NOVEL USES OF ATTENUATED TOTAL REFLECTANCE INFRARED MICROSPECTROSCOPY COMBINED WITH MULTIVARIATE ANALYSIS IN FOOD PROCESSING

Tilahun Kidanemariam Gelaw

Dipòsit Legal: T.1010-2013

TILAHUN KIDANEMARIAM GELAW

NOVEL USES OF ATTENUATED TOTAL REFLECTANCE INFRARED MICROSPECTROSCOPY COMBINED WITH MULTIVARIATE ANALYSIS IN FOOD PROCESSING

DOCTORAL THESIS

Department of Chemical Engineering

UNIVERSITAT ROVIRA I VIRGILI

Tarragona

2013

TILAHUN KIDANEMARIAM GELAW

NOVEL USES OF ATTENUATED TOTAL REFLECTANCE INFRARED MICROSPECTROSCOPY COMBINED WITH MULTIVARIATE ANALYSIS IN FOOD PROCESSING

DOCTORAL THESIS

Supervised by

Dr. SÍLVIA DE LAMO CASTELLVÍ

Department of Chemical Engineering

UNIVERSITAT ROVIRA I VIRGILI

Tarragona

2013

UNIVERSITAT ROVIRA I VIRGILI

Departament d'Enginyeria Química, ETSEQ
Avda. Països Catalans 26
Campus Sescelades
43007 Tarragona, Spain

Sílvia de Lamo Castellví, professora lectora del Departament d'Enginyeria Química de la Universitat Rovira i Virgili,

CERTIFICO:

Que el present treball, titulat "NOVEL USES OF ATTENUATED TOTAL REFLECTANCE INFRARED MICROSPECTROSCOPY COMBINED WITH MULTIVARIATE ANALYSIS IN FOOD PROCESSING", que presenta Tilahun Kidanemariam Gelaw per a l'obtenció del títol de Doctor, ha estat realitzat sota la meva direcció al Departament d'Enginyeria Química d'aquesta universitat.

Tarragona, 30 d'abril 2013

Sílvia de Lamo Castellví

EXAMINATION BOARD MEMBERS

Dr. Maria Izquierdo Pulido

University of Barcelona

Department of Nutrition and Bromatology

Barcelona, Spain

Dr. Nurcan Koca

Ege University

Department of Food Engineering

İzmir, Turky

Dr. Ricard Boqué Martí

University of Rovira I Virgili

Department of Analytical Chemistry and Organic Chemistry

Tarragona, Spain

Dr. Joan Ferré

University of Rovira I Virgili

Department of Analytical Chemistry and Organic Chemistry

Tarragona, Spain

Dr. Rosa María Lamuela Raventós

University of Barcelona

Department of Nutrition and Bromatology

Barcelona, Spain

Dr. Diego García Gonzalo

University of Zaragoza

Department of Animal Production and Food Science

Zaragoza, Spain

EXTERNAL REVIEWERS

Dr. Diana Behsnilian

Federal Research Institute of Nutrition and Food

Department of Food and Bio Process Engineering

Karlsruhe, Germany

Dr. Wojciech Kujawski

Nicolaus Copernicus University

Department of Physical Chemistry and Physical Chemistry of Polymers

Torun, Poland

ACKNOLEDGEMENTS

First and for most I would like to use this opportunity to express my sincere gratitude to my supervisor Dr. Sílvia De Lamo Castellví for her continuous guidance, support, motivation and help throughout the PhD work. I got an immense knowledge from her, not only the science, but also out of the science world. For that, I deeply thank her very much.

I also would like to sincerely thank Dr. Carme Güell and Dr. Montse Ferrando for their advice, encouragement and help me during my stay in the group. I would like to acknowledge Mrs. Tamara Esquitino and Alexandre Trentin for their techniqual assistance and providing data during the preparation of membrane samples and membrane cleaning.

I would like to extend my gratitude to Dr. Rafael Pagán, Dr. Diego García and Laura Espina from University of Zaragoza for providing me the microorganism samples, alive and inactivated different *Escherichia coli* 0157:H7 cells. It would not possible to have a complete work without their kind cooperation.

I also like to thank my colleges in FoodIE research group: Abreham Tesfaye, Rikkert Berendsen and Sarathi Raja. Moreover, I also sincerely thanks to my Ethiopian friends here in Tarragona for their encouragement, advice and the time we spent together.

I would like to thank the Department of Chemical Engineering of Universitat Rovira i Virgili and Generalitat de Catalunya for the financial and material support to carry out the PhD thesis.

My special heartfelt gratitude to my families, my beautiful and lovely wife Helen Temesgen, my mother Yamirot Mengistu, my brothers Dr. Awoke Kidanemariam, Geta Kidanemariam, Melkamu Kidanemariam and sisters Nigist Kidanemariam and Abebech Kidanemariam. They gave me valuable advices, encouragement, and above all love. I am so grateful to have you all besides me.

Acknowledgments

Lastly, I thank The Almighty God for giving me the wisdom, strength and all the patience to work and succeed in life

UNIVERSITAT ROVIRA I VIRGILI
NOVEL USES OF ATTENUATED TOTAL REFLECTANCE INFRARED MICROSPECTROSCOPY COMBINED WITHMULTIVARIATE ANALYSIS
IN FOOD PROCESSING
Tilahun Kidanemariam Gelaw
Dipòsit Legal: T.1010-2013

TO MY MOTHER….

TABLE OF CONTENTS

LIST OF TABLES

LIST OF FIGURES

NOMENCLATURE

ABBREVIATIONS

AFM	Atomic Force Microscopy
ANN	Artificial Neural Networks
ATR	Attenuated Total Reflectance
ATR-IRMS	Attenuated Total Reflectance Infrared Microspectroscopy
CDC	Center for Disease Control and Prevention
CECT	Colección Española de Cultivos Tipo (Spanish Culture Collection)
CFU	Colony Forming Unit
CLSM	Confocal Laser Scanning Microscopy
DTGS	Deuterated Triglycine Sulfate
ESEM	Environmental Scanning Electron Microscopy
FA	Factor Analysis
FSIS	Food Safety Inspection Service
FT-IRS	Fourier Transform Infrared Spectroscopy
HCA	Hierarchical Cluster Analysis
HGM	Hydrophobic Grid Membrane
ICD	Interclass Distance
IR	Infrared
LDA	Linear Discriminant Analysis
MCE	Nitrocellulose Mixed Esters
MCT	Mercury Cadmium Telluride
ME	Membrane Emulsification
PCA	Principal Component Analysis

PCR	Principal Component Regression
PEF	Pulsed Electric Field
PLSR	Partial Least Squares Regression
SEM	Scanning Electron Microscopy
SIMCA	Soft Independent Modeling of Class Analogy
STEC	Shiga Toxin-Producing *Escherichia coli*
TSAYE	Tryptic Soy Agar Yeast Extract
WFR	Water Flux Recovery
WHO	World Health Organization

SYMBOLS AND CHEMICAL FORMULAS

A	Absorbance
C	Carbon
CsI	Cesium iodide
θ_c	Critical angle
c	Concentration
N_o	Colony counts
D_p	Depth of penetration
E	Electric field
Ge	Germanium
H	Hydrogen
HBr	Hydrogen bromide
HCl	Hydrogen chloride
HF	Hydrogen flouride
I_o	Incident IR beam

I	Intensity
ε	Molar absorptivity
N	Nitrogen
N_2	Nitorgen gas
O	Oxygen
l	Path length
δ	Path difference
P	Phosphorus
KBr	Potassium bromide
n_1	Refractive index
AgBr	Silver bromide
AgCl	Silver chloride
S	Sulfur
KRS-5	Thallium bromoiodide
T	Transmittance
I	Transmitted IR beam
J	Water flux
λ	Wavelength
ῡ	Wavenumber
ZnSe	Zinc selenide

RESUMEN

El proceso de ensuciamiento de membrana es la principal limitación cuando se trabaja con membranas. Este fenómeno puede producirse por la deposición de partículas, suspensiones o materiales biológicos sobre la superficie o en el interior de los poros de la membrana. Diferentes técnicas tales como la microscopía confocal láser de barrido, la microscopía electrónica de barrido y la microscopía de fuerza atómica se han utilizado para caracterizar superficies membranas. Estas técnicas son empleadas principalmente para estudiar la morfología de las superficies y la distribución de poros en las membranas. La espectroscopía del infrarrojo con Transformada de Fourier (FTIR) también se ha dedicado para estudiar cualitativamente la composición y los grupos funcionales presentes en las superficies de las membranas. La técnica de la microespectroscopía del infrarrojo utilizando reflectancia total atenuada (ATR-IRMS) puede ser utilizada para detectar o identificar tanto cualitativa como cuantitativamente la composición química de las sustancias acumuladas sobre la superficie de la membrana sin necesidad de realizar un pretratamiento de la muestra. Además, también es posible estudiar la distribución de estas sustancias por microespectroscopía. Los métodos convencionales de cultivo utilizados para la detección e identificación de microorganismos requieren mucho tiempo y son bastante caros, Existe una necesidad imperiosa de desarrollar métodos rápidos, sensibles y fáciles de usar para reducir el tiempo de análisis y los costos, especialmente por parte de las industrias alimentarias donde el tiempo y el coste son aspectos claves. La técnica de la microespectroscopía del infrarrojo utilizando reflectancia total atenuada (ATR-IRMS) combinada con el análisis de datos multivariante puede ser utilizada como método rápido para el análisis de productos químicos y para clasificar y detectar microorganismos. Esta técnica tiene el potencial de detectar diferencias sutiles en la composición presente en los microorganismos. En general, los espectros de IR obtenidos para la mayoría de los microorganismos son casi idénticos, por lo tanto, es interesante aplicar una técnica de reconocimiento de patrones multivariante, como el *soft independent modeling of class analogy* (SIMCA) para detectar las pequeñas diferencias químicas que existen entre los microorganismos.

El objetivo general de esta tesis fue demostrar el uso de la técnica del ATR-IRMS combinada con el análisis multivariante como un método rápido, sencillo y robusto para poder caracterizar la superficie de membranas utilizadas para producir emulsiones alimentarias y estudiar diferentes microorganismos.

El primer estudio experimental se basó en la caracterización del proceso de ensuciamiento detectado en membranas usadas para la formación de emulsiones y su posterior proceso de limpieza mediante ATR-IRMS. Para esta investigación, se utilizaron dos membranas distintas, una de nylon y otra de ésteres orgánicos mixtos de nitrocelulosa (MCE) para estudiar el proceso de ensuciamiento y la eficiencia de los diferentes protocolos de limpieza aplicados. Emulsiones aceite-agua (O/W) fueron preparadas haciendo un primer pase a través de las membranas (nylon y MCE) con la ayuda de 900 kPa de presión N_2, utilizando como fase dispersa un 10% (v/v) de aceite de girasol y un 90% (v/v) de agua con 1% (w/v) de proteína de suero de leche como fase continua, Se aplicaron diferentes protocolos de limpieza a tres concentraciones distintas de Tween 20 (2, 3 y 4%) utilizando diferentes presiones de N_2 (150, 500 o 700 kPa) en el modo de lavado a contracorriente. Las membranas nuevas, sucias y limpiadas fueron caracterizadas por ATR-IRMS en la región del infrarrojo medio (4000-800 cm^{-1}) y los resultados analizados por análisis multivariante. Además, la eficiencia de los procesos de limpieza de las membranas se evaluó mediante el método tradicional (recuperación del flujo de agua) y por ATR-IRMS. Los espectros de IR de las membranas de nylon sucias y limpias mostraron principalmente la presencia de aceite de girasol con una banda clara detectada a 1743 cm^{-1}. Esta banda fue relacionada con *streching* del enlace >C=O de ácidos carboxílicos y ésteres y que no estaban presente en los espectros obtenidos de la membrana nueva. Sin embargo, no fue posible concluir a partir de los espectros adquiridos de las membranas de nylon sucias y limpiadas si el aceite de girasol fue el único componente de la emulsión causante de su ensuciamiento o si la proteína de suero de leche utilizada como emulsificante tuvo su papel en este fenómeno. Los espectros de IR obtenidos para la membrana de nylon nueva y para la proteína de suero, mostraron bandas similares de la región de las amida I y II (1629 cm^{-1} y 1550 cm^{-1}, respectivamente) no permitiendo discernir si la proteína de suero de leche participaba en el proceso de ensuciamiento de la membrana. El siguiente paso de esta investigación fue utilizar una membrana sin grupos funcionales amida (MCE). Los espectros de IR de membranas MCE limpias e ensuciadas mostraron la misma banda situada en 1743 cm^{-1} debido a la presencia de aceite de girasol. La banda asociada a la presencia de la proteína de suero (1535 cm^{-1}) no se observó en los espectros de membranas ensuciadas ni aplicando la segunda derivada a estos espectros. Los espectros de las diferentes muestras de membrana fueron analizados mediante soft independent modeling of class analogy (SIMCA). Las proyecciones de clases y las distancias entre clústers obtenidos mediante este análisis mostraron una clara diferenciación entre los clústers pertenecientes a los diferentes protocolos

de limpieza aplicados en membranas de nylon y MCE ensuciadas. Utilizando el poder de discriminación del modelo se detectaron las bandas que eran responsables de las diferencias químicas entre las muestras comparadas. Estas bandas estaban relacionadass con el aceite de girasol (1743, 1099 y 1057 cm^{-1}). Por lo tanto, el aceite de girasol fue identificado como el único agente responsable del ensuciamiento en ambas membranas testadas. Además, los modelos de SIMCA obtenidos con los espectros de membranas limpiadas y los resultados de eficiencia de limpieza obtenidos por los dos métodos, mostraron que loa condiciones más eficaces fueron cuando se utilizaron 3 y 4% de Tween 20 con 700 y 500 kPa de presión N_2, respectivamente.

El segundo estudio, se centró principalmente en la aplicación de la técnica del ATR-IRMS para detectar y discriminar microorganismos. Bacterias productoras de ácido acético (*Gluconobacter oxydans* y *Gluconacetobacter xylinus*) y dos cepas de *Saccharomyces cerevisiae* fueron cultivadas en mosto de uva roja durante 48 h. Estas muestras fueron posteriormente centrifugadas a 6000 rpm durante 5 minutos, los pellets se lavaron con solución salina y fueron después, a concentración de 10^8 UFC/mL, depositados sobre cuadrículas de una membrana hidrofóbica y secados para producir una película uniforme y delgada libre de agua. Los espectros se recogieron en modo de reflectancia total atenuada (ATR) en la región del infrarrojo medio (4000-700 cm^{-1}) y se analizaron mediante una técnica de análisis multivariante, SIMCA. El análisis de los espectros de IR (1600-900 cm^{-1}) obtenidos mostró una clara diferenciación entre las cepas de *S. cerevisiae* y las bacterías productoras de ácido acético. Los modelos obtenidos por la utilización del SIMCA mostraron que la diferenciación química entre las bacterías productoras de ácido acético se debió principalmente a las proteínas y lipopolisacáridos presentes en su pared celular. En el caso de las cepas de *S. cerevisiae*, su discriminación fue relacionada con strechings del grupo C-O-C e de β (1→3) polisacáridos (glucanos), así como manoproteínas y lípidos también presentan en sus paredes celulares.

En el tercer estudio, se evaluó el potencial de utilizar ATR-IRMS para diferenciar entre células bacterianas muertas, vivas y también lesionadas. Para ello, se utilizaron células de *Escherichia coli* O157:H7 tratadas por calor y campos eléctricos pulsados de alta intensidad (de sus siglas en inglés, PEF) para generar células lesionadas y muertas. Para la realización de estos experimentos, una alícuota del cultivo inicial de *E. coli* O157:H7 (0,25 mL) fue inoculada en 0,75 mL de solución tampón de fosfato y

citrato (tampón McIlvaine) a pH 4 y 7 y fue tratada térmicamente a 54 ± 0,2^{o}C durante 5, 10, 20 y 90 minutos. o por PEF utilizando 35 kV/cm durante 10, 25, 50 y 60 pulsos. Posteriormente, las muestras fueron centrifugadas a 6000 rpm durante 5 minutos y lavadas con solución salina al 0,9% tres veces. Los pellets de cada muestra fueron depositados en las cuadrículas de una membrana hidrófobica, secados durante 1 h y analizados por ATR-IRMS. El poder de discriminación del modelo SIMCA obtenido con los espectros de IR de las muestras de *E. coli* O157:H7 tratadas térmicamente a pH 4, mostró mayoritariamente dos bandas espectrales a 1638 y 1618 cm^{-1} responsables de su diferenciación química.. Estas bandas fueron relacionadas con proteínas secundarias β-plegadas que están presentes en su membrana celular. Estas bandas fueron también las principales bandas discriminantes entre células de *E. coli* O157:H7 vivas y tratadas por PEF a pH 4. A pH 7, en el modelo SIMCA creado comparando las muestras de *E. coli* O157:H7 vivas y tratadas térmicamente, también fue detectada la banda mecionada anteriormente a 1618 cm^{-1}. A más a más, en este modelo hubo una contribución de la banda 1215 cm^{-1} asociada a modos de vibración (*streching*) del grupo P=O (PO_2^-) presente en fosfodiésteres y lipopolisacáridos componentes también de la membrana celular de esta bacteria. Para la clasificación de células *E. coli* O157:H7 vivas y PEF tratadas a pH 7, dos bandas discriminantes fueron detectadas a 1078 y 993 cm^{-1}. Estas bandas también fueron vinculadas modos de vibración (*streching*) del grupo y a modos de vibración de los grupos C-O-C o C-O presentes en diferentes polisacáridos que forman parte de las membranas celulares, respectivamente. Las proyecciones de clase y las distancias de clase (de sus siglas en inglés, ICD) confirmaron los resultados obtenidos analizando el poder de discriminación en los dos modelos construidos a pH 4 y 7. Los clústers de muestras vivas y tratadas térmicamente i por PEF mostraron una buena separación y agrupación señalando las diferencias bioquímicas entre las muestras comparadas. Los valores de ICD aumentaron con el tiempo de tratamiento aplicado a ambos valores de pH. Para la realización de las mediciones cuantitativas, la regresión parcial por mínimos cuadrados (de sus siglas en inglés, PLSR) fue utilizada para predecir la inactivación bacteriana (térmica y por PEF) a partir de los espectros de IR. La predicción se realizó usando como método de referencia los recuentos en placa de las células de *E. coli* O157:H7 obtenidos en tres medios de cultivo distintos, agar Tripticasa de soya enriquecida con un 0,6% de extracto de levadura (de sus siglas en inglés, TSAYE), TSAYE con 3% de cloruro de sodio (de sus siglas en inglés, TSAYE -SC) y TSAYE con 0,35% de sales biliares (de sus siglas en inglés, TSAYE -BS). TSAYE, TSAYE-SC y TSAYE-BS se utilizaron para obtener el recuento total de células, células que tienen la membrana

citoplasmática dañada y células con la membrana externa dañada, respectivamente. Los valores de predicción que fueron obtenidos con los modelos de PLSR presentaron coeficientes de determinación (R^2) de 0,83 o superiores, y errores estándards de validación cruzada (de sus siglas en inglés, SECV) entre 0,114 y 0,369 unidades logarítmicas.

SUMMARY OF THE THESIS

Membrane fouling is the major limitation in membrane processes. This phenomenon could be due to the deposition of particulates, suspensions or biological materials on the membrane surface or inside the membrane pores. Different techniques such as confocal scanning laser microscopy, scanning electron microscopy and atomic force microscopy have been used to characterize membrane surfaces. These techniques mainly used to study the surface morphology and pore distributions of the membranes. Fourier transform infrared spectroscopy (FTIR) has been also used to study the composition and the functional groups present on membrane surfaces qualitatively. Attenuated total reflectance infrared microspectroscopy (ATR-IRMS) could be used to detect or identify qualitatively as well as quantitatively the chemical composition of foulants on the membrane surface without the need of sample pre-treatment. Moreover, the foulants distribution could be studied by taking IR scans at different site with the assistance of the microscope. Conventional culture methods for the detection and identification of microorganims are very labor intensive and time consuming. Hence, there is a strong need to develop rapid, sensitive and easy to use methods in attempt to reduce the analysis time and expenses, especially in food industries where time and cost are very sensitive issues. Attenuated total reflectance infrared microspectrsocpy (ATR-IRMS) combined with multivariate data analysis could be used as a rapid method for the analysis of chemicals and the classification and detection of microorganisms. This technique has the potential of detecting subtle compositional differences between microorganisms. Generally, raw spectra of microorganisms are nearly very similar, hence a multivariate pattern recognition technique such as soft independent modeling of class analogy (SIMCA) could be used to detect and classify microorganisms.

The overall objective of this thesis was to demonstrate the use of ATR-IRMS combined with multivariate analysis as a rapid, simple, and robust analytical technique for membrane characterization and studying microorganisms.

The first experimental study was the characterization of membrane fouling and cleaning using ATR-IRMS. For this research, nylon and nitrocellulose mixed esters (MCE) membranes were used to study the fouling and the efficiency of different cleaning protocols applied to remove membrane fouling after membrane emulsification. Oil-in-water (O/W) emulsions were prepared by passing 10% (v/v) sunflower oil as a dispersed phase and 90% (v/v) water with 1% (w/v) of whey protein as a continuous phase all together through the membranes (nylon and MCE) with the help of 900 kPa N_2 pressure. Different cleaning protocols were applied at three concentrations of Tween 20 (2, 3 and 4%) and using N_2 pressure (150, 500 or 700 kPa) in backwash mode. New, fouled and cleaned nylon and MCE membranes were characterized by ATR-IRMS in the mid-infrared region (4000-800 cm^{-1}) combined with multivariate analysis. Furthermore, the efficiency of the membrane cleaning processes was evaluated by using ATR-IRMS and water flux recovery. The raw ATR-IRMS spectra of fouled and cleaned nylon membranes showed mainly the presence of sunflower oil displaying a clear band at 1743 cm^{-1} related to >C=O stretching of carbonic acids and esters that was not present in the raw spectra of new nylon membrane. However, it was impossible to conclude from the raw spectra of fouled and cleaned nylon membranes if sunflower oil was the only compounent producing fouling or if whey protein was also involved on this phenomenon. The raw spectra of new nylon membrane and whey protein showed a similar band in the amide I and amide II regions (1629 cm^{-1} and 1550 cm^{-1} respectively) not allowing to discern the role of whey protein on this process. The next step of this research was to use a membrane without amide functional groups (MCE) to obtain further insight regarding the role of whey protein on the fouling process. The raw spectra of fouled and cleaned MCE membranes showed the same band at 1743 cm^{-1} due to the presence of sunflower oil. Whey protein band (1535 cm^{-1}) was not observed on the fouled membrane spectra and their 2nd derivative representation. The raw ATR-IRMS spectra of the membrane samples were further analyzed using soft independent modeling of class analogy (SIMCA) models. Class projections and interclass distances of SIMCA showed clear differentiation between the clusters of different cleaning protocols tested on nylon and MCE membranes. The discriminating power had the IR bands related to sunflower oil (1743, 1099

and 1057 cm^{-1}). Therefore, sunflower oil was identified as the only foulant agent on both membrane surfaces. Moreover, the cleaning efficiency results showed that, fouled nylon and MCE membranes cleaned with 3 and 4% of Tween 20 and 700 and 500 kPa of N_2 pressure, respectively were the conditions that produced the highest rates of cleaning efficiency using either water flux recovery or ATR-IRMS techniques.

In the second study, we mainly focused on the application of ATR-IRMS to detect and discriminate different microorganisms. Acetic acid bacteria (*Gluconobacter oxydans* and *Gluconacetobacter xylinus*) and *Saccharomyces cerevisiae* strains were grown in red grape must for 48 h, centrifuged at 6000 rpm for 5 min, washed with saline solution and pellets (10^8 CFU/mL) were deposited onto the grids of hydrophobic membrane filters and dried to produce a uniform and thin film. Spectra were collected in the attenuated total reflectance (ATR) mode in the mid-infrared region (4000-700 cm^{-1}) and were analyzed by a multivariate analysis technique, SIMCA. Infrared spectra analysis (1600-900 cm^{-1}) showed clear differentiation between *S. cerevisiae* and acetic acid bacteria strains. The SIMCA analysis of the raw spectra of acetic acid bacteria strains showed that their discrimination was mainly due to proteins and lypopolysaccharides presents in their cell wall. In the case of *S. cerevisiae* their discrimination was related to the C-O-C stretching of β (1→3) glucans polysaccharides as well as mannoproteins and lipids also presents in their cell walls.

In the third study, we evaluated the potencial of using ATR-IRMS to differentiate between alive, death and injured bacterial cells. For this purpose, *Escherichia coli* O157:H7 cells were inactivated by thermal and pulsed electric fields (PEF) treatments to produce different types of injured cells and analyzed by ATR-IRMS and multivariate analysis (SIMCA). *E. coli* O157:H7 cells (0.25 mL) were suspended into 0.75 mL of citrate phosphate (McIlvaine buffer) at pH 4 and 7 and treated thermally at 54 ± 0.2 ^oC for 5, 10, 20 and 90 min. Similarly, an aliquote of 0.25 mL *E. coli* O157:H7 cells were suspended into 0.75 mL of citrate phosphate (McIlvaine buffer) at pH 4 and 7 and treated by PEF 35 kV/cm for 10, 25, 50 and 60 pulses. Then, bacterial cells were centrifuged at 6000 rpm for 5 min and washed with 0.9% saline solution three times. Pellets

were placed onto the grids of hydrophobic membranes, dried out for 1 h and analyzed by ATR-IRMS. The discriminating power of alive and thermal treated *E. coli* O157:H7 cells at pH 4 showed two major spectral bands at 1638 and 1618 cm^{-1} responsible of their discrimination. These bands were due to the amide I band of β-pleated secondary proteins presents in their cell membrane. These bands were also the major discriminating bands of alive and PEF treated *E. coli* cells at pH 4. The major discriminating band responsible for the classification of alive and thermal treated *E. coli* O157:H7 cells at pH 7 was the amide I band at 1618 cm^{-1} due to the β-pleated secondary protein in the cell membrane. There was also a contribution of a band at 1215 cm^{-1} for the discrimination of alive and thermal treated *E. coli* O157:H7 cells at pH 7 linked to P=O (PO_2^-) stretching of phosphodiesters and lipopolysaccharides presents in the cell membrane. Two major discriminating bands were detected at 1078 and 993 cm^{-1} for the classification of alive and PEF treated *E. coli* O157:H7 cells at pH 7. These bands were also linked to P=O (PO_2^-) stretching of phosphodiesters or lipopolysaccharides and C-O-C or C-O strechings of different polysaccharides presents in the cell membranes, respectively. The class projections and interclass distances (ICD) values of thermal and PEF treated *E. coli* O157:H7 cells at pH 4 and 7 further proved the results obtained analyzing the IR bands of the discriminating power. Alive, thermal and PEF treated samples showed tight clustering pointing out the biochemical differences between the samples compared. The ICD values increased with the treatment time applied at both pH values. For quantitative measurements, partial least square regression (PLSR) was used to predict the bacterial inactivation (thermal and PEF) from IR data. The prediction was done using the inactivation values obtained from Tryptic Soy Agar with 0.6% of Yeast Extract added (TSAYE), TSAYE with 3% of sodium chloride (TSAYE-SC) and TSAYE with 0.35% of bile salts (TSAYE-BS) cell counts as reference data. TSAYE, TSAYE-SC and TSAYE-BS were used to have total cell counts, cells that have cytoplasmic membrane damaged and cells with outer membrane damaged respectively. The PLSR prediction of inactivation values obtained had a coefficient of determination (R^2) of 0.83 or higher with a standard error of cross validation (SECV) between 0.114 and 0.369 log units.

CHAPTER 1

Introduction

1.1. INTRODUCTION

1.1.1. A Brief Review of Membrane Fouling

1.1.1.1. Membrane Emulsification

A two-phase system of matter which is a mixture of two or more immiscible liquids is known as emulsion (Nazir *et al.*, 2010; Charcosset, 2011). A stabilized emulsion can be formed by using surface active components or surfactants. Most of the products of food, cosmetics and pharmaceutical industries are results of emulsions. Examples of emulsion are vinaigrettes, mayonnaise, milk, creams etc (Nazir *et al.*, 2010; Trentin *et al.*, 2010; Charcosset *et al.*, 2004; Karbstein and Schubert, 1995).

Depending on the application of the resulting emulsions conventional techniques including colloid mills, rotor-stator systems and high pressure homogenizers have been used for the preparation of emulsions (Joscelyne and Trägårdh, 2000; Charcosset, 2011). Usually, these techniques produce high shear force and heat which could cause the loss of the functional properties of the emulsion components. In addition to this, it is difficult to control the size and distribution of the droplets (Joscelyne and Trägårdh, 2000; Trentin *et al.*, 2010; Charcosset, 2011). Recently, membrane emulsification (ME) has been used to prepare emulsions. With this technology,it is possible to have very narrow particle size distributions without losing functional properties of the emulsion components and without needing high energy (Katoh *et al.*, 1996; Joscelyne and Trägårdh, 2000; Charcosset *et al.*, 2004; van der Graaf *et al.*, 2005; Vladisavljević *et al.*, 2006; Nazir *et al.*, 2010; Trentin *et al.*, 2010; Trentin *et al.*, 2011a). ME could be used in the production of simple and multiple emulsions in many fields and industries such as food, chemical, pharmaceutical and cosmetic. In ME, the dispersed phase is forced to pass through a microporous membrane, while the continuous phase flows along the membrane surface (Charcosset *et al.,* 2004; van der Graaf *et al.*, 2005; Vladisavljević *et al.*, 2006; Sawalha *et al.*, 2008; Trentin *et al.*, 2010; Trentin *et al.*, 2011a; Laouini *et al.*, 2012). Two operation methods are used in ME processes, direct and premix (Joscelyne and Trägårdh, 2000; Charcosset *et al.*,

2004; Trentin *et al.*, 2010). In direct ME, the dispersed phase is forced to pass through the membrane while the continuous phase flows along the membrane surface and detaches the droplet formed. In premix ME, first a coarse emulsion with non uniform droplet size distibution is prepared and this premix is pressed to pass through the membrane to form uniform and small droplets (Joscelyne and Trägårdh, 2000; Charcosset *et al.*, 2004; van der Graaf *et al.*, 2005; Surh *et al.*, 2008; Trentin *et al.*, 2010; Trentin *et al.*, 2011a). The main advantage of using premix ME process instead of direct ME is that, premix ME has a higher disperse phase flux.

1.1.1.2. Membrane Fouling

The main problem of ME processes is membrane fouling where different components of the emulsion are accumulated on the membrane surface or within the membrane pores. Fouling occurs due to the interaction between the membrane and the components of the emulsion (Güell *et al.*, 1996; Chang *et al.*, 2002; Van der Bruggen *et al.*, 2002; Lim and Bai, 2003; Schäfer *et al.*, 2004; Ferrando *et al.*, 2005; Zator *et al.*, 2009; Li and Chen, 2010; Trentin *et al.*, 2011b). The factors that affect membrane fouling are: membrane properties (surface chemistry, morphological structure, surface charge and hydrophilicity), properties of the feed solution (composition, concentration, pH, and ionic strength) and operational conditions (filtration mode, transmembrane pressure, cross-flow velocity of the feed and temperature) (Ho and Zydney, 1999; Makardij *et al.*, 1999; de Bruijn *et al.*, 2002; Marshall *et al.*, 2003; Al-Amoudi and Lovitt, 2007; Nigam *et al.*, 2008; Li and Chen, 2010). Membrane fouling can be sub-divided into different categories depending on the origin of the foulant: organic fouling (adsorption of organic molecules), colloidal fouling (deposition of particulates) and biofouling (growth and adhesion of microorganisms) (Flemming *et al.*, 1997; Zhu and Elimelech, 1997; Schäfer *et al.*, 2004; Costa *et al.,* 2006; Li and Chen, 2010).

1.1.1.2.1. Organic Fouling

Organic fouling is produced by the accumulation of dissolved or colloidal organic material on the membrane. Some examples of organic foulants are oils, proteins, carbohydrate, polysaccharides (Schäfer *et al.*, 2004; Ye *et al.*, 2005; Costa *et al.*, 2006; Al-Amoudi and Lovitt, 2007; Zator *et al.*, 2009; Li and Chen, 2010). This phenomenon has been reported by different researchers. For example, Costa *et al.* (2006), investigated the effect of membrane pore size and nature of the solution on the fouling of natural organic matter (NOM) on ultrafiltration (UF) membrane. These authors reported three mechanisms involved in fouling of NOM, pore blocking, pore constriction and cake formation. At an early stage of the UF process, pore blocking was the predominant fouling mechanism for both large (10 nm) and small (2 nm) pore size membranes. At longer filtration times there was a transition of fouling mechanism from pore blocking to cake layer formation and this phenomena occured faster on membranes with larger pore size than membranes with smaller pore size (Costa *et al*., 2006). Similarly, Van der Bruggen *et al.* (2002) studied the water flux decline of nanofiltration (NF) membrane due to the fouling of different organic compounds. From their study, almost 50% of the flux decline was observed when the solution concentration contained 10 mmol/L of organic compounds (Van der Bruggen *et al.*, 2002). Moreover, Violleau *et al*. (2005) studied the fouling of hydrophobic and hydrophilic NOM isolated from Blavet River on polyamide NF membrane. Streaming potential results showed that hydrophobic foulants were retained more inside the pores comparing with the hydrophilic foulants that were mainly adsorbed at the surface of the membrane (Violleau *et al.*, 2005).

1.1.1.2.2. Biofouling

Biofouling is produced by the accumulation and growth of microorganisms (microfouling) or plants, fungi and algae (macrofouling) on the membrane surface (Flemming et al., 1997; Baker and Dudley, 1998; Schäfer et al., 2004; Al-Amoudi and Lovitt, 2007; Li and Chen, 2010). Among

the fouling types, biofouling is hard to control in membrane process. The presence of small number of microorganisms in the feed solution could lead to the failure of the membrane, since these small numbers of microorganisms can easily and rapidly multiply using the nutrients available in the feed solutions (Flemming *et al.*, 1997; Ivnitsky *et al.*, 2005).

A variety of microorganisms have been detected to produce biofilms, *Pseudomonas*, *Bacillus,*, *Flavobacterium*, *Escherichia coli, Mycobacterium*, *Lactobacillus*, *Cytophaga*, *Micrococcus* and *Acinetobacter* (Flemming, 2002; Ivnitsky *et al.*, 2005; Schäfer *et al.*, 2004).

1.1.1.2.3. Colloidal Fouling

In this type of fouling, colloidal and particulate matters ranging from a few nanometers to a few micrometers are been accumulated on the membrane surface (Schäfer *et al.*, 2004; Kwon *et al.*, 2006; Al-Amoudi and Lovitt, 2007; Li and Chen, 2010). Zhu and Elimelech, 1997 investigated the effect of silica colloids on cellulose acetate and aromatic polyamide composite membrane. These authors observed greater flux decline when feed concentrations of silica colloids were higher due to the increase of the rate of convective transport of particles toward the membrane surface. This caused an increase in the overall rate of colloid deposition onto the membrane. They reported that for composite membrane, fouling was significant at all ionic strengths but for cellulose acetate membrane, fouling occurred only at high ionic strength values. Moreover, the effects of several parameters (pressure applied, shear rate, feed concentration, and particle size) on flux decline due to colloidal fouling has been studied in cross-flow membrane filtration (Zhang and Song, 2000). For this experiment, a model suspension of silica colloids with a diameter of 26 and 50 nm were used at two different pressure, ΔP= 41.4 kPa and 62.1 kPa. The result of the study showed that at the initial stage of the filtration the permeate flux for smaller particles decline faster than that of the larger particle permeate flux. However, when the filtration time was sufficiently long, the permeate flux for larger particles was smaller than the smaller particles (Zhang and Song, 2000).

Kwon *et al*. (2006) studied the organic nanocolloids fouling of drinking water on dialysis and UF membrane. These researchers used regenerated cellulose (RC) and polyethersulfone (PES) UF membranes. A flux decline difference was observed between RC and PES membranes when the pore size was in the same order as the dimensions of the organic nanocolloids. RC membranes experienced greater flux decline than the PES membranes due to internal pore blockage. On the other hand, organic nanocolloids were more strongly adsorbed on PES membrane surface.

1.1.1.3. Membrane Fouling Characterization

It is possible to minimize fouling phenomena using different strategies such as applying a pretreatment of the feeding, modifying the membrane surface and applying membrane cleaning process (chemically or physically) (Al-Amoudi and Lovitt, 2007). Different characterization techniques have been used to study membrane fouling. The methods most commonly used are macroscopic (calculating of flux decline) and microscopic (scanning electron microscope, confocal laser scanning microscope, atomic force microscope and spectroscopic techniques) (Güell *et al.*, 1996; Song, 1998; Väisänen *et al.*, 2002; Ferrando *et al.*, 2005; Delaunay *et al.*, 2008; Güell *et al.*, 2009; Torras *et al.*, 2009; Hilal, *et al.*, 2010). The following **Table 1.1** summarizes some of the techniques used for the characterization of membrane fouling in literature.

Table 1.1 *Membrane characterization techniques, their advantage and limitations*

Techniques	Advantages	Disadvantages	References
Scanning Electron Microscopy (SEM)/Environmental Scanning Electron Microscopy (ESEM)	• It provides high resolution images of the structure of fouling layer • It shows the size and shape of foulants that provides information about the origin of foulants • It provides micro-scale observation of membrane fouling behavior (surface morphology) • It monitors the effectiveness of fouling control methods (such as membrane cleaning)	• Coating of the sample (conductivity reasons) is needed unless ESEM is used • It destroys the original structure of fouling layer • The sample preparation is time consuming • Sample should be dried unless ESEM is used	Güell *et al.*, 1996; Le-Clech *et al.*, 2007; Meng *et al.*, 2010; Torras *et al.*, 2009; Väisänen *et al.*, 2002
Confocal Laser Scanning Microscopy (CLSM)	• Recording of thin layer images within the sample without cutting into slices • It displays and quantify the cross-section of the membrane sample (3D structure view) and morphology • Different states of membrane can be characterized (dry, hydrated, mounted in glycerol and in immersion oil) • It can differentiate membrane foulants by using fluorescence probe	• It has low magnification, hence, the resolution is lower than SEM • The effectiveness of laser penetration is poor • Losing signal or distortion might take place	Charcosset and Bernengo, 2000; Güell *et al.*, 2009; Ferrando *et al.*, 2005; Spettmann *et al.*, 2008; Yang *et al.*, 2007; Zator *et al.*, 2009

Techniques	Advantages	Disadvantages	References
Atomic Force Microscopy (AFM)	• It provides 3D images with resolutions at around atomic level • It provides quantitative information of cake morphology • No special sample pretreatment is required for its measurements It can measure both conducting and non-conducting surfaces	• It is difficult to find universal probes to simulate the affinity between foulants and membrane • Impossible to identify the composition of the foulants	Chan and Chen, 2004; Meng *et al.*, 2010; Singh *et al.*, 1998; Torras *et al.*, 2009
Fourier transform infrared (FTIR) spectroscopy	• It detects the chemical composition/chemical structure of membrane foulants • It is rapid and easy technique, • Samples can be re-used, since it is a non-destructive technique	• Membrane characterization is restricted to the surface of the membrane	Zhu and Nyström, 1998; Belfer *et al.*, 2000; Nataraj *et al.*, 2008; Meng *et al.*, 2010

1.1.2. Foodborne Pathogen Detection

In food processing industries, foodborne pathogens are the main food safety concerns and challenges during the processing of food and food products (Chemburu *et al.,* 2005; Elviss *et al.,* 2009; Jasson *et al.,* 2010; Ponniah *et al.,* 2010; Velusamy *et al., 2010*). When a food is contaminated with pathogenic microorganisms and is consumed by humans may cause a disease called foodborne illness (Velusamy *et al.,* 2010). Each year in USA 48 millions of illness and 3,000 deaths are estimated related to foodborne illness (FSIS, 2011). *Campylobacter jejuni, Salmonella, Escherichia coli* and *Listeria monocytogenes* have been identified as the four major foodborne pathogens that cause foodborne outbreaks (WHO, 2002; Alocilja and Radke, 2003; Chemburu *et al.,* 2005). Foodborne illness is considered as an outbreak, when two or more people become sick with a similar illness due to the consumption of food from the same source (Ray, 2003). Center for Disease Control and Prevention (CDC, 2013) reported that, during the period between 2009 and 2010 a total number of 1,527 foodborne outbreaks that produce 29,444 cases of illness, 1,184 hospitalizations, and 23 deaths were reported in the USA. In 2011, an outbreak of Shiga toxin-producing *Escherichia coli* (STEC) was reported in Germany due to the consumption of contaminated raw tomatoes, cucumbers and leafy salads (Frank *et al.,* 2011). During a traditional festival in Catalonia, Spain a large outbreak of *Salmonella* serotype Enteriditis was occurred due to the consumption of a hard pastry with vanilla cream in June 2002 (Camps *et al.*, 2005). From the onset to the end of the outbreak, 1435 cases and 117 hospitalizations were recorded. The reason for the outbreak was due to the inadequate handling of foods containing eggs which consumed on the day of the festival (Camps *et al.*, 2005). A summary of the recent outbreaks of foodborne pathogens is shown in **Table 1.2**.

Table 1.2 *Recent outbreaks of the major foodborne pathogen microorganisms*

Microorganisms	**Place and year of outbreak**	**No. of cases**	**Type of food**	**Cause of the outbreak**	**References**
Campylobacter jejuni	Barbecue party in Germany, 2001	5	Chicken meat	Slaughter house contamination	Allerberger *et al.*, 2002
Campylobacter jejuni	high school in Japan, 2005	33	Cooked chicken	Secondary contamination in cooking practice	Yoda and Uchimura, 2006
Salmonella Weltevreden	Denmark Finland and Norway, 2007	45	Alfalfa sprouts	Contaminated alfalfa sprouts	Emberland *et al.*, 2007
Salmonella Enteritidis	Nursing home in Germany, 2006	111	Cake	High ambient summer temperatures and failure to keep the cake refrigerated	Frank *et al.*, 2007
Salmonella Typhimurium	USA, 2009	714	Peanut butter	Contaminated peanut butter	CDC,2009
Salmonella Typhimurium	The Netherlands, 2009	23	Raw or under cooked beef	Contaminated beef	Whelan *et al*., 2010
Salmonella Thompson	The Netherlands, 2012	866	Smoked salmon	Contaminated smoked salmon from the producer	Friesema *et al.,* 2012
Escherichia coli O103:H25	Norway, 2006	17	Fermented sausage	Contaminated fermented sausage	Sekse *et al.*, 2009
Escherichia coli O14:H4	Germany, 2011	214	Raw tomatoes, cucumber and leaf salad	Contaminated tomatoes, cucumber and leaf salad	Frank *et al.*, 2011
Listeria monocytogenes	USA, 2002	54	Turkey deli meat	Contaminated turkey distributed by turkey processing plant	Gottlieb *et al.*, 2006

In any food industry, food safety and food quality are their main priorities. Before the distribution of their products for consumption, the food is analyzed for the presence of pathogenic and spoilage bacteria. However, the level of concentration of target pathogens in food are usually low and it is necessary to pre-enriched it prior to culturing step. This makes the detection and isolation methods difficult (De Boer and Beumer, 1999; Elmerdahl, 2000). Moreover, it has been stressed the importance of the detection and isolation of injured pathogen microorganisms prior to the distribution of processed (thermal, high pressure or other emerging techniques) foods. The sublethal injured pathogen microorganisms can easily recover and start to grow when they got suitable environment and cause illnesses (Mackey, 2000; Mañas and Pagán, 2005). In the following sections we will briefly introduce the conventional and alternative detection and isolation methods of foodborne pathogens, their advantages and limitations.

1.1.2.1. Conventional Methods for Pathogen Detection

The most common and standard methods of foodborne pathogen detection are the so called classical/conventional methods. These methods are based on nutritious or selective broth or agar media to detect viable bacterial cells or spores in foods (De Boer and Beumer, 1999; Lazcka *et al.*, 2007; Jasson *et al.*, 2010; Velusamy *et al.*, 2010; Arnandis-Chover *et al.*, 2012). The conventional methods are considered the standard methods being accurate, sensitive and can provide qualitative/quantitative information of pathogenic microorganisms present in foods (De Boer and Beumer, 1999; Velusamy *et al.*, 2010; López-Campos *et al.*, 2012). However, they have some limitations mainly related with sample preparation which is very labor intensive and time consuming. The concentration of pathogenic microorganisms found in food samples is normally low; for this reason, it is necessary to apply an initial enrichment step to be able to detect those microorganisms by conventional methods. These methods need several days to deliver a result and knowing if the pathogen is present or not in the food (De Boer and Beumer,

1999; Jasson *et al.*, 2010; López-Campos *et al.*, 2012). These can be minimized or avoided by using modified/automated conventional methods (De Boer and Beumer, 1999; Chemburu *et al.*, 2005; Jasson *et al.*, 2010; Velusamy *et al.*, 2010). The following **Table 1.3** summarizes conventional and automated conventional methods, their advantages and limitations.

Table 1.3 *Conventional method for the detection of foodborne pathogens: their advantages and limitations*

Methods	Description	Advantages	Limitations	Reference
Culture and colony counting	• It is an enumeration method based on the preparation of samples, plating, colony counting and identification of bacteria	• They are very sensitive and inexpensive, requiring no complex instrumentation • They give qualitative and quantitative information about the concentration and or type of microorganisms • They provide accurate results hence regarded as a reference/standard method	• Time consuming, it normally takes 2-3 days for initial results, and up to 7-10 days for confirmation • Labor intensive, it needs culture medium preparation, inoculation, colony counting and biochemical characterization	Brooks *et al.*, 2004; Leonard *et al*., 2004; De Boer and Beumer, 1999; Jasson *et al*., 2010; López-Campos *et al.*, 2012

Though conventional methods are accurate and sensitive for the detection of pathogenic microorganisms, food processing industries require rapid, reliable, simple, specific and sensitive detection methods (De Boer and Beumer 1999; Velusamy *et al.*, 2010). In the following section we will have a brief overview of the rapid methods that have been developed to analyze pathogenic microorganisms.

1.1.2.2. Rapid Methods

In food products, the detection methods need to be selective because low numbers of pathogenic bacteria are often present in this complex biological environment along with many other non-pathogenic microorganisms (Jasson *et al.*, 2010; López-Campos *et al.*, 2012; Velusamy *et al*., 2010). The rapid methods to detect foodborne pathogen microorganisms reported in literature with their advantages and limitations are listed in the following table (**Table 1.4**).

T*able 1.4* *Rapid methods for the detection of foodborne pathogens: Their advantage and limitations*

Methods	Description	Advantages	Limitations	**References**
Flow cytometry	•It is an optical technique where a suspension of microorganisms interacts with a beam of a laser and the light is been scattered and absorbed by the microorganisms.	•It has high sensitivity, the detection level could be as low as 10^2 yeast cells and about 10^2-10^3 bacterial cells per ml •It is suitable for detecting low numbers of specific microorganisms in fluids or food matrices •I t is possible to obtain information about the size, number and type of the microorganism.	•Most microorganisms are optically too similar to resolve from each other, hence it is necessary to label them with fluorescent dyes attached to specific antibodies	Jasson *et al.*, 2010; De Boer and Beumer, 1999; Gunasekera *et al.*, 2003
Impedimetry	•It is based on changes in conductance in a medium where microbial growth and metabolism takes place	•It is fully automated and computerized •It is used for the screening of large numbers of samples, hence saves substantial time and material.	•Its sensitivity is low, hence it is not suited for testing samples with low numbers of microorganisms •The food matrix will interfere with the impedance analysis which needs the determination of calibration curves for each food matrix examined	De Boer and Beumer, 1999; Grossi *et al.,* 2008; Jasson *et al.*, 2010

Methods	Description	Advantages	Limitations	**References**
Electrochemical biosensors	•It is an electronic analytical device which converts a biological response into an electrical signal. A bioreceptor/ biorecognition element interacts (binds or recognizes) the analyte under study and the transducer transforms the signal resulting from the interaction into another signal that can be more easily measured and quantified	•They require lower time between sampling and results compared to culture and colony counting methods •It is possible to work with small sample volumes (nanolitres or less), hence the reagents cost will not be high •They are label-free and "real-time" detection methods and hence simplifies sample preparation	•The biological sensing components are unstable and tend to degrade in a short-period of time and lose their effectiveness over a of the •These methods lack sufficient sensitivity and specificity of foodborne pathogen samples compared to optical methods •Generally they are complicated and expensive	Jasson *et al.*, 2010; Velusamy *et al.*, 2010; Boer and Beumer, 1999; Lazcka *et al.*, 2007; Ivnitski *et al*, 1999; Ellis and Goodacre, 2001; Warriner and Namvar, 2011; Palchetti and Mascini, 2008; Radke and Alocilja, 2005; Tully *et al.*, 2008

Methods	Description	Advantages	Limitations	**References**
Vibrational spectroscopy •Raman and Fourier transform infrared (FTIR) spectroscopy	• It is whole-organism fingerprinting techniques which is based on the interaction of radiation with the samples	•It provides comprehensive chemical information/chemical structure of biological cells at a molecular level •They require minimum/no pre-samples preparation, that will minimize the time to get the result •They are non-invasive investigation of biological samples •FT-IR provides the detection, enumeration, classification and identification at the same time	•Analysis of mixed cultures is difficult unless IR microscope is used • It requires a strict care on microbiological parameters (culture medium, cultivation time, and temperature)	Sengupta *et al.*, 2006; Alvarez-Ordóñez *et al.*, 2011; Burgula *et al.*, 2007; Maquelin *et al.*, 2006; Félix-Rivera and Hernández-Rivera, 2011; Velusamy *et al.*, 2010; Naumann, 2006

In the food industries, these rapid methods are a powerful tool for the early detection and quantification of pathogenic microorganisms. Currently, food safety rules and legislations are very strict with the presence and the concentration of some pathogenic microorganisms in food products (Fung, 1994; De Boer and Beumer, 1999; Fung, 2002; Velusamy *et al.*, 2010; Mandal *et al.*, 2011).

1.1.3. An Overview of Fourier Transform Infrared Spectroscopy (FTIR)

Infrared (IR) spectroscopy is a type of vibrational spectroscopy technique which is based on the interaction of electromagnetic radiation with atoms of molecules (Stuart, 2006; Griffiths and de Haseth, 2007; Smith, 2011). The basic principle is simple, when an IR radiation interacts with atoms of molecules, some of the radiation is absorbed by the chemical bonds and this absorbance can be measured. Generally, each compound absorbs specific amount of IR light at specific IR wavenumbers. The absorption of IR radiation at specific wavenumber produces the vibration in terms of stretchinging, contracting and bending. Spectral bands are derived from the motions of the chemical bonds and correlated with the chemical structures of the sample analyzed. The spectrum of each compound is unique and used as a "fingerprint" to identify the compound with certainty (Stuart, 2006; Griffiths and de Haseth, 2007; Smith, 2011).

However, the basic necessity for a molecule to have an IR spectrum is to have a dipole moment and the dipole moment must change during the vibration. Dipole moment is the magnitude of the product of charges on the molecules and the distance between the charges. Molecules need to be heteronuclear diatomic (a molecule with two different atoms, e.g. HF, HCl, HB) to have a change in the dipole moment (Stuart, 2004; Griffiths and de Haseth, 2007).

The IR spectrum extends from the visible until the microwave region of the electromagnetic spectrum (wavenumbers ranging from 14,000 to 10 cm^{-1}). The infrared range of the electromagnetic spectrum is divided into three regions named after their relation to the visible

spectrum; Near-infrared (wavenumber ranges from 14,000 to 4,000 cm^{-1}), Mid-Infrared (4,000 to 400 cm^{-1}) and Far-infrared (400 to 10 cm^{-1}) (Naumann, 2006; Stuart, 2006). However, the most useful IR spectrum region is the Mid-Infrared region, since the Far-Infrared and Near-Infrared regions are usually difficult to study and interpret (Naumann, 2006; Stuart, 2006; Alvarez-Ordóñez and Prieto, 2012).

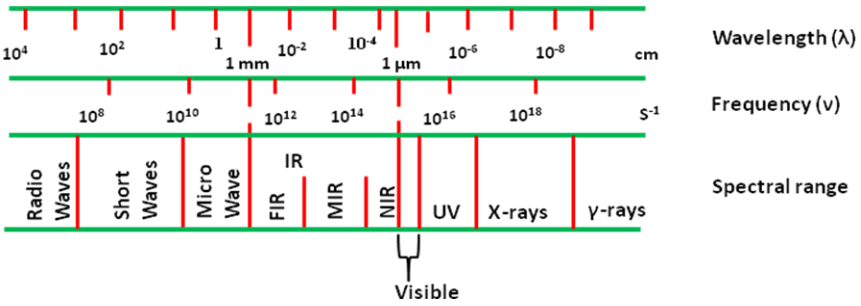

Figure 1.1. Schematic representation of the electromagnetic spectrum (Modified from Naumann, 2006)

As we aforementioned, spectral bands associated with the functional groups are used to identify and characterize specific compounds. The common functional groups at each corresponding group frequencies are shown in the following table (**Table 1.5**)

Table 1.5 *Characteristic FT-IR absorptions of common functional groups (adapted from Coates 2006)*

Functional Groups		**Group Frequencies (cm^{-1})**
Methyl ($-CH_3$)	C-H asym./sym.	2970-286
	C-H asym./sym. bending	1470-1365
Methylene ($>CH_2$)	C-H asym./sym.	2935-2845
	C-H asym./sym. bending	1485-1445
Methyne (>CH-)	C-H stretching	2900-2880
	C-H bending	1350-1330
Alkenes	C=C	1680-1600
	Vinyl C-H stretching	3095-3010
	Vinyl C-H in plane bending	1420-1410

Functional Groups		**Group Frequencies (cm^{-1})**
	Vinyl C-H out of plane	995-890
Alkynes	C=C (Terminal alkynes)	2140-2100
	C=C (Medial alkynes)	2260-2190
	C-H stretching	3320-3310
	C-H bending	680-610
Aromatic ring	C=C-C stretching	1615-1450
	C-H stretching	3130-3070
	C-H in plane bending	1225-950
	C-H out of plane bending	900-670
Alcohol and hydroxy	O-H stretching	3645-3200
	O-H in plane bending	1410-1260
	O-H out plane bending	720-590
	C-O stretching	1200-1050
Ether and oxy compounds	C-H (Methoxy)	2820-2810
	C-O-C (Alkyle)	1150-1050
	C-O-C (Cyclic ether)	1140-1070
	-O-H (Aromatic ether)	1270-1230
	C-O-(Epoxy and oxirane)	1250, 890-800
	C-O-O-C (Peroxides)	890-820
Amine and amino (primary amino)	N-H stretching	3510-3325
	N-H bending	1650-1590
	C-N stretching	1090-1020
Amine and amino (secondary amino)	>N-H stretching	3450-3310
	>N-H bending	1650-1550
	C-N stretching	1190-1130
Amine and amino (tertiary amino)	C-N stretching	1210-1150
Amine and amino (aromatic amino)	C-N stretching	1360-1250
Carbonyl groups (carboxylic acid)	>C=O stretching	1725-1700
Carbonyl groups (amide)	>C=O stretching	1680-1630
Carbonyl groups (ketone)	>C=O stretching	1725-1705
Carbonyl groups (aldehyde)	>C=O stretching	2800-2700/1740-1725
Carbonyl groups (ester)	>C=O stretching	1750-1725
Nitrogen multiple bonded (cyanate)	-OCN and C-OCN stretching	2260-2240/1190-1080
Nitrogen multiple bonded (isocyanate)	-N=C=O asym. stretching	2276-2240

Functional Groups		Group Frequencies (cm^{-1})
Nitrogen multiple bonded (thiocynate)	-SCN	2175-2140
Nitro compounds	N-O asym. stretching	1550-1475
	N-O sym. stretching	1360-1290
Phosphorus-oxy compounds	=PO stretching	1350-1250
	P-O-C stretching	1050-990
	P-O-C stretching	1240-1190/995-850
Thiols	S-H stretching	2600-2550
Thiols or thioether	CH_2-S-(C-S stretching)	710-685
Thioether	CH_3-S-(C-S stretching)	660-630
Disulfides	C-S stretching	705-570

When a compound is analyzed using IR spectrometer, the final result is displayed in terms of absorbance (A) or transmittance (T). Based on the intensity of the incident IR beam and the transmitted beam by the sample, the quantity of the transmittance (T) could be calculated using **equation 1.1**. The IR spectrum graph is plotted using the T and the wavenumbers of the radiation (Stuart, 2004; Naumann, 2006).

$$T = \frac{I}{I_o} \tag{1.1}$$

Where, where T is transmittance, I is the transmitted IR beam and I_o is the IR beam entering to the sample.

From the transmittance (T) and the wavenumbers of the radiation the IR spectrum graph can be plotted. Moreover, the concentration of the sample can be correlated with the intensity of the absorbance using the Beer-Lambert law (**equation 1.2**) (Naumann, 2006; Stuart, 2006; Burgula *et al*., 2007; Griffiths and de Haseth, 2007; Smith, 2011).

$$A = \varepsilon c l \tag{1.2}$$

Where A is the absorbance of the sample, *c* is the concentration, *l* is the path length of the sample and ε is the molar absorptivity. The absorbance also could be expressed in a logarithmic function using the difference of the intensity of the incident light (I_0) and the intensity of the transmitted light (*I*) (Stuart, 2006; Griffiths and de Haseth, 2007)

$$A = \log_{10}(\frac{I_o}{I}) \tag{1.3}$$

1.1.3.1. Equipments and Accessories of IR Spectroscopy

In IR analysis, the spectrum of a sample is produced using an instrument called a spectrometer (Smith, 2011). In a spectrometer there are three main parts, the IR source, the interferometer and the detector. The interferometer modulates the IR light intensities to encode their frequency information (Smiths Detection, IlluminatIR Users Manual). The most common interferometer used in IR instrument is Michelson interferometer (**Figure 1.2**). In Michelson interferometer, the IR light from the source transmitted in to two directions by the beam splitter. One travels toward a fixed mirror and the other travel toward a moving mirror. These light beams are then reflected back from their respective mirrors and travel to the beam splitter. The travelled back light beams are recombined into a single light at the beam splitter and travel into a sample holder, interact with the sample. Some of the light beam is absorbed by the sample and the remaing passes towards the detector (Burgula *et al*., 2007; Griffiths and de Haseth, 2007; Smith, 2011). During the recombination of the two light beams at the beam splitter, they interfere with each other in two ways. They interfere constructively when the path difference between the two beams is zero and they interfere destructively when the path difference between the two beams is half of the wavelength. As a result of these interferences an interferogram, which is a plot of light intensity versus optical path difference is produced (Griffiths and de Haseth, 2007; Smith 2011).

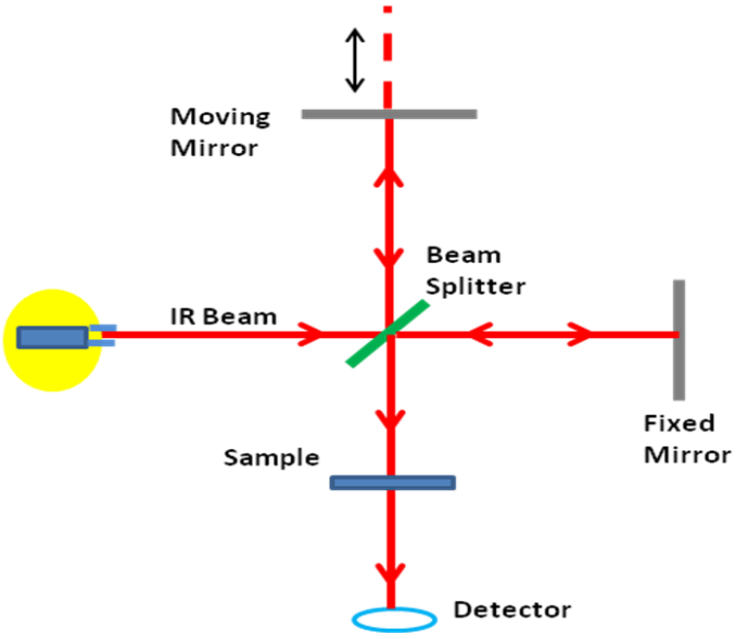

Figure 1.2. Schematic representation of Michelson interferometer (adapted from Smith, 2011)

The detector of the spectrometer acts as a transducer where the infrared light coming from the sample is changed into an electrical signal (voltage) (Griffiths and de Haseth, 2007; Smith, 2011). The common type of IR detector is deuterated triglycine sulfate (DTGS). It is a thermal detector which detects the change produced in the temperature of an absorbing material. When the temperature changes, the electrical polarization of DTGS varies, causing a flow of current. It is relatively inexpensive and it does not require any special treatment. However, DTGS is a slow detector, different materials respond to the change of IR intensity at different speed (Griffiths and de Haseth, 2007; Smith, 2011). The other type of detector is quantum detector called mercury cadmium telluride (MCT). It is a photodetector made with a photoconductive material where an electrical current is produced due to the photoexcitation of electrons by the absorbance of IR light (Griffiths and de Haseth, 2007; Smith, 2011). MCT detector is less noisy and faster than DTGS detector. Moreover, MCT detectors have a better sensitivity and more stable signal than the DTGS detectors. However, MCT detectors are very expensive and also they need to be cooled using liquid nitrogen (Griffiths and de Haseth, 2007; Smith, 2011).

1.1.3.2. Fourier Transformation (FT)

The first commercial spectrometer was available in the early 1940s. At that time, infrared spectra were obtained using dispersive elements (prism and gratings) in the spectrometer (Stuart, 2004). The infrared beams from the source were separated into individual wavelengths of the infrared light using the dispersive instruments and the detector the amount of energy at each frequency that was passing through the sample. It took longer time to obtain the spectral data, since the infrared frequencies were measured individually (Griffiths and de Haseth, 2007). Fourier transform (FT) has been in use since the invention of Michelson interferometer at the end of 1880s (Stuart, 2004). However, due to the lack of the mathematical algorithm and digital computers, it was not widely used until 1960s when James W. Cooley and John W. Tukey developed the mathematical algorism that produced the Fourier transform (Cooley and Tukey, 1965). Fourier transform is a mathematical function named in honor of the French mathematician Joseph Fourier (Smith, 2011). The main purpose of FT is to convert the interferogram obtained from the detector to the desired spectrum. Generally, an interferogram at a specific wavenumber of light is a cosine wave. The interferogram has intensity (I) as a function of path difference (δ), and using FT algorithm, this intensity is converted into a spectrum *B* as a function of wavenumber ($\bar{\upsilon}$) using the following equations (**equations 1.4 and 1.5**).

$$\mathrm{I}(\delta) = \int_{0}^{+\infty} \mathrm{B}(\bar{\upsilon})\ \cos(2\pi\bar{\upsilon}\delta)\mathrm{d}\bar{\upsilon} = F\left[\mathrm{B}(\bar{\upsilon})\right] \tag{1.4}$$

This is one of a cosine Fourier-transform pair that can be also written as:

$$\mathrm{B}(\bar{\upsilon}) = \int_{0}^{+\infty} \mathrm{I}(\delta)\cos(2\pi\bar{\upsilon}\delta)\mathrm{d}\delta = F^{-1}\left[\mathrm{I}(\delta)\right] \tag{1.5}$$

where I(δ) is the intensity of the interferogram as a function of path difference, B($\bar{\upsilon}$) is the output spectrum as a function of wavenumber and **equation 1.4** is the Fourier transform and **equation 1.5** is the inverse Fourier transform (Stuart, 2004; Griffiths and de Haseth, 2007).

The base of equation (**1.4** and **1.5**) is from the electric field of the IR light with a wavenumber ($\bar{\upsilon}$) and path length (x) and this electric field of the IR light at the beam splitter can be calculated using **equation 1.6**

$$\mathrm{E}(\mathrm{x}, \bar{\upsilon}) = E_0(\bar{\upsilon})e^{i(2\pi\bar{\upsilon}x-\omega t)} \tag{1.6}$$

Generally, the intensity of the spectrum *B* ($\bar{\upsilon}$) is proportional to E_0^2 ($\bar{\upsilon}$) (Jaggi and Vij, 2006). With a path difference (δ) due to the two mirrors in the interferometer, equation (1.6) can be written.

$$\mathrm{E}(\mathrm{x}_1, \mathrm{x}_2, \bar{\upsilon}) = E_0(\bar{\upsilon})[e^{i(2\pi\bar{\upsilon}x_1-\omega t)} - e^{i(2\pi\bar{\upsilon}x_2-\omega t)}] \tag{1.7}$$

The intensity of the interferogram (I) at a particular wavenumber is the square of the electric field of the IR beams coming from the two mirrors assuming that the beams recombined at the beam splitter of the interferometer has the same amplitude (Jaggi and Vij, 2006).

$$\mathrm{I}(\mathrm{x}_1, \mathrm{x}_2, \bar{\upsilon}) = 2E^2{}_0(\bar{\upsilon})[1+\cos 2\pi\bar{\upsilon}\delta] \tag{1.8}$$

Integrating **equation (1.8)** from δ = 0 to large path difference (δ=∞):

$$\mathrm{I}(\delta) = 2\int_0^\infty E^2{}_0(\bar{\upsilon})d(\bar{\upsilon}) + 2\int_0^\infty E^2{}_0(\bar{\upsilon})\cos(2\pi\bar{\upsilon}\delta)d(\bar{\upsilon}) \tag{1.9}$$

The intensity (I) at a path difference other than zero, **equation 1.9** can be rewritten as:

$$I(\delta) = 2\int_0^{\infty} E^2{}_0(\bar{\upsilon})\cos(2\pi\bar{\upsilon}\delta)d(\bar{\upsilon}) \qquad (1.10)$$

To obtain **equation 1.4**, 2 E_0^2 ($\bar{\upsilon}$) could be substituted by *B* ($\bar{\upsilon}$), since B ($\bar{\upsilon}$) is proportional to E_0^2 ($\bar{\upsilon}$).

The mathematical algorithm of the FT equation is done using a computer to obtain the final spectrum. **Figure 1.3** shows the output of this mathematical process.

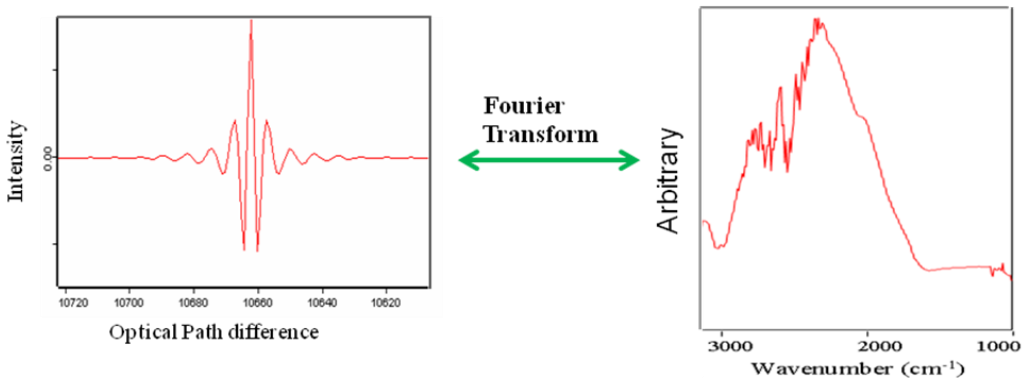

Figure 1.3. Graphical representation of the Fourier transform when an interferogram is converted into a single beam spectrum (adapted from Smith 2011)

1.1.3.3. Fourier Transform Infrared Interfaced with Microscopy

At the beginning FTIR technology, microsamples were measured by mounting the sample behind an optical material with an appropriate aperture (an opening/hole which determines the focusing of light on the sample). However, in this type of analysis, the infrared radiation is lost, because the samples are smaller than the infrared beam at its focus (Griffiths and de Haseth, 2007). The loss of this radiation was reduced by the introduction of a beam condenser in the sample compartment. When the samples were getting smaller and smaller,

spectrometers which use beam condenser were out of favor, instead a device called infrared microscopy with a remote aperture was started to function (Griffiths and de Haseth, 2007). The microscope provides physical information of the sample such as size, shape, color and morphology. In infrared microscopy, there is an aperture where only infrared radiation that has interacted with the sample passes and reaches at the detector (Smith, 2011).

1.1.3.4. Methods of IR Measurements

The common methods of mesurements are: transmission and reflectance spectroscopy (diffusion reflectance and attenuated total reflectance). These categories are mainly due to the difference in the interaction of the incident IR radiation with the sample (Naumann, 2006; Stuart, 2006; Alvarez-Ordóñez *et al*., 2011; Smith, 2011; Alvarez-Ordóñez and Prieto, 2012).

1.1.3.4.1. Transmission

Transmission FTIR technique is the most well known and successful method. It is based on the absorption of the radiation when it passes through the sample (Naumann, 2006; Stuart, 2006; Smith, 2011). Samples in different state (liquids, solids and gas) can be analyzed. The common infrared transparent materials used in transmission analyses are potassium bromide (KBr), cesium iodide (CsI), silver chloride (AgCl), silver bromide (AgBr), zinc selenide (ZnSe) and germanium (Ge). However, KBr is the most commonly used infrared transparent material, due to the fact that it is transparent over a broad spectra range. Moreover, it is relatively cheap and easy to prepare the IR transparent material which protects the detector from damage (windows) and liquid sample holders (cells) (Griffiths and de Haseth, 2007; Smith, 2011). There are some advantages of using transmission sampling techniques. The first advantage is that with the exception of a few sample types such as fibers and rubbers, it is possible to analyze all types of

samples. The cost of the equipment such as grinding and pressing machines needed to prepare the samples is relatively inexpensive (Smith, 2011). However, the main limitations of this method are the time required for sample preparation and the fact that it is a destructive technique due to the need of grinding, compressing, or dissolving the sample (Stuart, 2006; Smith, 2011).

1.1.3.4.2. Reflectance

Reflectance FTIR technique is based on the reflection of the light reflection from the surface of the sample. The intensity of the reflected light depends on the sample preparation size and shape of the particles/powder and how they are molecular organized (Smith, 2011). There are two ways of applying this technique: diffusion reflectance and attenuated total reflectance (Naumann, 2006; Smith, 2011). Generally, the main advantages of the reflectance technique are listed as follows; it is a nondestructive method and the sample after the analysis can be recovered for further analysis, and there is not or little sample preparation. However, the limitation of this technique is mainly related with the cost of the accessories which is higher than in the transmission method (Smith, 2011).

Diffusion reflectance: when a sample with a rough surface is in contact with an infrared beam, the incident light is reflected in different directions depending on the angle of incidence. Generally, highly scattering samples such as freeze-dried biological specimens and finely ground or powdered materials can be analyzed using this technique (Naumann, 2006). The main advantages of diffusion reflectance are nondestructive method (Smith, 2011), and there is no need to prepare a thin layer of sample. Its major limitation is that, the spectra obtained can be sometimes noisy since light is lost when it reflects from a rough surface. The other limitation is the cost of the accessories which is higher than the transmission method (Smith, 2011).

Attenuated total reflectance (ATR): is a type of reflectance technique based on the total internal reflection phenomenon (Naumann, 2006; Stuart, 2006; Smith, 2011; Alvarez-Ordóñez *et al*., 2011). In this technique, the sample is placed onto an optically denser (denser than the sample) material called attenuated total reflectance (ATR) crystal. When the IR radiation interacts with the crystal, an evanescent wave is produced and penetrates into the sample and into the detector (Naumann, 2006; Stuart, 2006; Smith, 2011; Alvarez-Ordóñez *et al*., 2011).

Table 1.6 *The properties of common ATR crystals (adapted from Smith, 2011)*

ATR Crystal	Refractive Index	Wavenumber Range (cm^{-1})	pH Range
ZnSe	2.42	15, 000 - 600	5 - 9
Ge	4.00	5, 500 - 600	1 - 14
KRS-5	2.37	20, 000 - 250	5 - 8
Diamond	2.42	30, 000 – 2, 200, 2000 - 400	1 -14

ATR crystals are made of a material with high refractive index and with long, thin parallelogram shape. These crystals have multiple evanescent wave sites at their surface (Smith, 2011). The most common ATR crystals used in IR measurements include, zinc selenide (ZnSe), germanium (Ge), and thallium/iodide (KRS-5) and diamond (Naumann, 2006; Stuart, 2006; Smith, 2011).The properties of the common ATR crystals are shown in **Table 1.6**.

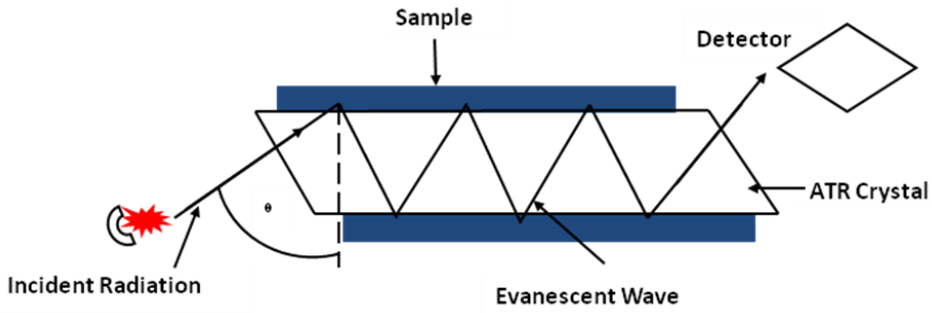

Figure 1.4. Schematic representation of attenuated total reflectance FT-IR method **(**Adapted from Stuart, 2004**)**

As it can be seen from **Figure 1.4,** the beam of radiation will undergo total internal reflection entering when it enters to the crystal. This phenomenon occurs when incident radiation interact with the sample at the angle greater the critical angle (θ_c). Critical angle is the minimum angle of incidence where a total internal reflectance can occur (Griffiths and de Haseth, 2007; Smith, 2011). When the beam of the radiation is in contact with the ATR crystal, the fraction of the beam penetrates the sample beyond the ATR crystal surface. The beam that totally internal reflected and in contact with the sample referred to as evanescent wave. The strength of the beam decreases exponentially as a function of the distance travelled inside the sample. This distance is called the depth of penetration. Depending on the interest of the person whether to analyze most of the bulk of the sample or only near the surface of the sample, an appropriate ATR crystal and incident angle of the IR beam should be selected before the analysis of the sample. The main parameter to select the crystal material and the incident angle is the depth of penetration (Griffiths and de Haseth, 2007). It is possible to calculate the depth of penetration of the evanescent wave of the incident radiation based on the wavelength values (λ) of the incident radiation, the refractive index of the ATR crystal (n_1) and sample (n_2) and the angle of incident of the radiation (θ) (Naumann, 2006; Stuart, 2006; Smith, 2011).

$$\text{Depth of penetration (Dp)} = \left(\frac{\lambda}{2\pi n_1 [\sin^2\theta - (n_2/n_1)^2]^{1/2}} \right) \quad (1.8)$$

The first advantage of this technique is that, there is no or little sample preparation needed, e.g. the time necessary for the grinding, squishing, pressing of the sample can be avoided using the ATR crystal directly.

The major limitations of reflectance techniques were aforementioned in the previous section. However, ATR method has additional limitation, the ATR crystals work at certain range of wavelengths limiting the infrared wavelength for the analysis (Stuart, 2006; Smith, 2011).

1.1.4. Multivariate Analysis Techniques

Multivariate analysis is a statistical method used to analyze multiple variables of data applying mathematical models (Miller and Miller, 2005; Naumann, 2006). There are two general categories of multivariate analysis depending on the previous knowledge of the data: supervised and unsupervised (Beebe *et al*., 1998; Brereton, 2003; Alvarez-Ordóñez *et al*., 2012). Supervised multivariate methods are methods where a previously set and defined spectra data are used for the prediction of unknown samples (Brereton, 2003; Naumann, 2006). Examples of supervised methods are artificial neural networks (ANN), linear discriminant analysis (LDA) and soft independent modeling of class analogy (SIMCA) (Kansiz *et al*., 1999; Dunn and Wold, 1995; Brereton, 2003). Unsupervised methods are used on the other hand, when there is no previous know how about the nature/class of the samples (Beebe *et al*., 1998; Brereton, 2003; Naumann, 2006). Examples of unsupervised methods are hierarchical cluster analysis (HCA), principal component analysis (PCA) and factor analysis (FA) (Dunn and Wold, 1995; Brereton, 2003; Naumann, 2006; Alvarez-Ordóñez *et al*., 2012). In addition to this for quantitative prediction, multivariate regression methods such as partial least squares regression (PLSR) and principal component regression (PCR) could be used (Haaland and Thomas, 1988; Beebe *et al*., 1998; Brereton, 2003; Miller and Miller, 2005).

1.1.4.1. Principal Component Analysis (PCA)

Principal component analysis (PCA) is based on the linear combination of the original independent variables (Pirouette, Version 4.0, 2008). It is used for the reduction of the original data and produces a new set of variables which are non-correlated (Dunn and Wold, 1995; Beebe *et al*., 1998; De Maesschalck *et al*., 1999; Pirouette, Version 4.0, 2008). It is the basis of other multivariate analysis methods such as soft independent modeling of class analogy and partial least square regression methods are based on PCA of the original data Pirouette, Version 4.0, 2008). PCA results can be represented graphically to show the inter-sample and inter-

variable relationships (Pirouette, Version 4.0, 2008). Different researchers used PCA methods to discriminate and classify microorganisms based on the IR spectral data (Kansiz *et al*., 1999; Rodriguez-Saona *et al*., 2001; Lin *et al*., 2004; Al-Qadiri *et al*., 2008b; Sundaram *et al*., 2012). Based on the results of scores and loadings of each principal component, the variation of IR spectral data is evaluated (Al-Qadiri *et al*., 2008b). Lin *et al*., (2004) used PCA analysis to detect the variation of the spectral data obtained from intact and sonication-injured *Listeria* strains (Lin *et al*., 2004). According to the results of the authors, sonication-injured *L. monocytogens* were well discriminated from the intact *L. monocytogens and L. innocua based* on the PCA scores of the IR spectra (Lin *et al*., 2004). Rodriguez-Saona *et al*. (2002) used Fourier-transform near infrared spectroscopy combined with PCA was used to discriminate different bacteria such as *Escherichia coli* spp., *Pseudomonas aeruginosa*, *Bacillus* spp. and *Listeria innocua* (Rodriguez-Saona *et al*., 2002). The authors claimed that the spectra region around 5000-4000 cm^1 exhibited clusters that discriminated between bacteria species at levels < 1 mg wet cells weight (approximately 10^6-10^7CFU/mg). The bacteria cells were concentrated on an aluminum oxide membrane to obtain a thin film prior to the spectral collections (Rodriguez-Saona *et al*., 2002).

1.1.4.2. Hierarchical Cluster Analysis (HCA)

In hierarchical cluster analysis (HCA) the clustering of samples is based on the distance between them. Samples considered similar when their distance is relatively smaller with respect to the measurements we set and different when they are separated with larger distance (Pirouette, Version 4.0, 2008). Different distance measurements such as Euclidean and Mahalanobis distances have been used to determine the similarity between samples (Naumann, 2006). Euclidean distance is the distance between two points in which one would measure with a standard ruler. This distance ignores the variability of the data sets. Mahalanobis distance is a multivariate distance which considers the correlation between variables (Yang and Trewn,

2004). In HCA analysis, first the distance between pairs of samples are computed, and then the samples with the smallest distance are grouped into one cluster. Second, the distance between this new cluster and all the remaining samples are computed, samples with the closest inter-cluster are collected again in one single cluster. This procedure continues until all the samples/clusters are grouped (Naumann, 2006; Pirouette, Version 4.0, 2008). The results of HCA are represented in the form of dendrogram which shows the classification of the samples visually (Pirouette, Version 4.0, 2008). HCA multivariate analysis method has been used for the classification of different microorganisms based on the infrared spectral data (Oust *et al*., 2004; Alvarez-Ordonez and Prieto, 2010; Hu *et al*., 2009; Choo-Smith *et al*., 2001 and Ngo Thi and Naumann , 2007).

1.1.4.3. Soft Independent Modeling of Class Analogy (SIMCA)

Soft independent modeling of class analogy (SIMCA) is used for the classification of samples according to the training sample data (Brereton, 2003; Alvarez-Ordóñez *et al*., 2012; Pirouette, Version 4.0, 2008). The SIMCA model is build based on the PCA of the training sample data (Al-Qadiri *et al*., 2008b; Alvarez-Ordóñez *et al*., 2012; Pirouette, Version 4.0, 2008). Although the main use of SIMCA is to predict correctly the class of unknown samples based on the training set, it is also possible to use this technique to analyze the important variables in the training sample (Brereton, 2003; Pirouette, Version 4.0, 2008). The distinct feature of SIMCA model is that, it is not a ridged model where unknown sample classified into a single class (Brereton, 2003; Pirouette, Version 4.0, 2008). In SIMCA prediction, there are three possibilities: the unknown sample fits only one of the pre-defined classes or the unknown sample does not fit in any of the pre-defined classes or the unknown sample fits into more than one pre-defined class (Pirouette, Version 4.0, 2008). SIMCA classification method has been reported by various authors as a tool to discriminate and classify different microorganisms based on their IR data (Kansiz *et al*., 1999; Lin *et al*., 2005; Subramanian *et al*., 2007; Al-Qadiri *et al*., 2008b; Grasso *et*

al., 2009; De Lamo-Castellví *et al*., 2010; De Lamo-Castellví and Rodriguez-Saona, 2011; Sundaram *et al*., 2012).

The main outputs are the interclass distances, class projections, misclassifications and the discriminating power (Brereton, 2003; Pirouette, Version 4.0, 2008). If the interclass distance value of two samples is above 3, the classes are considered as different classes (Brereton, 2003; Pirouette, Version 4.0, 2008). Class projection is a three-dimensional representation of the sample clusters where 95% probability clouds are built around the clusters based on PCA scores (Pirouette, Version 4.0, 2008). The measure of variable importance of the samples spectra is given by the discriminating power value (Brereton, 2003; Pirouette, Version 4.0, 2008). De Lamo-Castellví and Rodriguez-Saona, (2011) demonstrated the application of SIMCA for the discrimination of different strains of *Bacillus* spores. From the SIMCA model, three spectral bands at 1516, 1626 and 1724 cm^{-1} due to amide I, amide II and carbonic acids and esters from the spores coat protein were found to be the main contributors for the discrimination of *Bacillus* spores.

1.1.4.4. Partial Least Squares Regression (PLSR)

It is possible to predict IR spectral data quantitatively using a multivariate calibration method such as partial least squares regression (PLSR) based on reference data measured with a standard technique (Brereton, 2003; Al-Qadiri *et al*., 2008b; Pirouette, Version 4.0, 2008). In PLSR, the first step is the calibration process where predictive model using a training sample set is built. After the predictive model is built, it needs to be validated before using it for prediction (Pirouette, Version 4.0, 2008). PLSR analysis has been used to build calibration models based on FT-IR data by different researchers (Subramanian *et al*., 2006; Al-Qadiri *et al*., 2008b; Davis *et al*., 2010b). Al-Qadiri *et al*., (2008b) showed the possibility of using PLSR to predict the counts of sublethal injured *Salmonella enterica* serotype Typhimurium and *Listeria monocytogenes* after applying thermal treatments of 60^{o}C. They reported a high correlation coefficient (0.97 and

0.98) and a standard error of prediction (0.51 and 0.39 $\log_{10}$ CFU/mL) for *Salmonella enterica* serotype *typhimurium* and *Listeria monocytogenes* respectively (Al-Qadiri *et al*., 2008b).

1.1.5. State of the art of attenuated total reflectance (ATR) infrared spectroscopy

1.1.5.1. ATR-IR spectroscopy for the characterization of membrane fouling

For the characterization of membrane fouling, different techniques were listed in **Table 1.1.** In addition to these techniques, Fourier transform infrared (FTIR) spectroscopy has been used for the characterization of membrane fouling and cleaning (Belfer *et al*., 2000; Rabiller-Baudry *et al*., 2002; Nataraj *et al*., 2008). Zhu and Nyström, (1998) used FTIR to study the efficiency of a chemical cleaning used to remove fouled proteins (bovine serum albumin and lysozyme) on polysulfone membranes. The effectiveness of the chemical cleaning techniques was studied by comparing the IR spectral bands of the cleaned membrane after fouling and the virgin membranes. In their investigation, it is confirmed that the protein foulants are not totally removed from the membrane by the chemical cleanings (Zhu and Nyström, 1998). Moreover, Meng *et al*.(2010) reviewed the spectroscopic techniques used on MBR characterization, compared them with microscopic techniques and reported the advantages and their limitations (Meng *et al*., 2010). Generally, most of the researchers used FTIR techniques for the qualitative characterization of membrane fouling and surface (Zhu and Nyström, 1998; Belfer *et al*., 2000; Rabiller-Baudry *et al*., 2002; Nataraj *et al*., 2008). However, Delaunay and coworker (2008) used ATR-FTIR to report the quantitative analysis of membrane fouling (Delaunay *et al*., 2008). In their study, polyethersulfone (PES) or polysulfone (PSU) were used as an active layer or the intermediate one in the membrane composition. Using the height ratio of two targeted IR bands, 1539 cm^{-1} related to amide II vibration of proteins and 1240 cm^{-1} characteristic of the PES membrane, the fouling of protein was quantified (Delaunay *et al*., 2008). Recently, Diagne *et al*. (2013) used a similar procedure and studied the cleaning efficiency of fouled polyethersulfone (PES) membranes during the ultrafiltration of skimmed milk (Diagne *et al*.,

2013). The main advantage of FTIR over the other microscopy techniques is that, it provides information regarding the chemical structure and the chemical composition of the membrane surface (Delaunay *et al*., 2008; Nataraj *et al*., 2008; Meng *et al*., 2010). Moreover, it is possible to test the presence/absence of specific functional groups of the foulants on the membrane surface. It is also a non-destructive surface-sensitive technique. The other advantage is that, little or no sample pretreatment is required for its analysis (Zhu and Nyström, 1998; Chan and Chen, 2004; Delaunay *et al*., 2008; Nataraj *et al*., 2008; Meng *et al*., 2010; Diagne *et al*., 2013).

1.1.5.2. ATR-IR spectroscopy for the detection of microorganisms

Infrared spectroscopy has been used for microbiology analysis since 1950s when Goulden and Sharpe (1958) used this technology to classify a number of *Lactobacillus* species. In 1962, Scopes used IR spectroscopy (dispersive spectrometer) to discriminate acetic acid bacteria finding that the spectra of 22 strains of *Acetobacter* were different from that of 9 strains of *Acetomonas*. The lack of spectrum libraries and computer aided searching procedures limited the use of infrared spectroscopy for the identification and classification of microorganisms (Helm *et al*., 1991). Infrared spectroscopy starting having popularity with the development of spectrometer with an interferometer and the mathematical algorism of Fourier Transform (FT) with the assistance of computers (Naumann *et al*., 1982; Naumann *et al*., 1988; Helm *et al*., 1991; Mariey *et al*., 2001). The development of different sampling methods and also the use of different multivariate analysis helped the extraction of qualitative/quantitative information from the IR spectra, FTIR spectroscopy obtained recognitions among scientists. Since then, several researchers reported the use of FT-IR for the detection and classification of different microorganisms (Naumann *et al*., 1995; Goodacre *et al*., 1996; Kansiz *et al*., 1999; Naumann, 2001; Rodriguez-Saona *et al*., 2001; Grasso *et al*., 2009; De Lamo-Castellví *et al*., 2010; Preisner *et al*., 2010; De Lamo-Castellví and Rodriguez-Saona, 2011; Wang *et al*., 2011).

Nowadays, attenuated total reflectance (ATR) Fourier transform infrared (FTIR) spectroscopy is more preferable than transmission infrared spectroscopy, since no/little sample preparation is required for ATR- IR. Different scientists have used this advantage of ATR-IR spectroscopy to discriminate and identificatefoodborne pathogens (Lin *et al*., 2004; Lin *et al*., 2005; Al-Holy *et al*., 2006; Al-Qadiri *et al.*, 2006; Subramanian *et al*., 2006; Al-Qadiri *et al*., 2008a; Al-Qadiri *et al*., 2008b; Wang *et al*., 2011; Davis *et al*., 2012). Lin *et al*. (2005) used ATR-FTIR spectroscopy combined with multivariate statistical analysis technique for the discrimination of strains of *Alicyclobacillus* bacteria in apple juice. The second derivative of the spectra showed the strain dependence difference although two strains had similar spectral features. The authors used principal component analysis and the results proofed the similarities of the two strains (Lin *et al*. 2005).

Several researchers has been reported the use of Fourier-transform infrared microspectroscopy as a rapid technique for the identification and detection of different microorganisms (Wenning *et al*., 2006; Janbu *et al*., 2008; Grasso *et al*., 2009; De Lamo-Castellví *et al*., 2010; De Lamo-Castellví and Rodriguez-Saona, 2011; Davis *et al*., 2012). For instance, Janbu *et al*. (2008) investigated the potential application of FTIR microspectroscopy combined with multivariate analysis to identify species of *Listeria*. These authors stated that the greater variation was mainly observed in the polysaccharide region of the spectra (1200-900 cm^{-1}).

In addition to the classification and discrimination of foodborne pathogens at strain and serovar level, some researchers have reported the use of FTIR spectroscopy to detect the effect of different inactivation methods and antimicrobial compounds. The detection of the cellular structure modification by the application of thermal inactivation (Subramanian *et al*., 2007; Alvarez-Ordóñez and Prieto, 2010; Davis *et al*., 2010a), high pressure and pressure-assisted thermal processing (Subramanian *et al*., 2006; Subramanian *et al*., 2007), cold stress (Lu *et al*., 2010), antimicrobial compounds (Al-Qadiri *et al*., 2008a; Motta *et al*., 2008; Alvarez-Ordóñez *et al*., 2010; Zoumpopoulou *et al*., 2010) have been studied.

Table1.7. *Tentative assignment of FTIR spectra bands frequently found in microorganisms (4000-800 cm^{-1}) (adapted from Naumann, 2006; Lu et al., 2010; Alvarez-Ordóñez et al., 2011).*

Wavenumbers (cm^{-1})	**Assignment**
~3285	N-H streching of proteins and O-H streching of polysaccharides and water
~2966	C-H streching (asym.) of $-CH_3$ in fatty acids
~2929	C-H streching (asym.) of $>CH_2$ in fatty acids
~2852	C-H streching (sym.) of $>CH_2$ in fatty acids
~1740	>C=O streching of esters
~1715	>C=O streching of carbonic acid
~1695	Amide I band component
~1685	>C=O in nucleic acid
~1655	Amide I of α-helical structures
~1637	Amide I of β-pleated sheet structures
~1620	Streching base carbonyl and ring breathing mode of nucleic acid
~1550-1515	Amide II
~1469	CH_2 bending of the acyl chains (phospholipids)
~1458	C-H def of $>CH_2$ of proteins
~1395	C=O streching (sym.) of COO^- of proteins
~1235	P=O streching (asym.) of $>PO_2^-$ phosphodiesters
~1161	Streching C-OH of serine, threonine, and tyrosine residues of cellular
~1080	P=O streching (sym.) of $>PO_2^-$ in nucleic acid
1200-900	C-O-C of polysaccharide and, streching of phosphate
~1150	C-O streching of carbohydrate
~1078	C-OH streching of oligosaccharide
~1028	$-CH_2OH$ and C-O streching coupled with C-O bending of carbohydrate
1800-800	"Fingerprint" region

As we aforementioned in the section 1.1.2, the presence of injured pathogenic microorganisms in the food sample is considered a threat for food safety due to the fact that if the environment becomes suitable, the microorganism can start growing and multiplying (Lin *et al*., 2004; Al-Qadiri *et al*., 2008b). Several authors have proved the suitability of FTIR spectroscopy to detect the physiological state of different foodborne pathogens treated with different food preservation methods (Lin *et al*., 2004; Al-Qadiri *et al*., 2008b; Davis *et al*., 2010b; Sundaram *et*

al., 2012). Using FTIR made possible to obtain information about the mechanism involved on bacteria, yeast and spores inactivation by several treatments (Lin *et al*., 2004; Al-Qadiri *et al*., 2008b). Sundaram *et al*. (2012) were able to distinguish live and dead *S.* Typhimurium and *S.* Enteritidis cells treated by heat (100 ^{o}C) using FTIR spectroscopy. The maximum differences among alive and the dead cells were recorded in the spectral region of 1500 to 900 cm^{-1} (P=O and C-O-C stretching modes of polysaccharides and lipopolysaccharide, respectively). Similarly, Al-Qadiri *et al*. (2008b) reported the detection of sublethal heat injured *S.* Typhimurium and *L. monocytogenes* using this technique (Al-Qadiri *et al.,* 2008b).

All these investigations showed the potential of using FTIR spectroscopy as a rapid, non-destructive and easy technique for the classification and identification of different microorganisms. Moreover, some authors used FTIR spectroscopy for the detection of the extent of cellular injuries of foodborne pathogens produced by the application of different food preservation techniques.

1.2. OBJECTIVES

The main objectives of this dissertation were:

- To apply attenuated total reflectance infrared microspectroscopy (ATR-IRMS) combined with multivariate analysis for the characterization of membrane fouling and to study the efficiency of different cleaning protocols used to remove foulant residues remaining on the membrane.
- To evaluate the application of attenuated total reflectance infrared microspectroscopy (ATR-IRMS) combined with multivariate analysis to detect and discriminate different microorganisms and evaluate their physiological state.

These two main objectives were accomplished based on the following five specific objectives:

- Discriminate *Saccharomyces cerevisiae* and acetic acid bacteria (*Gluconacetobacter xylinus* and *Gluconobacter oxydans*) using ATR-IRMS combined with soft independent modeling of class analogy (SIMCA)
- Detect and discriminate inactivated *Escherichia coli* O157:H7 cells by thermal and pulsed electric field treatments using ATR-IRMS combined with soft independent modeling of class analogy (SIMCA)
- Predict the inactivated bacterial cell counts from ATR-IRMS spectral data using partial least squares regression (PLSR)
- Evaluate the application of ATR-IRMS combined with SIMCA to characterize membrane fouling
- Determine the cleaning efficiency of different cleaning protocols using the conventional method (flux) and the ATR-IRMS spectral data

1.3. REFERENCES

Abadias, M.; Usall J.; Anguera M.; Solsona C.; Viñas, I. Microbiological quality of fresh, minimally-processed fruit and vegetables, and sprouts from retail establishments. *International Journal of Food Microbiology* **2008,** 123, 121-129.

Al-Amoudi, A.; Lovitt, R. W. Fouling strategies and the cleaning system of NF membranes and factors affecting cleaning efficiency. *Journal of Membrane Science* **2007,** 303, (1-2), 4-28.

Allerberger, F.; Al-Jazrawi, N.; Kreidl, P.; Dierich, M.P.; Feierl, G.; Hein, I.; Wagner, M. Barbecued chicken causing a multi-state outbreak of *Campylobacter jejuni* enteritis. *Infection* **2003,** 31, (1), 19-23.

Al-Holy, M.A.; Lin, M.; Cavinato, A.G.; Rasco, B.A. The use of Fourier transform infrared spectroscopy to differentiate *Escherichia coli* O157:H7 from other bacteria inoculated into apple juice. *Food Microbiology* **2006,** 23, (2), 162-168.

Al-Qadiri, H.M.; Lin, M.S.; Cavinato, A.G.; Rasco, B.A. Fourier transform infrared spectroscopy, detection and identification of *Escherichia coli* O157: H7 and *Alicyclobacillus* strains in apple juice. *International Journal of Food Microbiology* **2006,** 111, (1), 73-80

Al-Qadiri, H.M.; Al-Alami, N.I.; Al-Holy, M.A.; Rasco, B.A. Using Fourier transform infrared (FT-IR) absorbance spectroscopy and multivariate analysis to study the effect of chlorine-induced bacterial injury in water. *Journal of Agricultural and Food Chemistry* **2008a,** 56, (19), 8992-8997.

Al-Qadiri, H.M.; Lin, M.; Al-Holy, M.A.; Cavinato, A.G.; Rasco, B.A. Detection of sublethal thermal injury in *Salmonella enterica* serotype *typhimurium* and *Listeria monocytogenes* using Fourier transform infrared (FT-IR) spectroscopy (4000 to 600 cm^{-1}). *Journal of Food Science* **2008b,** 73, (2), 54-61.

Alocilja E.C.; Radke S.M. Market analysis of biosensors for food safety. *Biosensors and Bioelectronics* **2003**, (18), 841- 846.

Alvarez-Ordonez, A.; Prieto, M. Changes in Ultrastructure and Fourier transform infrared spectrum of *Salmonella enterica* serovar *typhimurium* cells after exposure to stress conditions. *Applied and Environmental Microbiology* **2010,** 76, (22), 7598-7607.

Alvarez-Ordonez, A.; Mouwen, D.J.M.; Lopez, M.; Prieto, M. Fourier transform infrared spectroscopy as a tool to characterize molecular composition and stress response in foodborne pathogenic bacteria. *Journal of Microbiological Methods* **2011,** 84, (3), 369-378.

Alvarez-Ordonez, A.; Prieto, M. Technical and methodological aspects of Fourier transform infrared spectroscopy in food microbiology Research. In *Fourier Transform Infrared Spectroscopy in Food Microbiology*, Springer US: **2012**; pp 1-18.

Arnandis-Chover, T.; Morais, S.; Tortajada-Genaro, L.A.; Puchades, R.; Maquieira, Á.; Berganza, J.; Olabarria, G. Detection of food-borne pathogens with DNA arrays on disk. *Talanta* **2012,** (101),405-412.

Baldauf, N.A.; Rodriguez-Romo, L.A.; Mannig, A.; Yousef, A.E.; Rodriguez-Saona, L.E. Effect of selective growth media on the differentiation of *Salmonella* enterica serovars by Fourier-transform mid-infrared spectroscopy. *Journal of Microbiological Methods* **2007,** 68, (1), 106-114.

Baker, J.S.; Dudley, L.Y. Biofouling in membrane systems-A review. *Desalination* **1998,** 118, (1-3), 81-89.

Beebe, K.R., Pell, R.J., Seasholtz, M.B. Chemometrics: A pactical guide, Johan Wiley & Sons: New York, **1998**.

Belfer, S.; Fainchtain, R.; Purinson, Y.; Kedem, O. Surface characterization by FTIR-ATR spectroscopy of polyethersulfone membranes-unmodified, modified and protein fouled. *Journal of Membrane Science* **2000,** 172, (1-2), 113-124.

Bosilevac, J.M.; Koohmaraie, M. Prevalence and characterization of non-O157 shiga toxin-producing *Escherichia coli* isolates from commercial ground beef in the United States. *Applied and Environmental Microbiology* **2011,** 77, (6), 2103-2112.

Brereton, R.G. *Chemometrics: Data analysis for the laboratory and chemical plant.* John Wiley & Sons, Ltd.: Chichester, England, **2003**.

Brooks, B.W.; Devenish, J.; Lutze-Wallace, C.L.; Milnes, D.; Robertson, R.H.; Berlie-Surujballi, G. Evaluation of a monoclonal antibody-based enzyme-linked immunosorbent assay for detection of *Campylobacte*r fetus in bovine preputial washing and vaginal mucus samples. *Veterinary Microbiology* **2004,** 103, (1-2), 77-84.

Burgula, Y.; Khali, D.; Kim, S.; Krishnan, S.S.; Cousin, M.A.; Gore, J.P.; Reuhs, B.L.; Mauer, L.J. Review of mid-infrared Fourier transform-infrared spectroscopy applications for bacterial detection. *Journal of Rapid Methods & Automation in Microbiology* **2007,** 15, (2), 146-175.

Camps, N.; Dominguez, A.; Company, M.; Perez, M.; Pardos, J.; Llobet, T.; Usera, M.A.; Salleras L. *et al.* A foodborne outbreak of *Salmonella* infection due to overproduction of egg-containing foods for a festival. *Epidemiology and Infection* **2005**, 133, (05), 817-822.

Centers for Disease Control and Prevention (CDC). *Salmonella*–Investigation final update: Outbreak of *Salmonella* Typhimurium infections, 2008–2009: Available at: http://www.cdc.gov/salmonella/typhimurium/update.html#outbreakinvestigation. Accessed 27 Feb. 2013.

Centers for Disease Control and Prevention (CDC). Surveillance for foodborne disease outbreaks - United States, 2009–2010.*Morbidity and Mortality Weekly Report*, **2013**, 62(3), 41-60.

Ceuppens, S.; Boon, N.; Rajkovic, A.; Heyndrickx, M.; Van de Wiele, T.; Uyttendaele, M. Quantification methods for *Bacillus cereus* vegetative cells and spores in the gastrointestinal environment. *Journal of Microbiological Methods* **2010,** 83, (2), 202-210.

Chai, L.C.; Robin, T.; Ragavan, U.M.; Gunsalam, J.W.; Bakar, F.A.; Ghazali, F.M.; Radu, S.; Kumar, M.P. Thermophilic *Campylobacter* spp. in salad vegetables in Malaysia. *International Journal of Food Microbiology* **2007,** 117, (1), 106-111.

Chan, S.F.; Chan, Z.C.Y. A review of foodborne disease outbreaks from 1996 to 2005 in Hong Kong and its implications on food safety promotion. *Journal of Food Safety* **2008,** 28, (2), 276-299.

Chan, R.; Chen, V. Characterization of protein fouling on membranes: opportunities and challenges. *Journal of Membrane Science* **2004,** 242, (1-2), 169-188.

Chang, I.; Le Clech, P.; Jefferson, B.; Judd, S. Membrane fouling in membrane bioreactors for wastewater treatment. *Journal of Environmental Engineering* **2002,** 128, (11), 1018-1029.

Charcosset, C.; Bernengo, J.-C. Comparison of microporous membrane morphologies using confocal scanning laser microscopy. *Journal of Membrane Science* **2000,** 168, (1-2), 53-62.

Charcosset, C.; Limayem, I.; Fessi, H. The membrane emulsification process-a review. *Journal of Chemical Technology & Biotechnology* **2004,** 79, (3), 209-218.

Charcosset, C. Membrane systems and technology: In Murray M.Y. (Ed) *Comprehensive Biotechnology (Second Edition),* Academic Press, Burlington, **2011**, pp. 603-618.

Cheetangdee, N.; Fukada, K., Protein stabilized oil-in-water emulsions modified by uniformity of size by premix membrane extrusion and their colloidal stability. *Colloids and Surfaces A: Physicochemical and Engineering Aspects* **2012,** 403, 54-61.

Chemburu, S.; Wilkins, E.; Abdel-Hamid, I. Detection of pathogenic bacteria in food samples using highly-dispersed carbon particles. *Biosensors and Bioelectronics* **2005,** 21, (3), 491-499.

Chen, Y.; Knabel, S. J. Multiplex PCR for simultaneous detection of bacteria of the genus *Listeria*, *Listeria monocytogenes*, and major serotypes and epidemic clones of *L.. monocytogenes*. *Applied and Environmental Microbiology* **2007,** 73, (19), 6299-6304.

Christison, C.A.; Lindsay, D.; von Holy, A. Microbiological survey of ready-to-eat foods and associated preparation surfaces in retail delicatessens, Johannesburg, South Africa. *Food Control* **2008,** 19, (7), 727-733.

Coates, J. Interpretation of infrared spectra, a practical approach. In *Encyclopedia of Analytical Chemistry*, John Wiley & Sons, Ltd: **2006**.

Costa, A.R.; de Pinho, M.N.; Elimelech, M. Mechanisms of colloidal natural organic matter fouling in ultrafiltration. *Journal of Membrane Science* **2006,** 281, (1-2), 716-725.

Dao, H.T.A.; Yen, P.T. Study of *Salmonella*, *Campylobacter*, and *Escherichia coli* contamination in raw food available in factories, schools, and hospital canteens in Hanoi, Vietnam. *Annals of the New York Academy of Sciences* **2006,** 1081, (1), 262-265.

Davis, R.; Burgula, Y.; Deering, A.; Irudayaraj, J.; Reuhs, B.L.; Mauer, L.J. Detection and differentiation of live and heat-treated *Salmonella* enterica serovars inoculated onto chicken breast using fourier transform infrared (FT-IR) spectroscopy. *Journal of Applied Microbiology* **2010a,** 109, (6), 2019-2031.

Davis, R.; Irudayaraj, J.; Reuhs, B. L.; Mauer, L. J. Detection of *E. coli* O157:H7 from ground beef using Fourier transform infrared (FT-IR) spectroscopy and chemometrics. *Journal of Food Science* **2010b,** 75, (6), 340-346.

De Boer, E.; Beumer, R.R. Methodology for detection and typing of foodborne microorganisms. *International Journal of Food Microbiology* **1999,** 50, (1-2), 119-130.

De Bruijn, J.; Venegas, A.; Borquez, R. Influence of crossflow ultrafiltration on membrane fouling and apple juice quality. *Desalination* **2002,** 148, (1-3), 131-136.

De Lamo-Castellvi, S.; Manning, A.; Rodriguez-Saona, L.E. Fourier-transform infrared spectroscopy combined with immunomagnetic separation as a tool to discriminate *Salmonella* serovars. *Analyst* **2010,** 135, (11), 2987-2992.

De Lamo-Castellví, S.; Rodríguez-Saona, L.E. Use of attenuated total reflectance infrared microspectroscopy to discriminate *Bacillus* spores. *Journal of Food Safety* **2011,** 31, (3), 401-407.

Delaunay, D.; Rabiller-Baudry, M.; Gozálvez-Zafrilla, J.M.; Balannec, B.; Frappart, M.; Paugam, L. Mapping of protein fouling by FTIR-ATR as experimental tool to study membrane fouling and fluid velocity profile in various geometries and validation by CFD simulation. *Chemical Engineering and Processing: Process Intensification* **2008,** 47, (7), 1106-1117.

De Maesschalck, R.; Candolfi, A.; Massart, D.L.; Heuerding, S. Decision criteria for soft independent modelling of class analogy applied to near infrared data. *Chemometrics and Intelligent Laboratory Systems* **1999,** 47, (1), 65-77.

Diagne, W.N.; Rabiller-Baudry, M.; Paugam, L. On the actual clean-ability of polyethersulfone membrane fouled by proteins at critical or limiting flux. *Journal of Membrane Science* **2013,** 425-426, 40-47

Dunn, W.J., Wold, S. SIMCA pattern recognition and classification: In van de Waterbeemd H. (Ed) *Chemometric Methods in Molecular Design*. VCH Publishers, New York, NY. **1995**; pp. 179–193.

Ellis, D.I.; Goodacre, R. Rapid and quantitative detection of the microbial spoilage of muscle foods: current status and future trends. *Trends in Food Science & Technology* **2001,** 12, (11), 414-424.

Elviss, N.C.; Little, C.L.; Hucklesby, L.; Sagoo, S.; Surman-Lee, S.; de Pinna, E.; Threlfall, E.J. Microbiological study of fresh herbs from retail premises uncovers an international outbreak of *Salmonellosis*. *International Journal of Food Microbiology* **2009,** 134, (1-2), 83-88.

Elmerdahl Olsen, J. DNA-based methods for detection of food-borne bacterial pathogens. *Food Research International* **2000,** 33, (3-4), 257-266.

Emberland K.E.; Ethelberg S.; Kuusi M.; Vold, L.; Jensvoll, L.; Lindstedt, B.A.; Nygard , K.; Kjelsø, C.; Torpdahl, M.; Sørensen, G.; Jensen, T.; Lukinmaa, S.; Niskanen, T.; Kapperud, G. Outbreak of *Salmonella weltevreden* infections in Norway, Denmark and Finland associated with alfalfa sprouts, July-October 2007. *Euro Surveill* **2007**, 12, (48).

Esteban, J.I.; Oporto, B.; Aduriz, G.; Juste, R. A.; Hurtado, A. A survey of food-borne pathogens in free-range poultry *farms. International Journal of Food Microbiology* **2008,** 123, (1-2), 177-182.

Esteves, A.; Patarata, L.; Saraiva, C.; Martins, C. Assessment of the microbiological characteristics of industrially produced alheira, with particular reference to foodborne pathogens. *Journal of Food Safety* **2008,** 28, (1), 88-102.

Félix-Rivera, H.; Hernández-Rivera, S. Raman spectroscopy techniques for the detection of biological samples in suspensions and as aerosol particles: A Review. *Sensing and Imaging: An International Journal* **2011,** 13, (1), 1-25.

Ferrando, M.; Rŏzek, A.; Zator, M.; López, F.; Güell, C. An approach to membrane fouling characterization by confocal scanning laser microscopy. *Journal of Membrane Science* **2005,** 250, (1-2), 283-293.

Flemming, H.C.; Schaule, G.; Griebe, T.; Schmitt, J.; Tamachkiarowa, A. Biofouling-the Achilles heel of membrane processes. *Desalination* **1997,** 113, (2-3), 215-225.

Flemming, H.C. Biofouling in water systems -cases, causes and countermeasures. *Applied Microbiology and Biotechnology* **2002,** 59, (6), 629-640.

Frank, C.; Buchholz, U.; MaaSz, M.; Schroder, A.; Bracht, K.-H.; Domke, P.-G.; Rabsch, W.; Fell, G. Protracted outbreak of *Salmonella enteritidis* PT 21c in a large Hamburg nursing home. *BMC Public Health* **2007,** 7, (1), 243.

Frank C.; Faber M.S .; Askar M.; Bernard H.; Fruth A.; Gilsdorf A.; Höhle M; Karch H.; Krause G.; Prager R.; Spode A.; Stark K.; Werber D.; On behalf of the HUS investigation team. Large and ongoing outbreak of haemolytic uraemic syndrome, Germany, May 2011. *Euro Surveill* **2011**; 16 (21).

Friesema, I.H.; de Jong, A.E.; Fitz James, I.A.; Heck, M.E.; van den Kerkhof, J.H.; Notermans, D.W.; van Pelt, W.; Hofhuis, A. Outbreak of *Salmonella* Thompson in the Netherlands since July 2012. *Euro Surveill* **2012**; 17(43).

Fung, D.Y.C. Rapid methods and automation in food microbiology: A review. *Food Reviews International* **1994,** 10, (3), 357-375.

Fung, D.Y.C. Rapid methods and automation in microbiology. *Comprehensive Reviews in Food Science and Food Safety* **2002,** 1, (1), 3-22.

Gallay, A.; Bousquet, V.; Siret, V.; Prouzet-Mauléon, V.; de Valk, H.; Vaillant, V.; Simon, F.; Le Strat, Y.; Mégraud, F.; Desenclos, J.-C. Risk factors for acquiring sporadic *Campylobacter* infection in France: results from a national case-control study. *Journal of Infectious Diseases* **2008,** 197, (10), 1477-1484.

Gehring, A.G.; Irwin, P.L.; Reed, S.A.; Tu, S-I. Enzyme-linked immunimagnetic chemiluminescence incorporating anti-H7 and anti-O157 antibodies for the detection of *Escherichia coli* O157:H7. *Journal of Rapid Methods & Automation in Microbiology* **2006,** 14, (4), 349-361.

Germini, A.; Masola, A.; Carnevali, P.; Marchelli, R. Simultaneous detection of *Escherichia coli* O175:H7, *Salmonella* spp., and *Listeria monocytogenes* by multiplex PCR. *Food Control* **2009,** 20, (8), 733-738.

Gottlieb, S. L.; Newbern, E. C.; Griffin, P. M.; Graves, L. M.; Hoekstra, R. M.; Baker, N. L.; Hunter, S. B.; Holt, K. G.; Ramsey, F.; Head, M.; Levine, P.; Johnson, G.; Schoonmaker-Bopp, D.; Reddy, V.; Kornstein, L.; Gerwel, M.; Nsubuga, J.; Edwards, L.; Stonecipher, S.; Hurd, S.; Austin, D.; Jefferson, M. A.; Young, S. D.; Hise, K.; Chernak, E. D.; Sobel, J.; Listeriosis Outbreak Working, G. Multistate outbreak of *Listeriosis* linked to turkey deli meat and subsequent changes in us regulatory Policy. *Clinical Infectious Diseases* **2006,** 42, (1), 29-36.

Goulden, J.D.S.; Sharpe, M.E. The infra-red absorption spectra of *Lactobacilli*. *Journal of General Microbiology* **1958,** 19, (1), 76-86.

Grasso, E.M.; Yousef, A.E.; De Lamo Castellvi, S.; Rodriguez-Saona, L.E. Rapid detection and differentiation of *Alicyclobacillus* species in fruit juice using hydrophobic grid membranes and attenuated total reflectance infrared microspectroscopy. *Journal of Agricultural and Food Chemistry* **2009,** 57, (22), 10670-10674.

Griffiths P.; de Haseth, J. A. Fourier transform infrared spectrometry. 2nd Edition ; John Wiley & Sons, Inc.: New York, **2007**.

Grossi, M.; Lanzoni, M.; Pompei, A.; Lazzarini, R.; Matteuzzi, D.; Riccó, B. Detection of microbial concentration in ice-cream using the impedance technique. *Biosensors and Bioelectronics* **2008,** 23, (11), 1616-1623.

Gunasekera, T.S.; Veal, D.A.; Attfield, P.V. Potential for broad applications of flow cytometry and fluorescence techniques in microbiological and somatic cell analyses of milk. *International Journal of Food Microbiology* **2003,** 85, (3), 269-279.

Güell, C.; Davis, R.H. Membrane fouling during microfiltration of protein mixtures. *Journal of Membrane Science* **1996,** 119, (2), 269-284.

Güell C.; Ferrando M.; López, F. Confocal scanning laser microscopy: fundamentals and uses on membrane fouling characterization and opportunities for online monitoring: In Güell C.; Ferrando M.; López, F. (Eds) *Monitoring and Visualzing Membrane-Based Process*, Wiley VCH Verlag GmbH &Co. KGaA: Weinheim; **2009**, pp 55-75.

Haaland, D.M.; Thomas, E.V. Partial least-squares methods for spectral analyses. Relation to other quantitative calibration methods and the extraction of qualitative information. *Analytical Chemistry* **1988,** 60, (11), 1193-1202.

Hilal, N.; Johnson, D. The use of atomic force microscopy in membrane characterization: In Enrico, D.; Lidietta, G.(Eds) *Comprehensive Membrane Science and Engineering*, Elsevier: Oxford, **2010**; pp 337-354.

Ho, C.-C.; Zydney, A.L. Effect of membrane morphology on the initial rate of protein fouling during microfiltration. *Journal of Membrane Science* **1999,** 155, (2), 261-275.

Hussain, I.; Shahid Mahmood, M.; Akhtar, M.; Khan, A. Prevalence of *Campylobacter* species in meat, milk and other food commodities in Pakistan. *Food Microbiology* **2007,** 24, (3), 219-222.

Iqbal, S.S.; Mayo, M.W.; Bruno, J.G.; Bronk, B.V.; Batt, C.A.; Chambers, J.P. A review of molecular recognition technologies for detection of biological threat agents. *Biosensors and Bioelectronics* **2000,** 15, (11-12), 549-578.

Ivnitski, D.; Abdel-Hamid, I.; Atanasov, P.; Wilkins, E. Biosensors for detection of pathogenic bacteria. *Biosensors and Bioelectronics* **1999,** 14, (7), 599-624.

Ivnitsky, H.; Katz, I.; Minz, D.; Shimoni, E.; Chen, Y.; Tarchitzky, J.; Semiat, R.; Dosoretz, C.G. Characterization of membrane biofouling in nanofiltration processes of wastewater treatment. *Desalination* **2005,** 185, (1-3), 255-268.

Jaggi N.; Vij D.R. Fourier transform infrared spectroscopy: In Vij D.R. (Ed) Handbook of applied solid state spectroscopy. 1st edition, *Springer*, New York, NY, **2006**; 411 - 450.

Janbu, A.O.; Møretrø, T.; Bertrand, D.; Kohler, A. FT-IR microspectroscopy: a promising method for the rapid identification of *Listeria* species. *FEMS Microbiology Letters* **2008,** 278, (2), 164-170.

Jasson, V.; Jacxsens, L.; Luning, P.; Rajkovic, A.; Uyttendaele, M. Alternative microbial methods: An overview and selection criteria. *Food Microbiology* **2010,** 27, (6), 710-730.

Joscelyne, S.M.; Trägårdh, G. Membrane emulsification- a literature review. *Journal of Membrane Science* **2000,** 169, (1), 107-117.

Kansiz, M.; Heraud, P.; Wood, B.; Burden, F.; Beardall, J.; McNaughton, D. Fourier transform infrared microspectroscopy and chemometrics as a tool for the discrimination of cyanobacterial strains. *Phytochemistry* **1999,** 52, (3), 407-417.

Karbstein, H.; Schubert, H. Developments in the continuous mechanical production of oil-in-water macro-emulsions. *Chemical Engineering and Processing: Process Intensification* **1995,** 34, (3), 205-211.

Katoh, R.; Asano, Y.; Furuya, A.; Sotoyama, K.; Tomita, M. Preparation of food emulsions using a membrane emulsification system. *Journal of Membrane Science* **1996,** 113, (1), 131-135.

Khaitsa M.L.; Kegode R.B.; Doetkott, D.K. Occurrence of antimicrobial-resistant *Salmonella* species in raw and ready to eat turkey meat products from retail outlets in the Midwestern United States. *Foodborne Pathogens and Disease* **2007,** 4, (4), 517-525.

Kim, S.; Reuhs, B.L.; Mauer, L.J. Use of Fourier transform infrared spectra of crude bacterial lipopolysaccharides and chemometrics for differentiation of *Salmonella enterica* serotypes. *Journal of Applied Microbiology* **2005,** 99, (2), 411-417.

Kiess, A.S.; Kenney, P.B.; Nayak, R.R. *Campylobacter* detection in commercial turkeys. *British Poultry Science* **2007,** 48, (5), 567-572.

Knutson, H.J.; Carr, M.A.; Branham, L.A.; Scott, C.B.; Callaway, T.R. Effects of activated charcoal on binding *E. coli* O157:H7 and *Salmonella typhimurium* in sheep. *Small Ruminant Research* **2006,** 65, (1-2), 101-105.

Kumar, R.; Surendran, P.K.; Thampuran, N. Evaluation of culture, ELISA and PCR assays for the detection of *Salmonella* in seafood. *Letters in Applied Microbiology* **2008,** 46, (2), 221-226.

Kwon, B.; Cho, J.; Park, N.; Pellegrino, J. Organic nanocolloid fouling in UF membranes. *Journal of Membrane Science* **2006,** 279, (1-2), 209-219.

Laouini, A.; Fessi, H.; Charcosset, C. Membrane emulsification: A promising alternative for vitamin E encapsulation within nano-emulsion. *Journal of Membrane Science* **2012**, 423-424, (0), 85-96.

Lazcka, O.; Campo, F.J.D.; Muñoz, F.X. Pathogen detection: A perspective of traditional methods and biosensors. *Biosensors and Bioelectronics* **2007,** 22, (7), 1205-1217.

Le-Clech, P.; Marselina, Y.; Ye, Y.; Stuetz, R.M.; Chen, V. Visualisation of polysaccharide fouling on microporous membrane using different characterisation techniques. *Journal of Membrane Science* **2007,** 290, (1-2), 36-45.

Leonard, P.; Hearty, S.; Quinn, J.; O'Kennedy, R. A generic approach for the detection of whole *Listeria monocytogenes* cells in contaminated samples using surface plasmon resonance. *Biosensors and Bioelectronics* **2004,** 19, (10), 1331-1335.

Leon-Velarde, C.G.; Zosherafatein, L.; Odumeru, J.A. Application of an automated immunomagnetic separation-enzyme immunoassay for the detection of *Salmonella* enterica subspecies enterica from poultry environmental swabs. Journal of Microbiological Methods **2009,** 79, (1), 13-17.

Li, H.; Chen, V. Membrane fouling and cleaning in food and bioprocessing. In: Cui, Z.F.; Muralidhara, H.S. (Eds) *Membrane Technology*, Butterworth-Heinemann: Oxford, **2010**; pp 213-254.

Lim, A.L.; Bai, R. Membrane fouling and cleaning in microfiltration of activated sludge wastewater. *Journal of Membrane Science* **2003,** 216, (1-2), 279-290.

Lin, M.S.; Al-Holy, M.; Al-Qadiri, H.; Kang, D.H.; Cavinato, A.G.; Huang, Y.Q.; Rasco, B.A. Discrimination of intact and injured *Listeria monocytogenes* by Fourier transform infrared spectroscopy and principal component analysis. *Journal of Agricultural and Food Chemistry* **2004,** 52, (19), 5769-5772.

Lin, M.; Al-Holy, M.; Chang, S.-S.; Huang, Y.; Cavinato, A.G.; Kang, D.-H.; Rasco, B.A. Rapid discrimination of *Alicyclobacillus* strains in apple juice by Fourier transform infrared spectroscopy. *International Journal of Food Microbiology* **2005,** 105, (3), 369-376.

Little, C.L.; Rhoades, J.R.; Sagoo, S.K.; Harris, J.; Greenwood, M.; Mithani, V.; Grant, K.; McLauchlin, J. Microbiological quality of retail cheeses made from raw, thermized or pasteurized milk in the UK. *Food Microbiology* **2008a,** 25, (2), 304-312.

Little, C.L.; Richardson, J.F.; Owen, R.J.; de Pinna, E.; Threlfall, E.J. *Campylobacter* and *Salmonella* in raw red meats in the United Kingdom: Prevalence, characterization and antimicrobial resistance pattern, 2003-2005. *Food Microbiology* **2008b,** 25, (3), 538-543.

López-Campos, G.; Martínez-Suárez, J.; Aguado-Urda, M.; López-Alonso, V. Detection, identification, and analysis of foodborne pathogens. In *Microarray detection and characterization of bacterial foodborne pathogens*, Springer US: **2012**; pp 13-32.

Lu, X.; Liu, Q.; Wu, D.; Al-Qadiri, H.M.; Al-Alami, N.I.; Kang, D.-H.; Shin, J.-H.; Tang, J.; Jabal, J.M.F.; Aston, E.D.; Rasco, B.A. Using of infrared spectroscopy to study the survival and injury of *Escherichia coli* O157:H7, *Campylobacter jejuni* and *Pseudomonas aeruginosa* under cold stress in low nutrient media. Food Microbiology **2010,** 28, (3), 537-546.

Mackey, B.M. Injured bacteria: In Lund, B.; Baird-Parker, A.C.; Gould, G.W. (Eds) The microbiological safety and quality of food, Volume II. *Aspen publishers, Inc.,* Maryland **2000**; pp 315-341.

Magliulo, M.; Simoni, P.; Guardigli, M.; Michelini, E.; Luciani, M.; Lelli, R.; Roda, A. A Rapid multiplexed chemiluminescent immunoassay for the detection of *Escherichia coli* O157:H7, *Yersinia enterocolitica*, *Salmonella typhimurium*, and *Listeria monocytogenes* pathogen bacteria. *Journal of Agricultural and Food Chemistry* **2007,** 55, (13), 4933-4939.

Makardij, A.; Chen, X.D.; Farid, M.M. Microfiltration and ultrafiltration of milk:sSome aspects of fouling and cleaning. *Food and Bioproducts Processing* **1999,** 77, (2), 107-113.

Mandal P.K.; Biswas A. K.; Choi K.; Pal, U.K. Methods for rapid detection of foodborne pathogens: an overview. *American Journal of food Technology* **2011,** 6, (2), 87-102.

Maquelin, K.; Dijkshoorn, L.; van der Reijden, T.J.K.; Puppels, G.J. Rapid epidemiological analysis of *Acinetobacter* strains by Raman spectroscopy. *Journal of Microbiological Methods* **2006,** 64, (1), 126-131.

Marshall, A.D.; Munro, P.A.; Trägårdh, G. Influence of ionic calcium concentration on fouling during the cross-flow microfiltration of b-lactoglobulin solutions. *Journal of Membrane Science* **2003,** 217, (1-2), 131-140.

Meng, F.; Liao, B.; Liang, S.; Yang, F.; Zhang, H.; Song, L. Morphological visualization, componential characterization and microbiological identification of membrane fouling in membrane bioreactors (MBRs). *Journal of Membrane Science* **2010,** 361, (1-2), 1-14.

Miller J.N.; Miller, J.C. Statistics and Chemometrics for Analytical Chemistry. 5th ed.; Pearson Education Limited: Essex, **2005**.

Motta, A.; Flores, F.; Souto, A.A.; Brandelli, A. Antibacterial activity of a bacteriocin-like substance produced by *Bacillus* sp. P34 that targets the bacterial cell envelope. *Antonie van Leeuwenhoek* **2008,** 93, (3), 275-284.

Nataraj, S.; Schomäcker, R.; Kraume, M.; Mishra, I.M.; Drews, A. Analyses of polysaccharide fouling mechanisms during crossflow membrane filtration. *Journal of Membrane Science* **2008,** 308, (1-2), 152-161.

Naumann, D. Infrared spectroscopy in microbiology. In *Encyclopedia of Analytical Chemistry*, John Wiley & Sons, Ltd: **2006**.

Nazir, A.; Schroën, K.; Boom, R. Premix emulsification: A review. *Journal of Membrane Science* **2010,** 362, (1-2), 1-11.

Neves, E.; Silva, A.C.; Roche, S.M.; Velge, P.; Brito, L. Virulence of *Listeria monocytogenes* isolated from the cheese dairy environment, other foods and clinical cases. *Journal of Medical Microbiology* **2008,** 57, (4), 411-415.

Nigam, M.O.; Bansal, B.; Chen, X.D. Fouling and cleaning of whey protein concentrate fouled ultrafiltration membranes. *Desalination* **2008,** 218, (1-3), 313-322.

Palchetti, I.; Mascini, M. Electroanalytical biosensors and their potential for food pathogen and toxin detection. *Analytical and Bioanalytical Chemistry* **2008,** 391, (2), 455-471.

Pirouette, Multivariate data analysis version 4.0 user manual [online]. *Infometrix, Inc. Bothell, WA,* 2008.

Ponniah, J.; Robin, T.; Paie, M.S.; Radu, S.; Ghazali, F.M.; Kqueen, C.Y.; Nishibuchi, M.; Nakaguchi, Y.; Malakar, P.K. *Listeria monocytogenes* in raw salad vegetables sold at retail level in Malaysia. *Food Control* **2010,** 21, (5), 774-778.

Preisner, O.; Guiomar, R.; Machado, J.; Menezes, J.C.; Lopes, J.A. Application of Fourier transform infrared spectroscopy and chemometrics for differentiation of *Salmonella enterica* serovar *enteritidis* phage types. *Applied and Environmental Microbiology* **2010,** 76, (11), 3538-3544.

Rabiller-Baudry, M.; Le Maux, M.N.; Chaufer, B.; Begoin, L. Characterisation of cleaned and fouled membrane by ATR-FTIR and EDX analysis coupled with SEM: application to UF of skimmed milk with a PES membrane. *Desalination* **2002,** 146, (1-3), 123-128.

Radke, S.M.; Alocilja, E.C. A high density microelectrode array biosensor for detection of *E. coli* O157:H7. *Biosensors and Bioelectronics* **2005,** 20, (8), 1662-1667.

Ramaswamy, H.S.; Zaman, S.U.; Smith, J.P. High pressure destruction kinetics of *Escherichia coli* (O157:H7) and *Listeria monocytogenes* (Scott A) in a fish slurry. *Journal of Food Engineering* **2008,** 87, (1), 99-106.

Ray, B. Fundamental Food Microbiology, 3rd Edition; CRC Press LLC: Florida, **2003.**

Rebuffo-Scheer, C.A.; Schmitt, J.R.; Scherer, S. Differentiation of *Listeria monocytogenes serovars* by using artificial neural network analysis of Fourier-transformed infrared spectra. *Applied and Environmental Microbiology* **2007,** 73, (3), 1036-1040.

Rhoades, J.R.; Duffy, G.; Koutsoumanis, K. Prevalence and concentration of verocytotoxigenic *Escherichia coli*, *Salmonella enterica* and *Listeria monocytogenes* in the beef production chain: A review. *Food Microbiology* **2009,** 26, (4), 357-376.

Rodriguez-Saona, L.E.; Khambaty, F.M.; Fry, F.S.; Calvey, E.M. Rapid detection and identification of bacterial strains by Fourier transform near-infrared spectroscopy. *Journal of Agricultural and Food Chemistry* **2001,** 49, (2), 574-579.

Rodriguez-Saona, L.E.; Khambaty, F.M.; Fry, F.S.; Calvey, E.M. Discrimination of bacterial strains by Fourier-transform near-infrared spectroscopy using an aluminum oxide membrane. *Spectroscopic Properties of Biological Materials*, **2002**, 4574, 108-118.

Sallam, K.I. Prevalence of *Campylobacte*r in chicken and chicken by-products retailed in Sapporo area, Hokkaido, Japan. *Food Control* **2007,** 18, (9), 1113-1120.

Sawalha, H.; Fan, Y.; Schroën, K.; Boom, R. Preparation of hollow polylactide microcapsules through premix membrane emulsification-Effects of nonsolvent properties. *Journal of Membrane Science* **2008,** 325, (2), 665-671.

Schäfer, A.I. ; Andritsos, N. ; Karabelas, A.J. ; Hoek, E.M.V. ; Schneider, R. ; Nyström, M. Fouling in Nanofiltration: In Schäfer A.I., Waite T.D., Fane A.G. (Eds) Nanofiltration - Principles and Applications, Elsevier **2004**, 169-239.

Sengupta, A.; Mujacic, M.; Davis, E.J. Detection of bacteria by surface-enhanced Raman spectroscopy. *Analytical and Bioanalytical Chemistry* **2006,** 386, (5), 1379-1386.

Singh, S.; Khulbe, K.C.; Matsuura, T.; Ramamurthy, P. Membrane characterization by solute transport and atomic force microscopy. *Journal of Membrane Science* **1998,** 142, (1), 111-127.

Sekse, C.; O'Sullivan, K.; Granum, P.E.; Rørvik, L.M.; Wasteson, Y.; Jørgensen, H.J. An outbreak of *Escherichia coli* O103:H25 -Bacteriological investigations and genotyping of isolates from food. *International Journal of Food Microbiology* **2009,** 133, (3), 259-264.

Smith, B.C. Fundamentals of Fourier transform infrared spectroscopy. 2nd Edition; Taylor & Francis Group, LLC: New York, **2011**.

Smiths Detection, IlluminatIR Users Manual, The Genesis Centere Science Park South Birchwood, Warrington, England. Available at: http://www.smithsdetection.com.

Song, L., Flux decline in crossflow microfiltration and ultrafiltration: mechanisms and modeling of membrane fouling. *Journal of Membrane Science* **1998,** 139, (2), 183-200.

Spettmann, D.; Eppmann, S.; Flemming, H.-C.; Wingender, J. Visualization of membrane cleaning using confocal laser scanning microscopy. *Desalination* **2008,** 224, (1-3), 195-200.

Stuart, B.H. Infrared spectroscopy of biological applications. In *Encyclopedia of Analytical Chemistry*, John Wiley & Sons, Ltd: **2006.**

Subramanian, A.; Ahn, J.; Balasubramaniam, V.M.; Rodriguez-Saona, L. Determination of spore inactivation during thermal and pressure-assisted thermal processing using FT-IR spectroscopy. *Journal of Agricultural and Food Chemistry* **2006,** 54, (26), 10300-10306.

Subramanian, A.; Ahn, J.; Balasubramaniam, V.M.; Rodriguez-Saona, L. Monitoring biochemical changes in bacterial spore during thermal and pressure-assisted thermal processing using FT-IR Spectroscopy. *Journal of Agricultural and Food Chemistry* **2007,** 55, (22), 9311-9317.

Sumner, J.; Ross, T. A semi-quantitative seafood safety risk assessment. *International Journal of Food Microbiology* **2002,** 77, (1-2), 55-59.

Sundaram, J.; Park, B.; Hinton, A.; Yoon, S.C.; Windham, W.R.; Lawrence, K.C. Classification and structural analysis of live and dead *Salmonella* cells using Fourier transform infrared spectroscopy and principal component analysis. *Journal of Agricultural and Food Chemistry* **2012,** 60, (4), 991-1004.

Surh, J.; Jeong, Y.G.; Vladisavljević, G.T. On the preparation of lecithin-stabilized oil-in-water emulsions by multi-stage premix membrane emulsification. *Journal of Food Engineering* **2008,** 89, (2), 164-170.

Torras C.; Gumí T.; Garcia-Valls, R. Microscopy techniques for the characterization of membrane morphology: In Güell C.; Ferrando M.; López, F. (Eds) Monitoring and Visualzing Membrane-Based Process, Wiley VCH Verlag GmbH &Co. KGaA: Weinheim; **2009**, pp 33-54.

Trentin, A.; Güell, C.; López, F.; Ferrando, M. Microfiltration membranes to produce BSA-stabilized O/W emulsions by premix membrane emulsification. *Journal of Membrane Science* **2010,** 356, (1-2), 22-32.

Trentin, A.; De Lamo, S.; Güell, C.; López, F.; Ferrando, M. Protein-stabilized emulsions containing beta-carotene produced by premix membrane emulsification. *Journal of Food Engineering* **2011a,** 106, (4), 267-274.

Trentin, A.; Güell, C.; Gelaw, T.; De Lamo, S.; Ferrando, M. Cleaning protocols for organic microfiltration membranes used in premix membrane emulsification. *Separation and Purification Technology* **2011b,** 88, 70-78.

Tully, E.; Higson, S.P.; O'Kennedy, R. The development of a "labeless" immunosensor for the detection of *Listeria monocytogenes* cell surface protein, Internalin B. *Biosensors and Bioelectronics* **2008,** 23, (6), 906-912.

United States Department of Agriculture, Food Safety and Inspection Service (FSIS). Foodborne Illness: What Consumers Need to Know, Updated May 2011, Washington, Food Safety and Inspection service, **2011**.

Väisänen P.; Bird, M.R.; Nyström, M. Treatment of UF membranes with simple and formulated cleaning agents. *Food and Bioproducts Processing* **2002,** 80, (2), 98-108.

Van, T.T.H.; Moutafis, G.; Istivan, T.; Tran, L.T.; Coloe, P.J. Detection of *Salmonella* spp. in retail raw food samples from Vietnam and characterization of their antibiotic resistance. *Applied and Environmental Microbiology* **2007,** 73, (21), 6885-6890.

Van der Bruggen, B.; Braeken, L.; Vandecasteele, C. Flux decline in nanofiltration due to adsorption of organic compounds. *Separation and Purification Technology* **2002,** 29, (1), 23-31.

Van der Graaf, S.; Schroën, C.G.P.H.; Boom, R.M. Preparation of double emulsions by membrane emulsification-a review. *Journal of Membrane Science* **2005,** 251, (1-2), 7-15.

Velusamy, V.; Arshak, K.; Korostynska, O.; Oliwa, K.; Adley, C. An overview of foodborne pathogen detection: In the perspective of biosensors. *Biotechnology Advances* **2010,** 28, (2), 232-254.

Violleau, D.; Essis-Tome, H.; Habarou, H.; Croué, J.P.; Pontié, M. Fouling studies of a polyamide nanofiltration membrane by selected natural organic matter: an analytical approach. *Desalination* **2005,** 173, (3), 223-238.

Vladisavljević, G.T.; Surh, J.; McClements, J.D. Effect of emulsifier type on droplet disruption in repeated shirasu porous glass membrane homogenization. *Langmuir* **2006,** 22, (10), 4526-4533.

Wang, J.; Yue, T.; Yuan, Y.; Lu, X.; Shin, J.-H.; Rasco, B. Discrimination of *Alicyclobacillus* strains using nitrocellulose membrane filter and attenuated total reflectance Fourier transform infrared spectroscopy. *Journal of Food Science* **2011,** 76, (2), 137-142.

Warriner, K.; Namvar, A. Biosensors for Foodborne Pathogen Detection: In Murray, M.Y. (Ed) In *Comprehensive Biotechnology (Second Edition)*, Academic Press: Burlington **2011,** pp 659-674.

Whelan, J.; Noel, H.; Friesema, I.; Hofhuis, A.; de Jager, C.M.; Heck, M.; Heuvelink, A.; van Pelt, W. National outbreak of *Salmonella* Typhimurium (Dutch) phage-type132 in the Netherlands, October to December 2009. *Euro Surveill* **2010**, 15(44).

WHO. Food safety & food-borne illness. Fact sheet no. 237 (Revised January 2002). Geneva: World Health Organization; **2002**.

Workman, S.N.; Mathison, G.E.; Lavoie, M.C. An investigation of sources of *Campylobacter* in a poultry production and packing operation in Barbados. *International Journal of Food Microbiology* **2008,** 121, (1), 106-111.

Yang K. and Trewn J. Multivariate Statistical Methods in Quality Management. McGraw-Hill Companies, **2004**.

Yang, Z.; Peng, X.F.; Chen, M.-Y.; Lee, D.-J.; Lai, J.Y. Intra-layer flow in fouling layer on membranes. *Journal of Membrane Science* **2007,** 287, (2), 280-286.

Ye, Y.; Le Clech, P.; Chen, V.; Fane, A.G.; Jefferson, B. Fouling mechanisms of alginate solutions as model extracellular polymeric substances. *Desalination* **2005,** 175, (1), 7-20.

Yoda K.; Uchimura M. An outbreak of *Campylobacter jejuni* food poisoning caused by secondary contamination in cooking practice at a high school. *Japanese journal of infectious diseases* **2006**, 59, 408- 409.

Zator, M.; Warczok, J.; Ferrando, M.; López, F.; Güell, C. Chemical cleaning of polycarbonate membranes fouled by BSA/dextran mixtures. *Journal of Membrane Science* **2009,** 327, (1-2), 59-68.

Zhang, M.; Song, L. Mechanisms and parameters affecting flux decline in cross-flow microfiltration and ultrafiltration of colloids. *Environmental Science & Technology* **2000,** 34, (17), 3767-3773.

Zhu, X.; Elimelech, M. Colloidal fouling of reverse osmosis membranes: measurements and fouling mechanisms. *Environmental Science and Technology* **1997,** 31, (12), 3654-3662.

Zoumpopoulou, G.; Papadimitriou, K.; Polissiou, M.G.; Tarantilis, P.A.; Tsakalidou, E. Detection of changes in the cellular composition of *Salmonella enterica* serovar Typhimurium in the presence of antimicrobial compound(s) of *Lactobacillus* strains using Fourier transform infrared spectroscopy. *International Journal of Food Microbiology* **2010,** 144, (1), 202-207.

CHAPTER 2

Attenuated total reflectance infrared microspectroscopy combined with multivariate analysis, a novel tool to characterize membrane fouling and cleaning efficiency of organic microfiltration membranes[1]

[1]Part of this chapter has been published at: Alexandre Trentin, Carme Güell, Tilahun K. Gelaw, Sílvia de Lamo-Castellví, Montse Ferrando (2012) *Cleaning protocols for organic microfiltration membranes used in premix membrane emulsification*, **Separation and Purification Technology**, 88, 70-78 and Tilahun K. Gelaw, Alexandre Trentin, Carme Güell, Montse Ferrando, Luis E. Rodríguez-Saona, Sílvia de Lamo-Castellví (2011) *Attenuated total reflectance infrared microspectroscopy combined with multivariate analysis, a novel tool to characterize cleaning efficiency of organic microfiltration membranes*, **Journal of Membrane Science**, 376, 35-39

2.1. INTRODUCTION

Emulsification is a structure-forming process where two or more immiscible phases can be mixed to one another. Traditionally, colloid mills, rotor stator systems, high pressure homogenizers and ultrasonic homogenizers have been used to prepare emulsions. However, these techniques can cause loss of functional properties of the components which have heat and shear sensitivity, and it is also difficult to control the droplet size and their distribution (Karbstein and Schubert, 1995; Nazir *et al.,* 2010). Though, these techniques produce mono dispersed emulsion the energy consumption is high. A relatively new technique to produce emulsions is membrane emulsification (ME). It is a process in which a to-be-dispersed phase is pressed through a membrane and the droplets formed are carried away with a continuous phase flowing across the membrane (van der Graaf *et al.,* 2005; Piacentini *et al.,* 2010; Silvestre de los Reyes and Charcosset, 2010; Trentin *et al.,* 2010). ME produces an emulsion with a narrow droplet-size distribution with a less energy demand. Moreover this technique is simple to design and needs less amount of surfactant (Nakashima *et al.,* 1992; Dickinson, 1994; Kandori, 1995). In ME process, the accumulation of the different components of the emulsion on the membrane surface or within the membrane pores causes fouling that will inevitably result in a flux decline (Mallevialle *et al.,* 1989; Scott, 1995; Chang *et al.,* 2002; Charcosset, 2011; Trentin *et al.,* 2011). Membrane fouling has been classified into different types depending on the components that act as fouling agents, the adsorption of organic molecules produces organic fouling, the deposition of colloidal particulates is called colloidal fouling and the growth and adhesion of microorganisms is known as biofouling (Mallevialle *et al.,* 1989; Scott, 2003). Although membrane fouling is an inevitable phenomenon during membrane processes, it has been minimized by strategies such as appropriate membrane selection, choice of operating conditions and membrane cleaning. Among these strategies, the most feasible one to extend the life of membranes used in membrane emulsification is to perform physical or chemical/biochemical cleaning. Biological cleaning uses biocides to remove all viable microorganisms, whereas chemical cleaning involves the use of acids and/or bases to

remove foulants and impurities (Argüello *et al.,* 2002; Kuzmenk *et al.,* 2005). The most straight forward methodology to test the efficiency of membrane cleaning is measuring the water flux of the new and cleaned membranes and calculating the water flux recovery. However, additional membrane characterization to determine which compounds/species have been left or removed from the membrane has been also widely applied. In the past decade, membrane surface has been characterized with different methods such as scanning electron microscope (SEM) (Güell and Davis, 1996; Väisänen *et al.,* 2002), confocal scanning laser microscopy (CSLM) (Ferrando *et al.,* 2005; Zator *et al.,* 2007), spectroscopic techniques (Carlsson *et al.,* 1998; Belfer *et al.,* 2000) and atomic force microscopy (AFM) which has been used to study surface topography and pore size distribution (Hilal and Johnson, 2010).

Fourier transform infrared microspectroscopy (FT-IRMS) combined with multivariate data analysis is a well known method for the analysis of chemicals and microorganisms (Männig *et al.,* 2008; Grasso *et al.,* 2009). Specifically, attenuated total reflectance infrared microspectroscopy (IRMS) has the potential of detecting subtle compositional differences between samples. FTIR could be an interesting technique to analyze and identify chemical components on the membrane surface (Argüello *et al.,* 2002; Kuzmenk *et al.,* 2005; Barbar *et al.,* 2008; Nataraj *et al.,* 2008).

In fact, a wide application of FTIR for membrane characterization, membrane fouling and/or membrane cleaning can be found in the literature. Among the studies on membrane fouling it is possible to find, among others, applications to obtain qualitative information about the foulants during ultrafiltration of polysaccharide suspensions (Nataraj *et al.,* 2008), application to study fouling on ultrafiltration membrane used in waste water treatment (Shon *et al*., 2006), studies on BSA or hemoglobin adsorption during filtration using several organic membranes (Loh *et al.,* 2009), studies on fouling of lactose and calcium phosphate from skimmed milk nanofiltration (Rice *et al.,* 2009*)* and applications on fouling control in bioreactors (Li *et al.,* 2010). The characterization of membranes by FTIR before and after cleaning has been studied, among others, by Kuzmenko *et al.* (2005) who studied the extend of membrane alteration after

chemical cleaning with NaOH or NaOCl of membranes fouled with BSA; by Wu and Bird (2007) who combined the study of membrane fouling during tea microfiltration and the effectiveness of cleaning with NaOH; by Rabiller-Baudry *et al*. (2008) who studied membrane cleaning (with NaOH, Tween 20 or Ultrasil 10) of polyethersulfone (PES) membranes used for skimmed milk ultra filtration and by Väisänen *et al.* (2002) who studied the effect of the cleaning agent composition upon ultrafiltration membranes fouled with whey protein concentrate or ground mill circulation water. It is possible to find some applications of FTIR for the characterization of membranes used either to treat oily waters (Rezvanpour *et al.,* 2009) or to disrupt oil in water emulsions (Barbar *et al.,*2008). Although some authors mention that the intensity of infrared absorption bands can be used to quantify the amount of material present on the membrane (Loh *et al.,* 2009; Rabillier-Baudry *et al.*, 2008;), most of the published work using FTIR characterization in the membrane field, limits its application to the acquisition of qualitative information. Wems Diagne *et al.* (2013) studied the cleaning efficiency of fouled polyethersulfone (PES) membranes by ultrafiltration of skimmed milk using the height ratio of two targeted IR bands, 1539 cm^{-1} related to amide II vibration of proteins and 1240 cm^{-1} characteristic of the PES membrane.

The objective of this research was to evaluate the potential of using attenuated total reflectance infrared microspectroscopy (ATR-IRMS) combined with multivariate analysis (soft independent modeling of class analogy, SIMCA) to obtain qualitative information on the foulant residues remaining on the membrane after the application of several cleaning protocols. Moreover, the cleaning efficiency of the different protocols applied was also evaluated by calculating the area of the discriminating band at 1743 cm^{-1} and these results were compared with the water flux recovery. The SIMCA models were also used to identify the most effective cleaning protocol among those tested. For this research, nylon and nitrocellulose mixed ester (MCE) membranes were used to produce O/W emulsions stabilized by whey protein. This study should provide qualitative and quantitative information on the efficiency of the cleaning protocols and will serve as a first approach to apply ATR-FTIR combined with multivariable

analysis to membrane characterization, which, to the author's knowledge has not been applied before in this field.

2.2. MATERIALS and METHODS

2.2.1. Materials and Membrane

O/W emulsions were prepared using commercial sunflower oil as a disperse phase, MiliQ water (18.2 MΩ cm) as a continuous phase and whey protein (WPC, Lactalbumin® 75L, from Milei-Sttuttgart, Germany) as emulsifier. Nylon membrane (0.8 µm pore size, Whatman® ref. 7408-004, Scheicher and Schuell, Whatman international Ltd, Maidstone, England) with an effective membrane diameter of 41 mm and nitrocellulose mixed esters (MCE) membrane (0.8 µm pore size, Sterlitech Corporation, Kent, WA 98032-1911 USA) with an effective membrane diameter of 47 mm were used for premix membrane emulsification. The effective membrane diameter gives an effective filtration area of $1.32x10^{-3}$ m^2 (nylon membrane) and $1.73\ x10^{-3}$ m^2 (MCE membrane) for the membrane module employed in this research.

2.2.2. Premix Emulsification Procedure

O/W emulsions were prepared in a two step emulsification system (Trentin *et al.,* 2010). The first step consisted of preparing a coarse O/W emulsion by mixing the disperse phase and the continuous phase containing the emulsifier by means of a rotor-stator (Ultra-Turrax®, model T18, IKA) at 15500 rpm for 2 min. In the second step of the process the coarse emulsion was forced to pass through the membranes by using nitrogen pressure (500 or 900 kPa) resulting in a reduction of the droplet size. This second step was repeated five times (cycles) to obtain the final emulsion droplet size.

Figure 2.1 shows the flowchart which represents the experimental procedure of premix membrane emulsification. This procedure was done three times where at the beginning of each cycle a new membrane was placed on the membrane module.

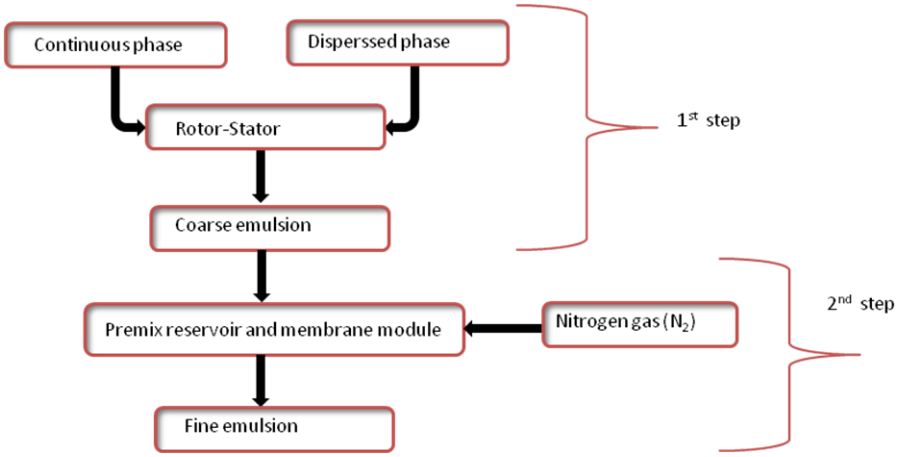

Figure 2.1. Oil-in-water premix membrane emulsification process

More details in the experimental procedure and equipment can be found in Trentin *et al* (2010). Each experimental condition tested in the present study was repeated three times and a new membrane was loaded into the membrane module at the beginning (1st cycle) of each experiment. Membrane cleaning was performed after emulsification using Tween 20 (polyoxyethylene sorbitan monolaurate; CAS no. 9005-64-5 Sigma–Aldrich, Spain) dissolved in milliQ water at different concentrations. The procedure for membrane cleaning consisted of forcing 700 mL of the cleaning agent (divided in four batches) at room temperature (22 $\pm$ 2 ^{o}C) through the membrane in a backwash mode at different N_2 pressures (150-700 kPa). The cleaning protocols applied are listed in **Table 2.1**. Three cleaning procedures, 2% Tween 20 and 150 kPa N_2 pressure (TW2P1.5), 3% Tween 20 and 700 kPa N_2 pressure (TW3P7) and 4% Tween 20 and 500 kPa N_2 pressure (TW4P5) were selected and used during the cleaning of MCE

membrane, based on the cleaning efficiencies obtained during the cleaning of nylon membranes.

Table2.1 *Cleaning protocols applied to nylon and nitrocellulose mixed esters membranes*

Samples	Tween 20 (TW, %)	N_2 pressure (P, kPa)
TW2P1.5	2	150
TW2P5	2	500
TW3P5	3	500
TW3P7	3	700
TW4P5	4	500

2.2.3. Water Flux Recovery

Water flux recovery (WFR) of new and cleaned membranes was obtained by pushing 170 mL of water at 150 kPa through the membrane. To calculate the efficiency of the cleaning method, WFR was calculated according to **equation 2.1**:

$$WFR = \left(\frac{J_c}{J_0} \right) * 100 \qquad (2.1)$$

Where J_0 is the water flux of the new membrane and J_c is the water flux of the cleaned membrane**.**

2.2.4. Sample preparation for ATR-IRMS analysis

Nylon and MCE membranes were used as a support to obtain spectra of sunflower oil, whey protein and Tween 20 (polyoxyethylene sorbitan monolaurate, from Sigma–Aldrich, Spain) by attenuated total reflectance infrared microspectroscopy (ATR-IRMS). In the case of whey protein, an aqueous solution of 10 % (w/w) was prepared by mixing 3 mg of whey protein

powder with 30 mL of deionized water. The mixture was left in a magnetic stirrer until all the powder was dissolved. An aliquot of the prepared solution (5 µmL) was placed onto half of the membrane. The membrane was air dried overnight to minimize the overlapping effect of water absorption bands (3400 and 1700 cm^{-1}) in the sample spectral signal. For sunflower oil, 5 µmL of this solution was deposited onto half of the membrane and left in an open air for drying. The same procedure was used for pure Tween 20 solution. Each dry membrane was mounted on different glass slide before being analyzed by ATR- IRMS.

For the characterization of fouled and cleaned membranes with ATR-IRMS, half of the membrane was divided into two parts in such a way that one part towards the center and the other part was towards the edge of the membrane (**Figure 2.2**)

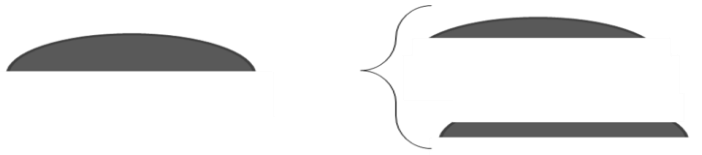

Figure 2.2. Schematic drawing of fouled and cleaned membrane (cut in to two halves)

Each of the two sections of the membrane samples were mounted onto different glass slides and were analyzed by ATR-IRMS in the mid-infrared region (4000-800 cm^{-1}). **Figure 2.3** shows the sample preparation process used to analyze nylon and MCE membranes by ATR-IRMS.

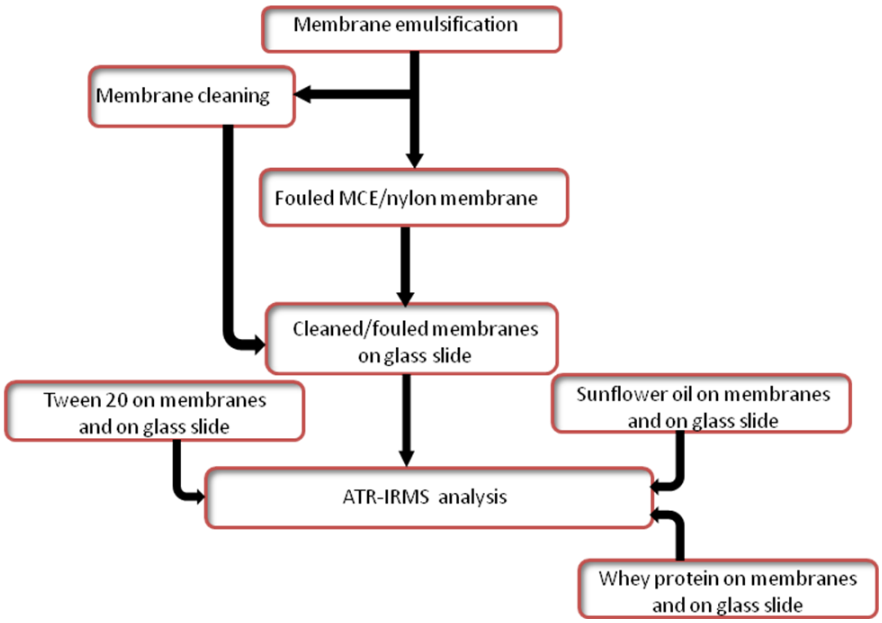

Figure 2.3. Membrane sample preparation steps for ATR-IRMS analysis

2.2.5. ATR-IRMS Spectra Acquisition

ATR-IRMS spectra were collected from different samples using FTIR microscope (Illuminate IR, Smiths detection) interfaced with mercury-cadmium-telluride (MCT) photoconductive detector and equipped with a microscope with a motorized x-y stage, 5x and 50x objectives, and slide-on attenuated total reflection (ATR) diamond objective (Smiths detection). The inside of the ATR-IRMS equipment used is shown in **Figure 2.4**. The IR radiation from the source collimated using a parabolic mirror (M1) and enters to the interferometer where the KBr (Potassium bromide) beam splitter splits the IR beam into a fixed mirror and a moving mirror. The beam splitter redirects the two beams coming back from the mirrors to a flat mirror (M2) which keeps the IR beam collimated but change the direction to another parabolic mirror (M3). M3 focuses the IR beam and sends to the sample via the masking apertures. The IR beam reflected from the sample recollimated by another parabolic mirror (M4) and sends to Trichroic beam splitter. From the Trichroic optical element, the mid IR beams reflected from the sample are directed to a parabolic mirror (M5), where the beams are focused and inter to the MCT detector. On the

other hand, the near IR beam reflected from the sample directed to the video camera by the Trichroic beam splitter.

The samples were placed on the stage of the microscope and a specific position was selected with the assistance of the live camera (Lecica OM 2500, Modulo FT-IR, Renishaw plc). The microscope was software-controlled using Wire 3.2 version software (Renishaw plc, New Mills, Wotton-under-Edge, Gloucestershire, GL12 8JR, United Kingdom).

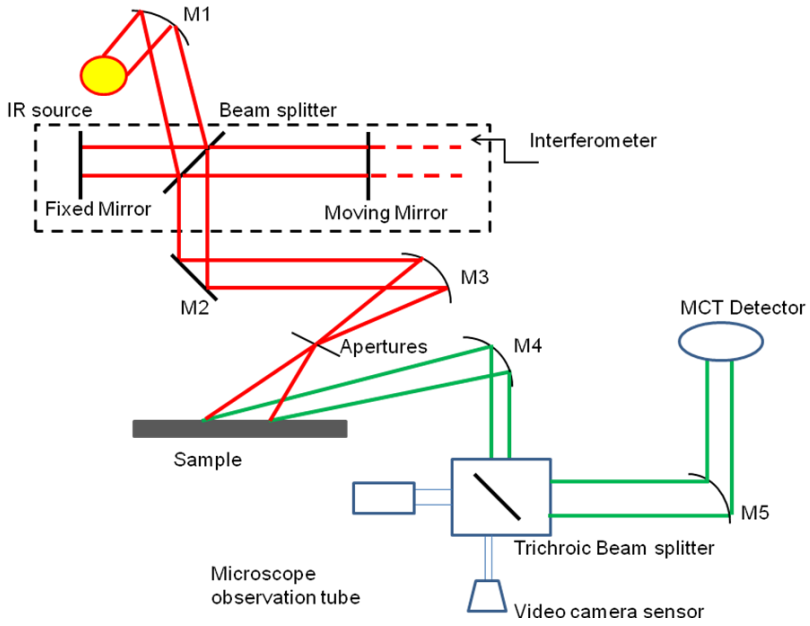

Figure 2.4. The schematic drawing of the IlluminateIR FT-IR spectrometer (adapted from Illuminate IR user manual, Smiths detection)

Spectra were collected from 4000 to 800 cm^{-1} with a resolution of 4 cm^{-1}. The spectrum of each sample was obtained by taking the average of 128 scans to improve the signal-to-noise ratio. Spectra were displayed in terms of the absorbance obtained by rationing the single beam spectrum against that of the air background. The spectrometer was completely software

controlled by synchronize IR basic version 1.1 software (SensIR Technologies, Smiths detection). The time required to obtain one spectrum was about 40 s.

2.2.6. Multivariate Analysis

Pirouette® multivariate analysis software (version 4.0, InfoMetrix, Inc., Woodville, WA) was used to analyze the raw spectra of the samples. The spectra were exported to as ".spc" files. The FT-IR spectral data were mean-centered, transformed to their second derivative using a 15-point Savitzky-Golay polynomial filter, and vector-length normalized; sample residuals and Mahalanobis distance were used to determine outliers (Kansiz *et al.* 1999; De Maesschalck *et al.* 2000). Spectral data were statistically analyzed using soft independent modeling of class analogy (SIMCA). SIMCA was used to build a predictive based model on the construction of separate PCA models for each class to describe and model the variation (De Maesschalck *et al.* 1999; Kansiz *et al.*, 1999). SIMCA class models were interpreted based on class projections, misclassifications, discriminating power, and interclass distances. Class projections were visible through a three-dimensional graph of clustered membranes. Probability clouds (95%) were built around the clusters based on PCA scores, allowing SIMCA to be used as a predictive modeling system. Total misclassifications were analyzed and interpreted for the input data and also validation unknowns to assess the power of the model. Variable importance, also known as discriminating power, was used to define the variables (wavenumbers) that have a predominant effect on cleaned membrane classification, minimizing the difference between samples within a cluster, and maximizing differences between samples from different clusters (Dunn and Wold, 1995).

2.2.7. Cleaning Efficiency

The efficiency of each cleaning protocol was obtained by calculating the area of the ~1743 cm^{-1} band, which was the most consistent among the bands found only on the fouling membrane spectra, and applying equation 2.2. The area of ~1743 cm^{-1} was calculated with Grams/AI version 8.0 (Thermo Fisher Scientific Inc., Smiths Detection) software.

$$Efficiency = \left(\frac{A - Bn}{A} \right) * 100 \quad (2.2)$$

Where A is the average area IR band at 1743 cm^{-1} for the fouled membrane and Bn is the average area of the same band for each cleaned membrane.

2.3. RESULTS AND DISCUSSION

2.3.1. Preliminary Study

A preliminary ATR-IRMS analysis was performed using the two sections of fouled nylon membrane to study the uniformity of the membrane surface regarding the distribution of fouling. The spectral data of the two sections were analyzed using SIMCA to study fouling distribution on the membrane surface and the models created were interpreted based on class projections, discriminating power, and interclass distances. Class projections illustrate the ability of SIMCA to differentiate IR data based on the first three principal components (Helm *et al.,* 1991; Beekes *et al.,* 2007).

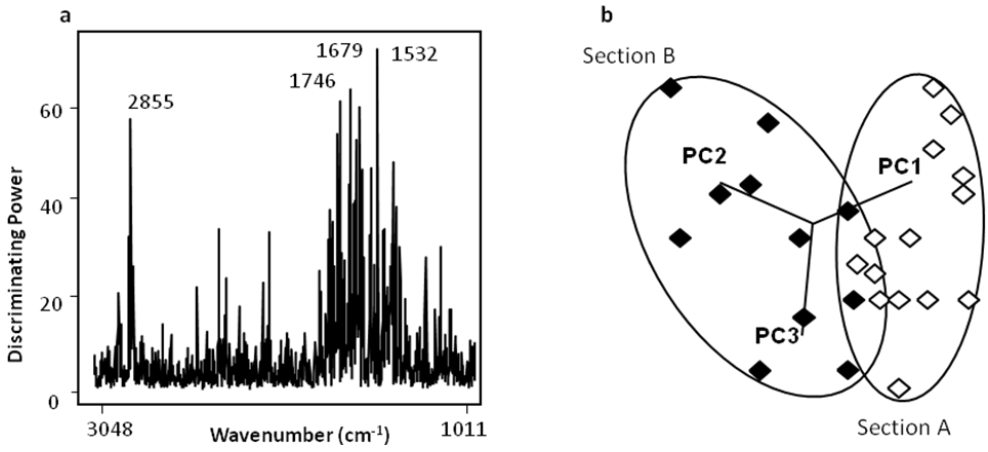

Figure 2.5. SIMCA discriminating power (a) and class projection (b) of a transformed (second derivative, 15 points window) ATR-IRMS spectra of fouled nylon membrane cut into two parts: the parts towards the center of the membrane (section A) and the parts towards the edge of the membrane (section B)

Infrared spectra analysis (3048 - 1011 cm^{-1}) using SIMCA classification models of section A and B did not permitted tight clustering, and clear differentiation among samples (**Figure 2.5**) showing that the two sections of the fouled nylon membrane were very similar. Discriminating power of SIMCA, which is a measure of variable importance in infrared frequency and contributes to the development of the classification models (Helm et al., 1991) showed discriminating bands at around 2885, 1746, 1679 and 1530 cm^{-1}. These bands could be linked to C-H stretching of CH_2, >C=O stretching of carboxylic acid from sunflower oil, >C=O stretching of amide and N-H bending of secondary amine from whey protein and the nylon membrane respectively (Coates, 2006). The interclass distances (ICD) are Euclidean distances between centers of clusters and values above 3.0 are considered good for class discrimination (Beekes *et al.,* 2007; Pirouette, Version 4.0, 2008). The ICD value was 1.6, pointing out that the two sections could be considered similar. These results indicated that the distribution of the fouling on the membrane surface was homogenous.

2.3.2. ATR-IRMS Characterization of New and Fouled Nylon Membranes

The raw spectrum of new, after emulsification (fouled), and pure components (sunflower oil and whey protein) is shown in **Figure 2.6.** A band, attributed to >C=O stretching of carbonic acids and esters (1743 cm^{-1}) (Mayo, 2003; Nigam *et al.,* 2008), was clearly observed for the fouled membrane, for pure sunflower oil and for whey protein samples, but not in the new membrane. Thus, this band was selected to differentiate between fouled and new membrane spectra. Raw spectra of sunflower oil and fouled membrane were more similar than the spectra of whey protein and fouled membrane (**Figure 2.6**). When the 2nd derivative was applied to their raw spectra, two bands at ~3008 cm^{-1} and ~1389 cm^{-1} related to the stretching of carbonic acids were detected on the sunflower oil and the fouled membrane but not in the whey protein spectra (**Figures 2.7 a and b**). These findings showed the presence of sunflower oil on the fouled membrane. Therefore, we can conclude that sunflower oil may be the dominant fouling agent on the membrane surface during the emulsification process.

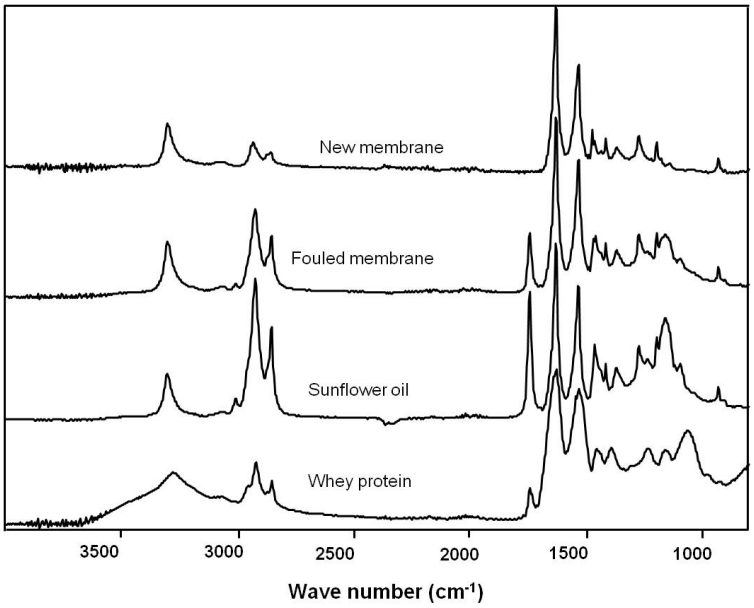

Figure 2.6. ATR-IRMS spectra of new nylon membrane, fouled nylon membrane and the two components of the emulsion, sunflower oil and whey protein using ATR diamond crystal in reflectance mode (from 4000 cm^{-1} to 800 cm^{-1})

Nonetheless, it is important to underscore that the whey protein also showed a band around ~1743 cm^{-1} which may overlap with the strong band coming from the sunflower oil. These results may indicate that proteins also contributed to the fouling of the membrane. Several studies have identified protein as the main fouling agent during membrane filtration processes (Bird and Bartlett, 2002; Rabiller-Baudry *et al.,* 2002; Wu and Bird, 2007), which may also be applicable to membrane emulsification process. Nevertheless, protein fouling would affect the membrane surface as well as inside the membrane pores. This last phenomenon cannot be detected using ATR-IRMS, because this technique was only used to characterize the surface chemistry of the membrane.

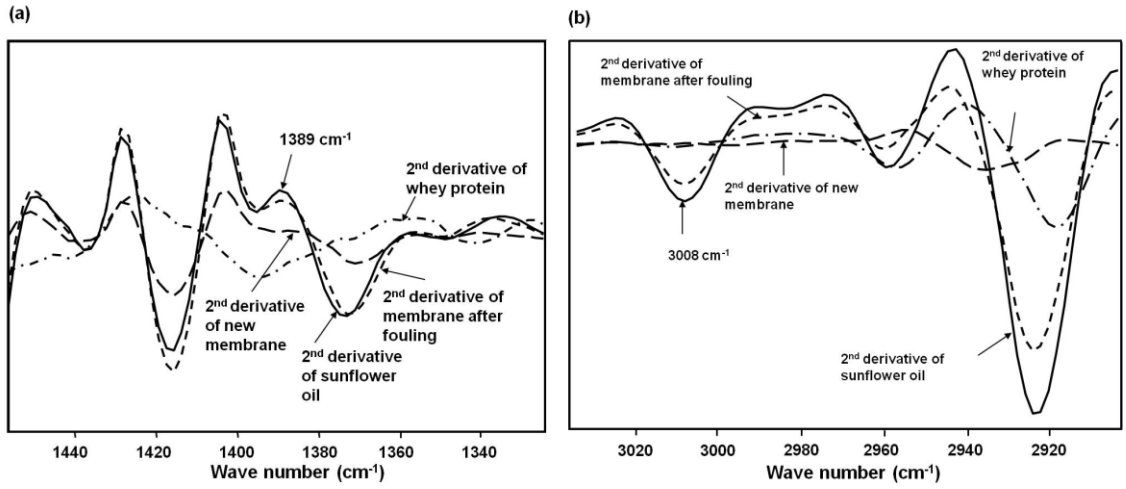

Figure 2.7. Secondary derivative transformations of IRMS spectra (15 points window) of new nylon membrane, fouled nylon membrane and the two components of the emulsion, sunflower oil and whey protein a) from 1320 cm^{-1} to 1460 cm^{-1} and b) from 2900 cm^{-1} to 3040 cm^{-1}.

2.3.3. Evaluation of the Efficiency of Cleaning Protocols on Membrane Emulsification by ATR-IRMS

To obtain more insight into the efficiency of a widely used non-ionic and food-grade surfactant in removing the major foulants present in the feed, particularly sunflower oil, membranes that

underwent the five different cleaning procedures with Tween 20 (TW2P1.5, TW2P5, TW3P5, TW3P7 and TW4P5) were characterized using ATR-IRMS. As shown in **Figure 2.8** (the raw spectra of the membrane after each cleaning procedure and the fouled membrane after emulsification) a band of around 1743 cm^{-1} remained after each cleaning procedure and was also present in the membrane after the premix emulsification process, but did not appear in the new membrane (**Figure 2.6**).

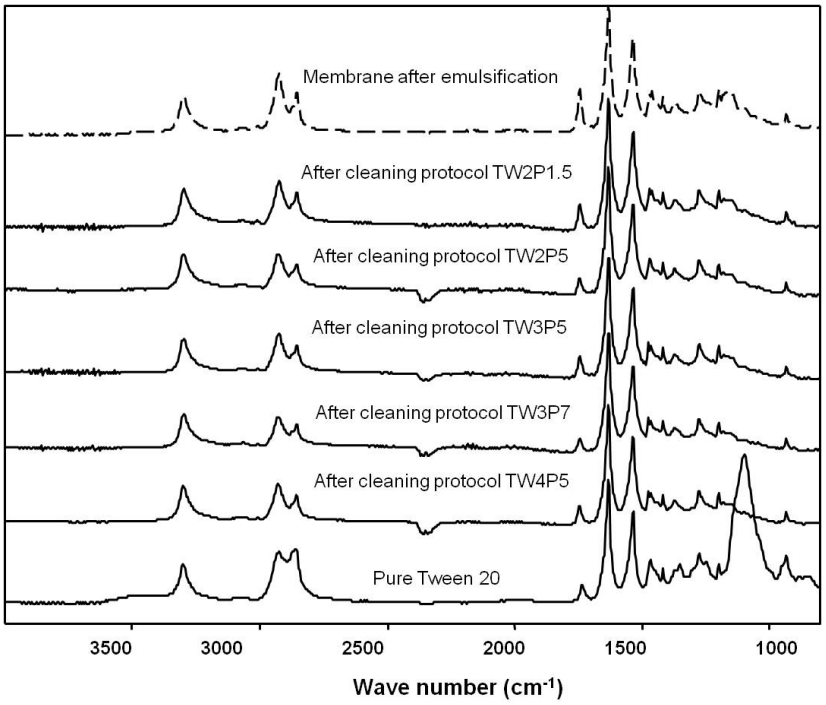

Figure 2.8. ATR-IRMS spectra of pure Tween 20 and fouled and cleaned nylon membrane after applying different cleaning conditions: TW2P1.5, TW2P5, TW3P5, TW3P7 and TW4P5 using ATR diamond crystal in reflectance mode (from 4000 cm^{-1} to 800 cm^{-1}).

This indicates that with the cleaning protocols using Tween 20, it is not possible to completely remove all the fouling components, which was also found when analyzing the water flux recovery (**Table 2.2**). However, of the cleaning procedures studied using the ATR-IRMS technique, and according to the results shown in **Figure 2.8**, TW3P7 is the most efficient cleaning process and TW2P1.5 is the least efficient. Efficiency values were obtained by

calculating the area of the 1743 cm^{-1} band, which is very clearly distinguished and the most consistent of the bands found solely on the fouling membrane spectra. The average area of the band on the fouled membrane was taken as 100%, and the reduction in the area of this band after each cleaning procedure was calculated. Therefore, the efficiency ratings (**Table 2.2**) clearly show that the TW3P7 cleaning procedure was the most efficient and TW2P1.5 the least efficient. The results obtained using ATR-IRMS characterization completely agree with the water flux recovery values presented in T**able 2.2**.

Table 2.2. *Percentage of water flux recovery calculated according to equation.2.1 and cleaning efficiency of each cleaning procedure calculated according to equation 2.2 after each cleaning step of fouled nylon membranes.*

Samples	Water flux recovery (%)	Av. Area of 1743 cm^{-1}	Efficiency
TW2P1.5	26.9	0,36689	77 % $\pm$ 0.08
TW2P5	41.7	0,27308	83 % $\pm$ 0.04
TW4P5	50.2	0,27173	83 % $\pm$ 0.12
TW3P7	54.6	0,16785	89 % $\pm$ 0.06
TW3P5	51.0	0,23821	85 % $\pm$ 0.13

According to those values the lowest water flux recovery was obtained for Tween 2% at 150 kPa (TW2P1.5) and the highest water flux recovery was obtained when using 3% Tween 20 at 700 kPa (TW3P7) (**Table 2.2**). Looking at both ATR-IRMS membrane characterization and water flux recovery values, it is clear that complete cleaning of the membranes was not achieved in any case. In the membrane cleaning process, the fouling residues in the membrane could be mainly coming from adsorbed protein, but ATR-IRMS characterization could not detect it because the band for the amines from the proteins will show together with the band for the amines coming from the nylon membrane. It is also worthy to mention that although the adsorption between the surfactant and the membrane surface has been reported (Al-Almoudi and Lovitt, 2007), ATR-IRMS results show that Tween 20 was not present in the membrane surface after the

cleaning protocols that used that agent. The typical band of Tween 20 at 1100 cm^{-1} (**Figure 2.8**) did not appear in any of the membranes cleaned with Tween 20. We assumed that the adsorption of the surfactant has been limited in our case to the internal porous structure of the membrane.

2.3.4. SIMCA Analysis of New and Fouled Nylon Membranes

Infrared spectra analysis (1800-900 cm^{-1}) using SIMCA classification models of new and fouled membranes as well as membranes with sunflower oil and whey protein, permitted tight clustering, clear differentiation and zero misclassifications among samples (**Figure 2.9a**). Discriminating power of SIMCA mainly showed four strong spectral bands at 1550, 1516, 1099 and 1057 cm^{-1} (**Figure 2.9b**). The first two absorption bands, 1550 and 1516 cm^{-1}, were associated to N-H bending and carbonyl stretching bands, respectively (Helm *et al.,* 1991). These two bands are diagnostic of secondary amides (whey protein and nylon membrane).The last two absorption peaks, 1099 and 1057 cm^{-1}, were related with asymmetric and symmetric stretching modes of C-O-C (polysaccharides) of esters presents in sunflower oil and whey protein (Helm *et al.,* 1991). These four bands clearly differentiate between fouled and new membranes spectra. Interclass distances (ICD) ranged from 6.1 to 39.7 (**Table 2.3**) showing chemical differences among samples.

Table 2.3. *SIMCA interclass distances of fouled and new nylon membrane and the two components of the emulsion, sunflower oil and whey protein. These distances were obtained using transformed (second derivative, 15 points window) ATR-IRMS spectra using diamond crystal accessory in reflectance mode and collected in the 1800-900 cm^{-1} region.*

	Fouled membrane	New membrane	Sunflower oil	Whey protein
Fouled membrane	0.0			
New membrane	25.0	0.0		
Sunflower oil	6.1	39.7	0.0	
Whey protein	19.5	21.8	18.1	0.0

Sunflower oil showed a similar pattern of clustering to fouled membrane indicating similarities in their chemical composition (**Figure 2.9a**). Thus, fouled membrane had more sunflower oil than whey protein on its surface.

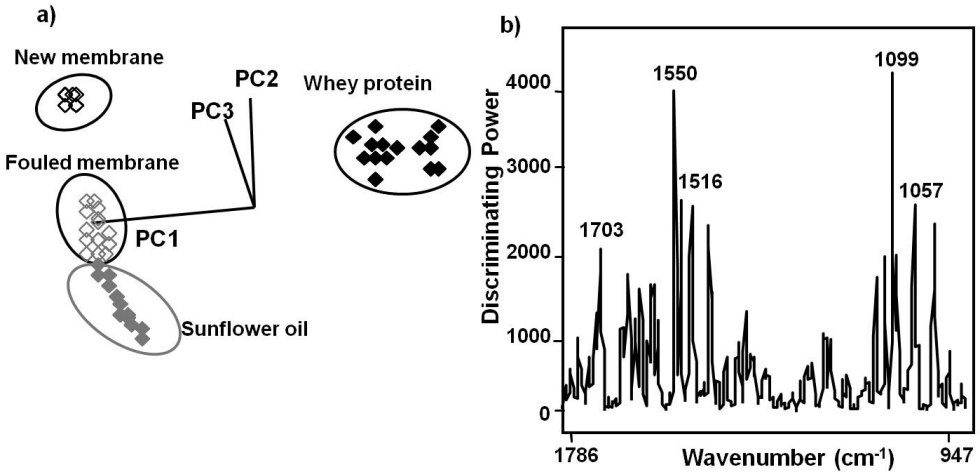

Figure 2.9. SIMCA class projections (a) and discriminating power (b) of transformed (second derivative, 15 points window) ATR-IRMS spectra of new and fouled nylon membrane and the two components of emulsion, sunflower oil and whey protein.

This finding was also supported with the ICD results (**Table 2.4**), the ICD value between sunflower oil and fouled membrane was remarkably smaller than the ICD between whey protein and fouled membrane, 6.11 and 19.47 respectively.

2.3.5. SIMCA Analysis of Cleaned and Fouled Nylon Membranes

Infrared spectra analysis (1800-900 cm^{-1}) using SIMCA classification model of cleaned membranes, permitted tight clustering and clear differentiation between fouled membrane and the cleaning protocols applied (**Figure 2.10a**).

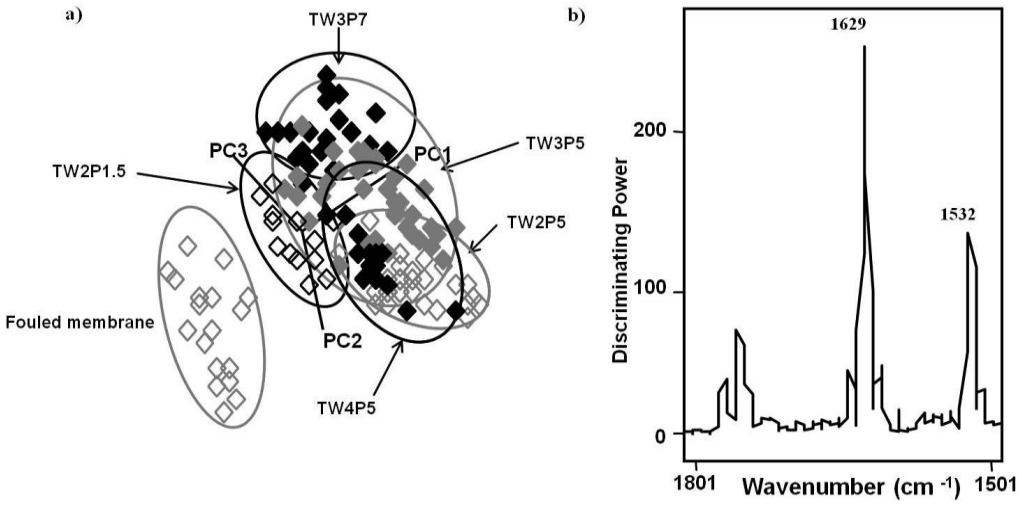

Figure 2.10. SIMCA class projections (a) and discriminating power (b) of transformed (second derivative, 15 points window) ATR-IRMS spectra of fouled and nylon membrane after applying different cleaning conditions: 2% of Tween 20 and 150 kPa pressure (TW2P1.5) , 2% of Tween 20 and 500 kPa pressure (TW2P5), 3% of Tween 20 and 500 kPa pressure (TW3P5), 3% of Tween 20 and 700 kPa pressure (TW3P7) and 4% of Tween 20 and 500 kPa pressure (TW4P5).

The ICD values between cleaned and fouled membranes (**Table 2.4**) showed that TW4P5 and TW3P7 were especially different from the fouled membrane (ICD 9.7 and 9.6 respectively). Therefore, the application of 3 or 4% of Tween 20 using N_2 pressure of with 700 or 500 kPa, were the most effective protocols among those tested, to regenerate the nylon membrane after the emulsification process. On the other hand, the application of 2% of Tween 20 and 150 kPa of N_2 pressure was the less effective cleaning protocol applied (TW2P1.5 ICD 5.4). These results are in agreement with flux recovery data obtained for these membranes (**Table 2.2**).

Discriminating power of SIMCA model showed a dominant band at 1629 cm^{-1} (**Figure 2.10b**) that allowed differentiating between fouled and cleaned membranes. This band is related to the amide I band of the whey protein or nylon membrane (Bird and Bartlett, 2002). ATR-IRMS combined with multivariate analysis, is a simple and rapid technique to discriminate between

fouled and clean membranes and to detect the most effective cleaning protocol among the treatments applied.

Table 2.4. *SIMCA interclass distances of fouled and nylon membrane after applying different cleaning conditions: TW2P1.5 TW2P5 TW3P5, TW3P7 and TW4P5 as explained in Table 2.1. These distances were obtained using transformed (second derivative, 15 points window) ATR-IRMS spectra using diamond crystal accessory in reflectance mode and collected in the 1800-900 cm^{-1} region.*

	Fouled membrane	TW2P1.5	TW2P5	TW3P5	TW3P7	TW4P5
Fouled membrane	0.0					
TW2P1.5	5.4	0.0				
TW2P5	7.5	1.0	0.0			
TW3P5	8.6	1.1	1.1	0.0		
TW3P7	9.6	1.2	0.9	0.8	0.0	
TW4P5	9.7	2.1	0.6	1.7	1.8	0.0

The current applications of ATR-FTIR in membrane characterization have been mainly based on qualitative analysis of the spectra of the membranes, as mentioned in the introduction section. ATR-IRMS coupled with SIMCA could provide valuable information about the microscopic phenomena detecting the components responsible for membrane fouling.

2.3.6. Detection of Sunflower Oil and Whey Protein on MCE Membrane

Raw spectra and secondary derivative transformations of new and fouled MCE membranes, sunflower oil and whey protein are shown in **Figure 2.11a** and **b**, respectively. The raw spectrum (**Figure 2.11a**) and the 2nd derivative (**Figure 2.11b**) of fouled membrane showed an IR band at 1743 cm^{-1} that was not present in the spectrum of new MCE membrane. This IR band was linked to stretching modes of carboxylic acids and esters present in the sunflower oil pointing out the presence of sunflower oil on the fouled membrane (Tait *et al.,* 1997; Hirschman, 2001; Mayo, 2004). Moreover, another IR band at 2920 cm^{-1} linked to CH_2 and CH_3 stretching vibrations of fatty acids (Tait *et al.,* 1997) was also a clear indication of the role of

sunflower oil as a foulant. From the raw spectra (**Figure 2.11a**), the protein band at 1640 cm^{-1} (amide I) was overlapped with the IR band of NO_2 (symmetric stretching) present in MCE membrane but not with the protein band at 1535 cm^{-1} (amide II). Moreover, the amide II band (>N-H stretching) at 1535 cm^{-1} linked to whey protein was not observed on the fouled membrane spectra and their 2nd derivative representation but found on the whey protein (Tait *et al.,* 1997; Mayo, 2004).

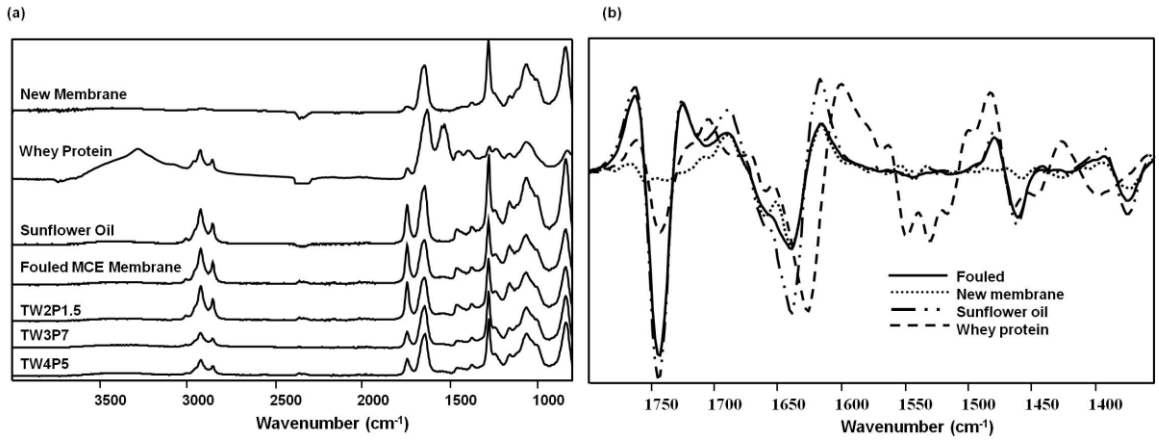

Figure 2.11. Typical ATR-IRMS spectrum (a) and secondary derivative transformations (b) of whey protein, sunflower oil and new and fouled MCE membranes using a diamond crystal accessory in reflectance mode.

The ATR-IRMS and SIMCA results of section **2.3.4** and **2.3.5** showed that sunflower oil was the main foulant agent on nylon microfiltration membranes used in premix emulsification. The nylon membrane showed two IR bands at 1640 and 1535 cm^{-1} that were overlapping with amide I and II bands of whey protein (Mayo, 2004). Therefore, it was not possible to determine the role of whey protein on the fouling. However, whey protein has been reported to cause fouling on microfiltration membranes (Güell and Davis, 1996; Paugam *et al.,* 2010). These differences may be explained by the fact that whey protein could be located mainly inside the membrane pores (Hilal and Johnso, 2010) and therefore can not be detected by ATR-IRMS.

2.3.7. SIMCA analysis of New and Fouled MCE Membrane

Further analysis of the raw spectra using SIMCA classification model of the MCE membrane samples (**Figure 2.12a**) helped to determine the role of whey protein as a foulant agent. We have demonstrated the advantage of using SIMCA for further analysis of raw infrared spectra during the characterization of new and fouled nylon membranes.

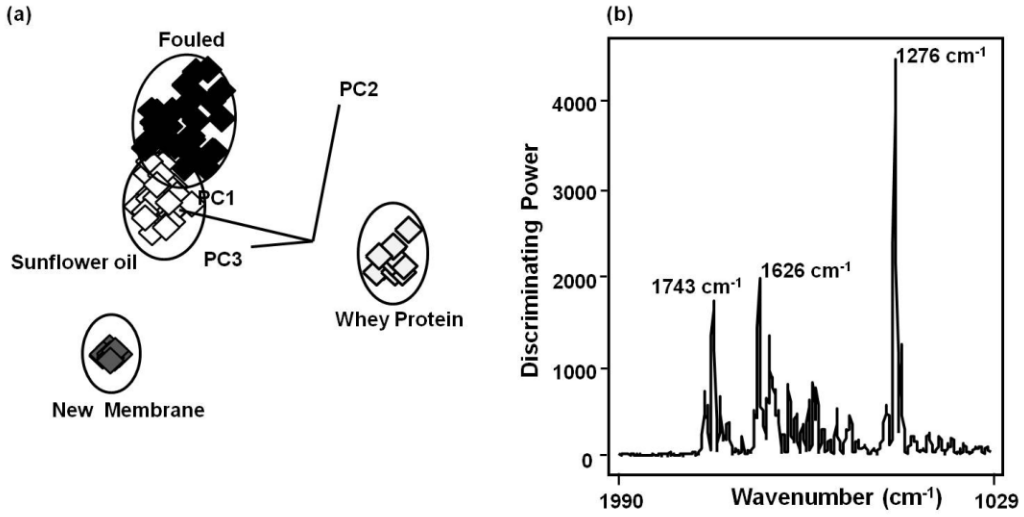

Figure 2.12. SIMCA of class projections (a) and discriminating power (b) of transformed (second derivative, 15 points window) ATR-IRMS spectra of new and fouled membranes and membrane with sunflower oil and whey protein.

Infrared spectra analysis (2000–1000 cm^{-1}) using SIMCA classification models of whey protein, sunflower oil, new and fouled MCE membranes showed tight clustering and clear separation between samples (**Figure 2.12**). Discriminating power of SIMCA model between protein, sunflower oil, new and fouled MCE membranes showed three major bands at 1743, 1626 and 1276 cm^{-1}. These bands were due to the >C=O stretching modes of carbonyl group and esters of the sunflower oil, the amide I of the whey protein and the NO_2 symmetric stretching of the nitro group present in the MCE membrane respectively (**Figure 2.12b**) (Tait *et al.,* 1997; Mayo, 2004). Figure 8a showed that the fouled MCE membrane was clustered very close to the

sunflower oil than to the whey protein. This observation was supported with the interclass distance values (**Table 2.5**). ICD value between fouled membrane and sunflower oil was 2.0 (**Table 2.5**) indicating similarities in their chemical composition between these two samples but not between fouled membrane and whey protein (ICD 12.5).

Table 2.5. *Interclass distance of SIMCA of transformed (second derivative, 15 points window) ATR-IRMS spectra (1990–1029 cm^{-1}) of new and fouled membranes and membrane with sunflower oil and whey protein.*

	New membrane	Fouled membrane	Sunflower oil	Whey protein
New membrane	0.0			
Fouled membrane	11.1	0.0		
Sunflower oil	11.1	2.0	0.0	
Whey protein	21.5	12.5	18.4	0.0

Discriminating power of SIMCA model between new and fouled MCE membrane (**Figure 2.13b**) showed two IR bands at 1743 and 1278 cm^{-1} associated to >C=O stretchinging modes of carbonyl group and esters of the sunflower oil and the NO_2 symmetric stretching of the nitro group present in the MCE membrane, respectively (Tait *et al.,* 1997; Mayo, 2004) but no IR band related with whey protein. This further indicates that, sunflower oil was the dominating foulant as it has been observed on the nylon membrane.

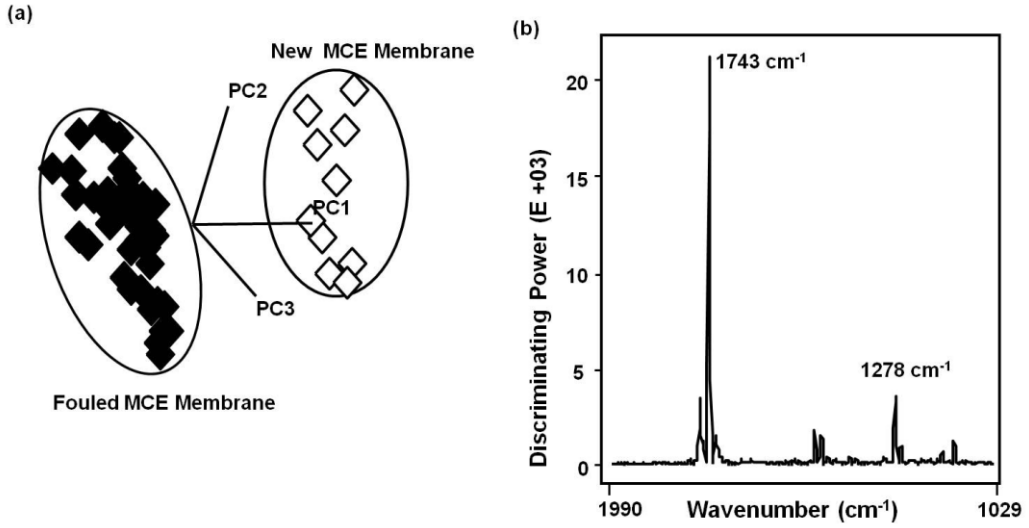

Figure 2.13. Soft independent modeling class analogy (SIMCA) of class projections (a) and discriminating power (b) of transformed (second derivative, 15 points window) ATR-IRMS spectra of new and fouled MCE membranes.

2.3.8. SIMCA Analysis of Cleaned and Fouled MCE Membranes

Three cleaning protocols using different Tween 20 solutions in a backwash mode, (TW2P1.5, 2% Tween 20 and 150 kPa pressure, TW4P5, 4% Tween 20 and 500 kPa pressure, TW3P7, 3% Tween 20 and 700 kPa pressure) were used to clean MCE membranes used in premix ME processes. These cleaning protocols were selected for this experiment based on their performance efficiency during the cleaning of fouled nylon membrane (**Table 2.2**). Some researchers have reported a quantitative application of ATR-IR based on the height ratio of two targeted bands (Wemsy Diagne *et al.,* 2013). Here, a specific IR band was selected based on the intensity and consistency. To study the efficiency of the cleaning protocols used for the cleaning of fouled MCE, the approach to evaluate the effectiveness of cleaning fouled nylon membranes were followed based on the IR band at 1743 cm^{-1}, as this band was the consistent and present in all fouled MCE membrane spectra.

Table 2.6. *SIMCA interclass distances of new, fouled and MCE membrane after applying different cleaning conditions: TW2P1.5, TW3P7 and TW4P5. These distances were obtained using transformed (second derivative, 15 points window) ATR-IRMS spectra using a diamond crystal accessory in reflectance mode and collected in the 2000–900 cm^{-1} region.*

	New membrane	Fouled membrane	TW2P1.5	TW3P7	TW4P5
New membrane	0.0				
Fouled membrane	12.7	0.0			
TW2P1.5	9.8	1.1	0.0		
TW3P7	6.4	2.2	0.9	0.0	
TW4P5	7.2	2.4	1.1	0.4	0.0

Therefore, the area of this distinct spectral band (1743 cm^{-1}) of fouled and cleaned membranes was calculated using **equation 2.2**. The cleaning efficiency of TW2P1.5, TW3P7 and TW4P5 was 4.2, 37.8 and 31.6% respectively (**Table 2.6**). Thus, TW4P5 and TW3P7 cleaning protocols were relatively better than the TW2P1.5, which is the one with lower surfactant concentration and lower transmembrane pressure.

Table 2.7. *Percentage of water flux recovery calculated according to equation 2.1 and cleaning efficiency of each cleaning procedure calculated according to equation 2.2 after each cleaning step of MCE membranes.*

Samples	Water flux recovery (%)	Av. area of 1743 cm^{-1}	Efficiency
TW2P1.5	19.9 ± 1.6	2.0 ± 0.0	4.2 ± 1.9
TW3P7	63.1 ± 0.3	1.3 ± 0.1	37.8 ± 9.6
TW4P5	59.3 ± 0.2	1.4 ± 0.2	31.6 ± 8.2

Moreover, in our study the water flux recovery (WFR) was calculated by equation 2.1 using the water flux before and after the cleaning of fouled membranes (**Table 2.7)**. From WFR values, TW4P5 and TW3P7 cleaning protocols were also better than the TW2P1.5 showing the same trend regarding cleaning efficiencies than the one found when analysing the data obtained by ATR-IRMS. The WFR values are directly related with the degree of cleaning achieved after each treatment on the membrane surface and inside the pores (Trentin *et al.,* 2011). Since ATR-IRMS

spectra mainly provide information regarding the membrane surface, we can assume that the cleaning efficiency values obtained by ATR-IRMS will be directly related to the membrane surface cleaning efficiency.

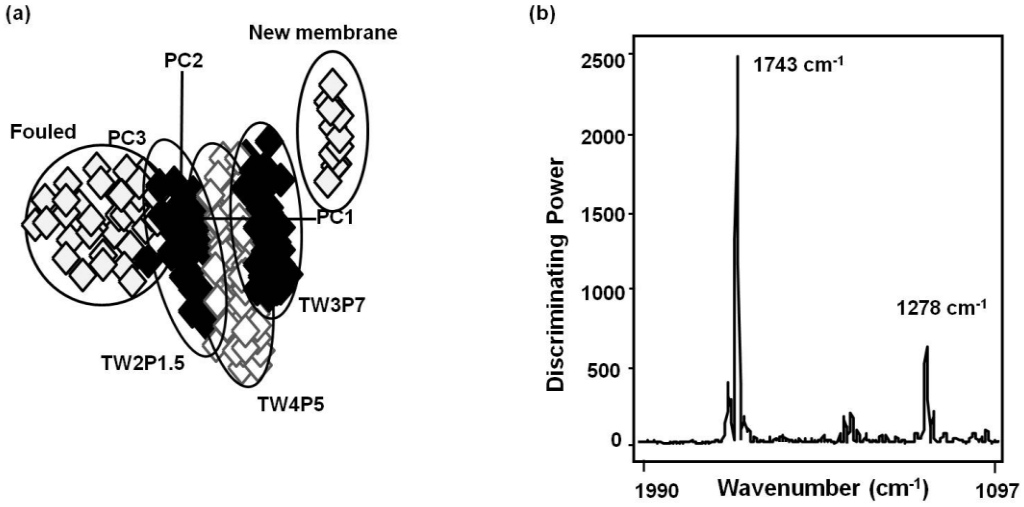

Figure 2.14. SIMCA of class projections (a) and discriminating power (b) of transformed (second derivative, 15 points window) ATR-IRMS spectra of new, fouled and MCE membrane after applying different cleaning conditions: TW2P1.5, TW3P5, TW3P7 and TW4P5.

The SIMCA classification model of the transformed spectra between 2000-1000 cm^{-1} of fouled and cleaned MCE membranes is shown in **Figure 2.14**. The class projection plot in **Figure 2.14a** of the SIMCA analysis showed cleaned membranes clustering close to each other. From these results, there was no clear difference on their performances regarding the cleaning of the fouled MCE membranes. The ICD values further confirm the class projection results where, the values range from 0.9 to 1.1 (**Table 2.7**). However, the membrane cleaned with 2% Tween 20 at 150 kPa (TW2P1.5) is closer to the fouled membrane than the membranes cleaned with 3 or 4% Tween 20. From this observation we can conclude that, TW2P1.5 had lower efficiency than TW4P5 and TW3P7.

2.4. CONCLUSIONS

ATR-IRMS combined with multivariate analysis technique provides qualitative information regarding the efficiency of cleaning protocols for organic microfiltration membranes used in premix ME. The results showed that the main foulant on both nylon and MCE membrane surfaces after the emulsification process was sunflower oil, while whey protein could not be significantly detected. This technique allowed to differentiate new, fouled and cleaned membranes and detect the most and less effective membrane cleaning protocols among those tested. When nylon membrane was used, the amide band overlapping has been observed that made the result inconclusive regarding the fouling of protein on nylon membrane. However, using a MCE membrane it was possible to conclude that whey protein was not present on the membrane surface after applying cleaning with Tween 20, regardless of its concentration or the pressure applied. Since the MCE membrane did not show an amide band that could overlap with the one from the protein. However, whey protein could still be adsorbed and/or blocking some membrane pores, since the results on water flux recovery indicate that the cleanings were not complete. ATR-FTIR has been used in membrane characterization, it is believed that this work further proofs the potential of ATR-IRMS combined with multivariate analysis technique for characterization of membrane fouling as well as membrane cleaning protocols. However, it must be mentioned that the characterization is restricted to the surface under the present experimental conditions, even though it would be possible to prepare cross sections of the membrane samples to obtain information on foulants retained inside the membrane.

2.5. REFERENCES

Al-Amoudi, A.; Lovitt, R.W. Fouling strategies and the cleaning system of NF membranes and factors affecting cleaning efficiency. *Journal of Membrane Science* **2007,** 303, (1-2), 4-28.

Argüello, M.A.; Álvarez, S.; Riera, F.A.; Álvarez, R. Enzymatic cleaning of inorganic ultrafiltration membranes fouled by whey proteins. *Journal of Agricultural and Food Chemistry* **2002,** 50, (7), 1951-1958.

Barbar, R.; Durand, A.; Ehrhardt, J.J.; Fanni, J.; Parmentier, M. Physicochemical characterization of a modified cellulose acetate membrane for the design of oil-in-water emulsion disruption devices. *Journal of Membrane Science* **2008**, 310, (1-2), 446-454.

Beekes, M.; Lasch, P.; Naumann, D. Analytical applications of Fourier transform-infrared (FT-IR) spectroscopy in microbiology and prion research. *Veterinary Microbiology* **2007**, 123, (4), 305-319.

Belfer, S.; Fainchtain, R.; Purinson, Y.; Kedem, O. Surface characterization by FTIR-ATR spectroscopy of polyethersulfone membranes-unmodified, modified and protein fouled. *Journal of Membrane Science* **2000**, 172, (1-2), 113-124.

Bird, M.R.; Bartlett, M. Measuring and modelling flux recovery during the chemical cleaning of MF membranes for the processing of whey protein concentrate. *Journal of Food Engineering* **2002**, 53, (2), 143-152.

Carlsson, D.J.; Dal-Cin, M.M.; Black, P.; Lick, C.N. A surface spectroscopic study of membranes fouled by pulp mill effluent. *Journal of Membrane Science* **1998,** 142, (1), 1-11.

Chang, I.; Le Clech, P.; Jefferson, B.; Judd, S. Membrane fouling in membrane bioreactors for wastewater treatment. *Journal of Environmental Engineering* **2002**, 128, (11), 1018-1029.

Charcosset C., Membrane systems and technology. In: Murray M.Y. (Ed) *Comprehensive biotechnology, Academic Press*, Burlington, MA, **2011,** pp. 603-618.

De Maesschalck, R.; Jouan-Rimbaud, D.; Massart, D.L. The Mahalanobis distance. *Chemometrics and intelligent laboratory systems* **2000**, 50, (1), 1-18.

Dickinson, E. Emulsions and droplet size control. In: Wedlock, D.J. (Ed) Controlled particle, droplet and bubble formation, Butterworth-Heinemann, Oxford: **1994**, pp.189-216, Chapter 7.

Dunn W.J.; Wold, S. SIMCA pattern recognition and classification. *In:* van de Waterbeemd H. (Ed) Chemometric methods in molecular design. VCH Publishers, NY **1995**, pp. 179-193.

Ferrando, M.; Rŏżek, A.; Zator, M.; López, F.; Güell, C. An approach to membrane fouling characterization by confocal scanning laser microscopy. *Journal of Membrane Science* **2005**, 250, (1-2), 283-293.

Grasso, E.M.; Yousef, A.E.; Castellvi, S.D.; Rodriguez-Saona, L.E. Rapid detection and differentiation of *Alicyclobacillus* species in fruit juice using hydrophobic grid membranes and attenuated total reflectance infrared microspectroscopy. *Journal of Agricultural and Food Chemistry* **2009**, 57, (22), 10670-10674.

Güell, C.; Davis, R.H. Membrane fouling during microfiltration of protein mixtures. *Journal of Membrane Science* **1996**, 119, (2), 269-284.

Helm, D.; Labischinski, H.; Naumann, D. Elaboration of a procedure for identification of bacteria using Fourier-Transform IR spectral libraries: a stepwise correlation approach. *Journal of Microbiological Methods* **1991**, 14, (2), 127-142.

Hilal, N.; Johnson, D. The use of atomic force microscopy in membrane characterization In: Enrico, D.; Lidietta, G. (Eds) Comprehensive membrane science and engineering, *Elsevier:* Oxford, **2010**; pp 337-354.

Hruschka, W.R.; Williams, P.; Norris, K. Near infrared technology in the agricultural and food industries. In: Williams P.; Norris K. (Eds) Data analysis: Wavelength selection methods. *American Association of Cereal Chemists:* Minnesota, **2001**, pp. 39-58.

Kandori, K. Applications of microporous glass membranes: membrane emulsification. In: Gaonkar, A.G. (Ed) Food Processing: Recent Development. *Elsevier*, Amsterdam **1995**, 113-142.

Kansiz, M.; Heraud, P.; Wood, B.; Burden, F.; Beardall, J.; McNaughton, D. Fourier transform infrared microspectroscopy and chemometrics as a tool for the discrimination of *cyanobacterial* strains. *Phytochemistry* **1999,** 52, (3), 407-417.

Karbstein, H.; Schubert, H. Developments in the continuous mechanical production of oil-in-water macro-emulsions. *Chemical Engineering and Processing: Process Intensification* **1995**, 34, (3), 205-211.

Kuzmenko, D.; Arkhangelsky, E.; Belfer, S.; Freger, V.; Gitis, V. Chemical cleaning of UF membranes fouled by BSA. *Desalination* **2005**, 179, (1-3), 323-333.

Li, W.; Zhou, J.; Gu, J.-S.; Yu, H.-Y. Fouling control in a submerged membrane-bioreactor by the membrane surface modification. *Journal of Applied Polymer Science* **2010,** 115, (4), 2302-2309.

Loh, S.; Beuscher, U.; Poddar, T.K.; Porter, A.G.; Wingard, J.M.; Husson, S.M.; Wickramasinghe, S.R. Interplay among membrane properties, protein properties and operating conditions on protein fouling during normal-flow microfiltration. *Journal of Membrane Science* **2009**, 332, (1-2), 93-103.

Mallevialle, J.; Anselme, C.; Marsigny, O. Effects of humic substances on membrane processes. In: Suffet I.H.; MacCarthy Patrick (Eds) Aquatic humic substances. *American Chemical Society*: Denver, Colorado **1989**; pp 749-767.

Männig, A.; Baldauf, N.A.; Rodriguez-Romo, L.A.; Yousef, A.E.; Rodriguez-Saona, L.E. Differentiation of *Salmonella enterica* serovars and strains in cultures and food using infrared spectroscopic and microspectroscopic techniques combined with soft independent modeling of class analogy pattern recognition analysis. *Journal of Food Protection* **2008**, 71, (11), 2249-2256.

Mayo, D.W. Spectra of carbonyl compounds of all kinds (factors affecting carbonyl group frequencies). In: Mayo D.W.; Miller F.A.; Hannah R.W. (Eds) Course notes on the interpretation of infrared and Raman spectra. *John Wiley & Sons, Inc.*: New Jersey, **2004**, pp 179-204.

Nakashima, T.; Shimizu, M.; Kukizaki, M. Membrane emulsification by microporous glass. *Key Engineering Materials* **1992**, 61, 513-516.

Nataraj, S.; Schomäcker, R.; Kraume, M.; Mishra, I.M.; Drews, A. Analyses of polysaccharide fouling mechanisms during crossflow membrane filtration. *Journal of Membrane Science* **2008**, 308, (1-2), 152-161.

Nazir, A.; Schroën, K.; Boom, R. Premix emulsification: A review. *Journal of Membrane Science* **2010**, 362, (1-2), 1-11.

Nigam, M.O.; Bansal, B.; Chen, X.D. Fouling and cleaning of whey protein concentrate fouled ultrafiltration membranes. *Desalination* **2008**, 218, (1-3), 313-322.

Paugam, L.; Delaunay, D.; Rabiller-Baudry, M. Cleaning efficiency and impact on production fluxes of oxidising disinfectants on a pes ultrafiltration membrane fouled with proteins. *Food and Bioproducts Processing* **2010**, 88, (4), 425-429.

Piacentini, E.; Figoli, A.; Giorno, L.; Drioli, E. Membrane emulsification. In: Drioli, E.; Giorno, L.(Eds) Comprehensive Membrane Science and Engineering. *Elsevier*: Oxford, **2010**, pp 47-78.

Pirouette, Multivariate data analysis version 4.0 User Manual [online]. Infometrix, Inc. Bothell, WA, **2008**.

Rabiller-Baudry, M.; Le Maux, M.; Chaufer, B.; Begoin, L. Characterization of cleaned and fouled membrane by ATR-FTIR and EDX analysis coupled with SEM: application to UF of skimmed milk with a PES membrane. Desalination **2002**, 146, (1-2), 123-128.

Rabiller-Baudry, M.; Bégoin, L.; Delaunay, D.; Paugam, L.; Chaufer, B. A dual approach of membrane cleaning based on physico-chemistry and hydrodynamics: Application to PES membrane of dairy industry. *Chemical Engineering and Processing: Process Intensification* **2008**, 47, (3), 267-275.

Rezvanpour, A.; Roostaazad, R.; Hesampour, M.; Nyström, M.; Ghotbi, C. Effective factors in the treatment of kerosene-water emulsion by using UF membranes. *Journal of Hazardous Materials* **2009**, 161, (2-3), 1216-1224.

Rice, G.; Barber, A.; O'Connor, A.; Stevens, G.; Kentish, S. Fouling of NF membranes by dairy ultrafiltration permeates. *Journal of Membrane Science* **2009,** 330, (1-2), 117-126.

Scott K., Handbook of industrial membranes (2nd ed.), Elsevier Science, Lancaster, PA **2003.**

Silvestre de los Reyes, J.; Charcosset, C. Preparation of water-in-oil and ethanol-in-oil emulsions by membrane emulsification. *Fuel* **2010**, 89, (11), 3482-3488.

Shon, H.K.; Vigneswaran, S.; Kim, I.S.; Cho, J.; Ngo, H.H. Fouling of ultrafiltration membrane by effluent organic matter: A detailed characterization using different organic fractions in wastewater. *Journal of Membrane Science* **2006**, 278, (1-2), 232-238.

Tait, J.K.F.; Davies, G.; McIntyre, R.; Yarwood, J. FTIR-ATR studies of interfacial interactions in epoxy resin/polymer laminate structures. *Vibrational Spectroscopy* **1997,** 15, (1), 79-89.

Trentin, A.; Güell, C.; López, F.; Ferrando, M. Microfiltration membranes to produce BSA-stabilized O/W emulsions by premix membrane emulsification. *Journal of Membrane Science* **2010,** 356, (1-2), 22-32.

Trentin, A.; De Lamo, S.; Güell, C.; López, F.; Ferrando, M. Protein-stabilized emulsions containing beta-carotene produced by premix membrane emulsification. *Journal of Food Engineering* **2011,** 106, (4), 267-274.

Väisänen, P.; Bird, M.R.; Nyström, M. Treatment of UF membranes with simple and formulated cleaning agents*. Food and Bioproducts Processing* **2002,** 80, (2), 98-108.

Van der Graaf, S.; Schroën, C.G.P.H.; Boom, R.M. Preparation of double emulsions by membrane emulsification-a review. *Journal of Membrane Science* **2005**, 251, (1-2), 7-15.

Wemsy Diagne, N.; Rabiller-Baudry, M.; Paugam, L. On the actual clean-ability of polyethersulfone membrane fouled by proteins at critical or limiting flux. *Journal of Membrane Science* **2013,** 425-426, 40-47.

Wold, S.; Albano, C.; Blomquist, G.; Coomans, D.; Dunn, W.J.; Edlund ,U.; Eliasson, B.; Hellberg, S.; Johansson, E.; Norden, B.; Sjastrem, M.; Saderstrem, B. and Wold, H. Pattern recognition by means of disjoint principal component models (SIMCA), In: Haskuldson, A. (Ed) *Proceedings of the symposium on applied statistics*. Technical University Copenhagen, Copenhagen, **1981**, pp. 475-487

Wu, D.A.N.; Bird, M.R. The fouling and cleaning of ultrafiltration membranes during the filtration of model tea component solutions. *Journal of Food Process Engineering* **2007,** 30, (3), 293-323.

Zator, M.; Ferrando, M.; López, F.; Güell, C. Membrane fouling characterization by confocal microscopy during filtration of BSA/dextran mixtures. *Journal of Membrane Science* **2007**, 301, (1-2), 57-66.

CHAPTER 3

Discrimination and classification of acetic acid bacteria and Saccharomyces cerevisiae *strains by attenuated total reflectance microspectroscopy*

3.1. INTRODUCTION

In the last decade, Fourier transform infrared spectroscopy (FTIR) technique has been used to detect and discriminate microorganisms in different food products, such as, *Alicyclobacillus* in fruit juice (Grasso *et a*l. 2009), *Lactobacilli* in meat and cheese (Oust *et al.* 2004) and *Salmonella* in apple juice (Yu *et al.* 2004). The advantage of using FTIR is that it is rapid, sensitive, can provide a real time measurement, simplify data acquisition and enable immediate predictions (Shiroma-Kian *et al.* 2008; De Nardo *et al.* 2009). Attenuated total reflectance infrared microspectroscopy (ATR-IRMS) provides bands from all the cellular components of microorganism (e.g. cell membrane and wall components, proteins and nucleic acid), giving spectral signatures or "fingerprints" that permit the classification of microorganisms at the strain and serovar level (Armenta *et al.* 2005; Baldauf *et al.* 2007). The raw spectra of microorganisms are nearly very similar, hence a supervised multivariate pattern recognition technique needs to be used to detect and classify microbial samples in to their different classes (Armenta *et al.* 2005; Baldauf *et al.* 2007; Shiroma-Kian *et al.* 2008; De Nardo *et al.* 2009). Recently, in literature it is reported that using a supervised multivariate classification models microorganisms can be classified at the strain and species/variety levels (Shiroma-Kian *et al.* 2008; De Nardo *et al.* 2009; Grasso *et al.* 2009).

Wine is a complex mixture of compounds which largely define its appearance, aroma, flavor and mouthful properties. In wine processing, there are different microorganisms that are known to have an effect on wine quality (color, test, and chemical composition) and participate during the fermentation process (alcoholic or malolactic) (Nieuwoudt *et al.* 2006). Among the microorganisms found in the wine production, yeast (*Saccharomyces cerevisiae*) (Nieuwoudt *et al.* 2006; König *et al.* 2009) lactic acid bacteria (Wibowo *et al.* 1985; Davis *et al.* 1988; König *et al.* 2009), and acetic acid bacteria (König *et al.* 2009) are the common ones. These microorganisms are present in the grape must or added at the beginning or during the fermentation process after being pre-incubated in a culture media. However, even though these microorganisms have positive effect on wine quality, some of them are considered causes

of wine spoilage (Bartowsky *et al.* 2003; Bartowsky and Henschke 2008). Hence, there is a strong need to rapidly detect the bacteria and yeast populations during wine fermentation. The microorganisms involved in a wine fermentation process have been studied by conventional culture techniques but are time consuming and may underestimate the number of viable bacteria. There are interesting alternatives to the traditional methods such as polymerase chain reaction (PCR) technique and flow cytometry (Bartowsky *et al.* 2003). Nevertheless, these methods need special personnel training. Developing a simple, rapid, reproducible and sensitive infrared spectroscopy method to study yeast and acid acetic bacteria populations during grape must fermentation, will be a breakthrough for wine industry.

The main objective of this research was to evaluate the potential of ATR-IRMS coupled with multivariate analysis to discriminate and classify *Saccharomyces cerevisiae* and acetic bacteria strains using hydrophobic membranes as a support.

3.2. MATERIALS and METHODS

3.2.1. Bacteria and Yeasts Growing Conditions

Gluconacetobacter xylinus (CECT 473, CECT, Colección Española de Cultivos Tipo, Universidad de Valencia, Valencia), *Gluconobacter oxydans* (CECT 315) and two strains of *Saccharomyces cerevisiae* (CECT 1327 and commercial, ref. 001412 AEB Iberica S.A, Castellbisbal, Spain) were selected for this study. Stock cultures were stored at -20^{o}C in cryobeads (Microbank™, Pro-Lab Diagnostics,). The stock cultures were transferred into 10 mL of Glucose Yeast Extract Broth (GYB, 10% w/v of glucose, Aldrich, Sigma-Aldrich., Steinhein, Germany and 1% w/v of yeast extract, Fluka, Sigma-Aldrich) for 24 h at 26^{o}C. For the second transfer, an aliquot of each activated culture (0.4 mL) was inoculated in 40 mL of commercial red grape juice (Carrefour, Madrid, España) and incubated with agitation (150 rpm) at 26^{o}C for 48 h.

3.2.2. Sample Preparation

Vegetative cells were harvested by centrifugation (6000 rpm for 5 min at room temperature) and washed twice under the same conditions using 30 mL of saline solution (SS, 0.85% NaCl) and finally re-suspended in 1 mL of SS. An aliquot of each pellet (10 µL) was deposited by vacuum filtration onto a grid of a hydrophobic membrane (HGM; ISO-GRID, Neogen Corporation, Lansing, MI). In each membrane, 4 grids were used to place the suspension of bacterial/ yeast cells and this operation was repeated three times per each strain.

Then, membranes were dried for 1 h to produce an uniform and thin film and minimize the overlapping effect of water absorption bands (3400 and 1700 cm^{-1}) in the sample spectral signal. Eight spectra (two per grid) per each sample and day of experiment were collected in the attenuated total reflectance (ATR) mode in the mid-infrared region (4000-800 cm^{-1}).

3.3. RESULTS and DISCUSSION

3.3.1. Discrimination of Acetic Acid Bacteria and Yeast Placed Onto Grids of HGM by ATR-IRMS

For this study, two strains of acetic acid bacteria and two strains of *S. cerevisiae* were used to evaluate the potential of ATR-IRMS technique to discriminate between acid acetic bacteria and yeast. **Figure 3.1** shows the raw spectra of *G. oxydans* (CECT 315) and *S. cerevisiae* **(**CECT 1327). Analyzing the IR bands obtained for the bacteria and yeast, the raw spectra of these strains are quite similar.

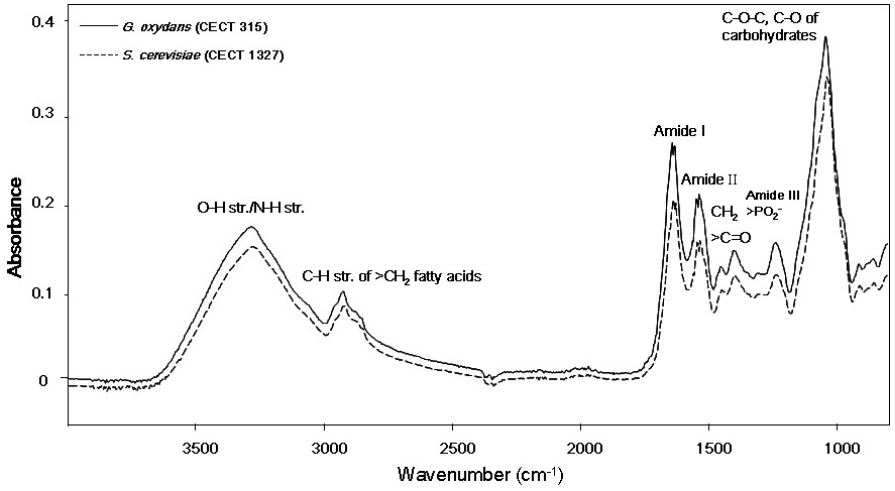

Figure 3.1. ATR-IRMS spectrum of *G. oxydans* (CECT 315) and *S. cerevisiae* **(**CECT 1327) using ATR diamond crystal in reflectance mode (from 4000 - 800 cm^{-1}).

The bands of highest proportion at approximately 1037, 1639 and 1546 cm^{-1} were associated with C-O-C and amide I and amide II group vibrations, respectively. Cell walls of Gram-negative bacteria in general composed of peptidoglaycan (5-20%) and lipopoysaccharides where as the cell walls of *Saccharomyces* are composed of mannoprotiens and β-glucans (85–90% of the cell wall dry mass) and a smaller amount of chitin (1–3%) and lipids (2–5%) which gives a structural function for the cell (Galichet *et al.* 2001; Lesage and Bussey 2006; Huanga *et al.* 2008).

Class projections illustrate the ability of SIMCA to differentiate IR data based on the first 3 principal components. Infrared spectra analysis (1600-900 cm^{-1}) of acid bacteria and yeast strains (**Figure 3.2a**) permitted tight clustering and clear differentiation among strains. Interclass distances (ICD) are Euclidian distances between centers of clusters and above 3.0 are considered as significant to identify two groups of samples as different classes (Dunn and Wold, 1995).

Table 3.1. *SIMCA interclass distances of* S. cerevisiae *(CECT 1327 and commercial) strains and acetic acid bacteria,* G. oxydans *(CECT 315) and* G. xylinus *(CECT 473). These distances were obtained using transformed (second derivative, 15 points window) ATR-IRMS spectra using a diamond crystal accessory in reflectance mode and collected in the 1675-1004 cm^{-1} region.*

	S. cerevisiae[†]	*S. cerevisiae*[‡]	*G. oxydans*	*G. xylinus*
S. cerevisiae	0.0			
S. cerevisiae	5.1	0.0		
G. oxydans	5.2	4.0	0.0	
G. xylinus	4.3	6.1	3.5	0.0

[†]*S. cerevisiae* **(**CECT 1327); [‡]*S. cerevisiae* commercial

In this experiment, ICD ranged from 3.2 to 6.3 (**Table 3.1**) showing differences between strains in their biochemical patterns. Discriminating power of SIMCA, which is a measure of variable importance in infrared frequency and contributes to the development of the classification models (Dunn and Wold. 1995), showed three strong spectral bands at 1130, 1026 and 1666 cm^{-1} (**Figure 3.2b**) located in the bacteria fingerprint region which is very reproducible spectrum region mainly associated with major cellular constituent of the total biochemical composition of the microorganism (Armenta *et al.* 2005; Baldauf *et al.* 2007). These IR peaks were related to >PO_2^- stretching of nucleic acids, O-H group of cellulose present in the bacterial cell, and amide I bands linked to the presence of mannoprotiens in yeast or peptidoglycan in bacterial cell walls, respectively (Galichet *et al.* 2001; Maquelin *et al.* 2002; Pawlak *et al.* 2003; Stark *et al.* 2004; Huanga *et al.* 2008).

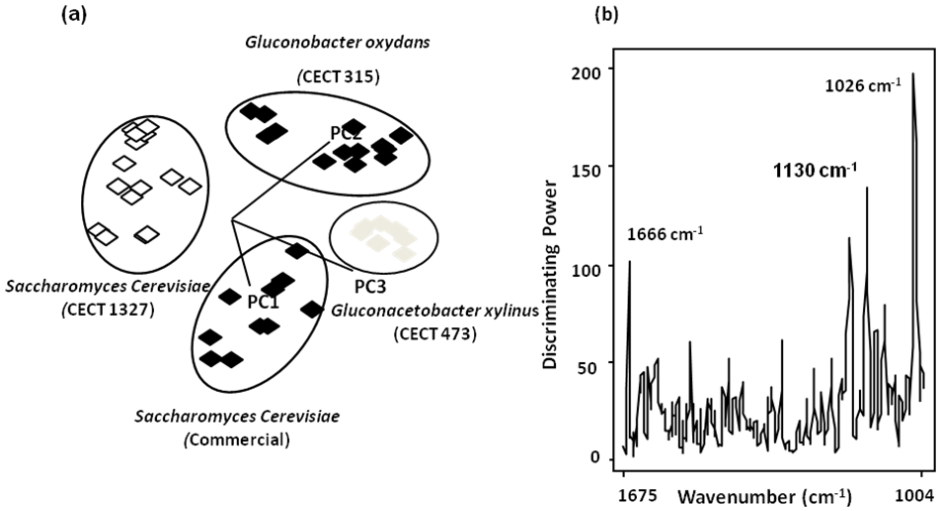

Figure 3.2. SIMCA class projections (a) and discriminating power (b) of transformed (second derivative, 15 points window) ATR-IRMS spectra of *G. oxydans* (CECT 315), *G. xylinus* (CECT 473) and *S. cerevisiae* (CECT 1327 and commercial).

3.3.2. Discrimination of Acetic Acid Bacteria or S. cerevisiae *Strains Placed onto Grids of HGM by ATR-IRMS*

It is also important to check if we can discriminate among *G. oxydans* and *G. xylinus or S. cerevisiae* strains and to detect which functional groups are related to their discrimination. The SIMCA class projection plot showed well-separated and nonoverlapping clusters among *G. oxydans* and *G. xylinu* (**Figure 3.3a**) and *S. cerevisiae* (**Figure 3.4a**) strains. Moreover, ICD was 3.5 for acetic acid bacteria strains and 5.1 for *S. cerevisiae* strains showing differences in their biochemical patterns. In the case of acetic acid bacteria strains, discriminating power of SIMCA showed two strong spectral bands at 1570 cm^{-1} and 1138 cm^{-1} (**Figure 3.3b**).

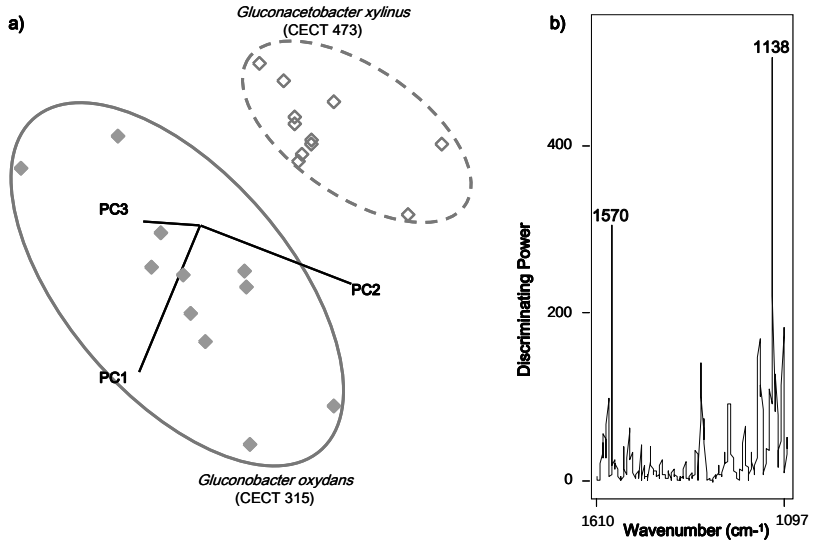

Figure 3.3. SIMCA discriminating power (a) and class projections (b) of transformed (second derivative, 15 points window) ATR-IRMS spectra of *G. oxydans* (CECT 315) and *G. xylinus* (CECT 473).

The absorption peak at 1570 cm^{-1} were linked to N-H bending of amide II protein groups present in one of the major components of *G. oxydans* and *G. xylinus* cell wall, peptidoglycan. The IR band at 1138 cm^{-1} was associated to stretching modes of O-specific polysaccharides chains of lypopolysaccharides of their cell envelope. Three bands had a predominant effect on the classification of *Saccharomyces* strains (**Figure 3. 4b**), 1590 cm^{-1}, 1438 cm^{-1} and 1168 cm^{-1}. These bands were associated to amide II (amino group) of mannoprotiens presents in their cell wall, $-CH_2$ and $-CH_3$ deformation of proteins and lipids, and C-O-C stretching of polysaccharides β (1→3) glucans, respectively (Adhikari *et al.* 1995; Lucassen *et al.* 1998; Galichet *et al.* 2001; Yu and Irudayaraj 2005).

Therefore, ATR-IRM allowed a clear discrimination among the acetic acid bacteria and yeast strains tested providing evidence that the signal responsible for their differentiation was mainly associated with IR frequencies of bacteria and yeast cell walls

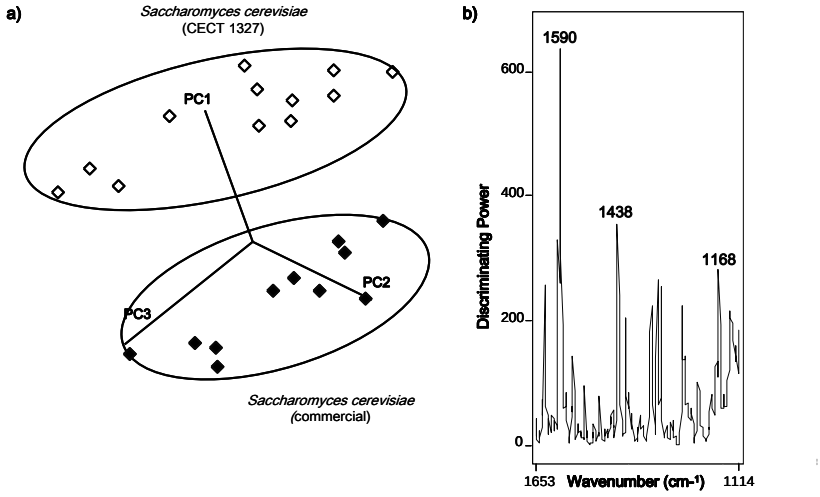

Figure 3.4. SIMCA discriminating power (a) and class projections (b) of transformed (second derivative, 15 points window) ATR-IRMS spectra of *S. cerevisiae* (CECT 1327 and commercial).

3.4. CONCLUSIONS

ATR-IRMS combined with multivariate analysis is a valuable method to acquire highly reproducible spectra and discriminate different strains of acetic acid bacteria and *Saccharomyces*. ATR-IRMS provides a simple, rapid and accurate tool for detecting secondary fermentations produced by undesirable microorganisms.

3.5. REFERENCES

Adhikari, C.; Proctor, A.; Blyholder, G.D. Diffuse reflectance Fourier transform infrared spectroscopy of phospholipid adsorption onto silicic acid. *Journal of the American Oil Chemists' Society* **1995,** 72, (3), 337-341.

Armenta, S.; Garrigues, S.; Miguel de la Guariia, Pondeau, P. Attenuated total reflection Fourier transform infrared analysis of the fermentation process of pineapple. *Analytical Chemica Acta* **2005,** 545, 99-106.

Baldauf, N.A.; Rodriguez-Romo, L.A.; Männig, A.; Yousef, A.E.; Roderiguez-Saona, L.E. Effect of selective growth media on the differentiation of *Salmonella* enterica serovars by Fourier transform mid-infrared spectroscopy. *Journal of Microbiological Methods* **2007,** 68, 106-114.

Bartowsky, E.J.; Henschke, P.A. Acetic acid bacteria spoilage of bottled red wine-A review. *International Journal of Food Microbiology* **2008,** 125, 60-70.

Bartowsky, E.J.; Xia, D.; Gibson, R.L.; Fleet, G.H.; Henschke, P.A. Spoilage of bottled red wine by acetic acid bacteria. *Letters in Applied Microbiology* **2003**, 36, 307-314.

Beekes, M.; Lasch, P.; Naumann, D. Analytical applications of Fourier transform-infrared (FT-IR) spectroscopy in microbiology and prion research. *Veterinary Microbiology* **2007,** 123, 305-319.

Davis, C.R.; Wibowo, D.; Fleet, G.H.; Lee, T.H. Properties of wine lactic acid bacteria: Their potential enological significance. *American Journal of Enology and Viticulture* **1988**, 39, (2), (1988), 137-142.

De Nardo, T.; Shiroma-Kian, C.; Yuwana, H.; Rodriguez-Saona, L.E. Rapid and simultaneous determination of lycopene and β-carotene contents in tomato juice by infrared spectroscopy. *Journal of Agricultural and Food Chemistry* **2009,** 57, 1105-1112.

Dunn, W.J.; Wold, S. SIMCA pattern recognition and classification. *In:* van de Waterbeemd H. (Ed) Chemometric methods in molecular design. VCH Publishers, NY **1995**, pp. 179-193.

Galichet, A.G.; Sockalingum, D.; Belarbi, A.; Manfait, M. FTIR spectroscopic analysis of *Saccharomyces cerevisiae* cell walls: study of an anomalous strain exhibiting a pink-colored cell phenotype. *FEMS Microbiology Letters* **2001**, 197, 179-186.

Grasso, E.M.; Yousef, A.E.; De Lamo Castellvi, S.; Rodriguez-Saona, L.E. Rapid detection and differentiation of *Alicyclobacillus* species in fruit juice using hydrophobic grids membranes and attenuated total reflectance infrared microspectroscopy. *Journal of Agricultural and Food Chemistry* **2009,** 57, 10670-10674.

Hruschka, W.R.; Williams, P.; Norris, K. Near infrared technology in the agricultural and food industries. In: P. Williams, K. Norris (Eds) Data analysis: Wavelength selection methods, *American Association of Cereal Chemists:* Minnesota, **2001**, pp. 39-58.

Huang, K.C.; Mukhopadhyay, R.; Wen, B.; Gitai, Z.; Wingreen, N.S. Cell shape and cell-wall organization in gram-negative bacteria. *Proceedings of the National Academy of Sciences of the United States of America* **2008,** 105, 19282-19287

Kansiz, M.; Heraud, P.; Wood, B.; Burden, F.; Beardall, J.; McNaughton, D. Fourier transform infrared microspectroscopy and chemometrics as a tool for the discrimination of *cyanobacterial* strains. *Phytochemistry* **1999,** 52, 407-417.

König, H.; Unden, G.; Fröhlich, J. Biology of microorganisms on grapes, in must and wine. *Springer*, Verlag Berline Heidelberg, Germany **2009**.

Lesage, G.; Bussey, H. Cell wall assembly in *Saccharomyces cerevisiae. Microbiology and molecular biology reviews* **2006,** 70, 317-343.

Lucassen, G.W.; Caspers, P.J.; Puppels, G.J. Infrared spectroscopy: New tool in medicine In: Mantsch H.H., Jackson M. (Eds) *Society of photo-optical instrumentation engineers (SPIE) conference series.*Bellingham, WA, SPIE, **1998,** 3257, 52-61.

Maquelin, K.; Kirschner, C.; Choo-Smith, L.P.; van den Braak, N.; Endtz, H.; Naumann, D.; Puppels, G.J. Identification of medically relevant microorganisms by vibrational spectroscopy. *Journal of Microbiological Methods* **2002,** 51, 255-271.

Nieuwoudt, H.H.; Pretorius, I.S.; Bauer, F.F.; Nel, D.G.; Prior, B.A. Rapid fermentation profiles of wine yeast s by Fourier transform infrared spectroscopy. *Journal of Microbiological Methods* **2006,** 67, 248-256.

Oust, A.; M∅retr∅, T.; Kirschner, C.; Narvhus, J.A.; Kohler, A. FT-IR spectroscopy for identification of closely related lactobacilli. *Journal of Microbiological Methods* **2004,** 59, 149-162.

Pawlak, A.; Mucha, M. Thermogravimetric and FTIR studies of chitosan blends. *Thermochimica Acta* **2003,** 396, 153-166.

Shiroma-Kian, C.; Tay, D.; Manrique, I.; Giusti, M.M.; Rodriguez-Saona, L.E. Improving the screeing process for the selection of potato breeding lines with enhanced polyphenolics content. *Journal of Agricultural and Food Chemistry* **2008,** 56, 9835-9842.

Stark, N.M.; Matuana, L.M.; Clemons, C.M. Effect of processing method on surface and weathering characteristics of wood–flour/HDPE composites. *Journal of Applied Polymer Science* **2004,** 93, 1021-1030.

Wibowo, D.; Eschenbruch, R.; Davis, C.R.; Fleet, G.H.; Lee, T.H. Occurrence and growth of lactic acid bacteria in wine: A review. *American Journal of Enology and Viticulture* **1985,** 36, (4), 303-313.

Wold, S.; Albano, C.; Blomquist, G.; Coomans, D.; Dunn, W.J.; Edlund, U.; Eliasson, B.; Hellberg, S.; Johansson, E.; Norden, B.; Sjastrem, M.; Saderstrem, B.; Wold, H. Pattern recognition by means of disjoint principal component models (SIMCA), In: Haskuldson A. (Ed) *Proceedings of the symposium on applied statistics*. Technical University Copenhagen, Copenhagen, **1981**, pp. 475-487.

Yu, C.; Irudayaraj, J. Spectroscopic characterization of microorganisms by Fourier transform infrared microspectroscopy. *Biopolymers,* **2005,** 77, 368-377.

CHAPTER 4

Detection of injured population of Escherichia coli *O157:H7 produced by thermal and pulsed electric field treatment with attenuated total reflectance infrared microspectroscopy*

4.1. INTRODUCTION

Escherichia coli O157:H7 is an enterohemorrhagic bacterium that causes foodborne illness. It is reported that, this bacteria is an important cause of bacterial gastrointestinal illness in the United States (Mead *et al.*, 1999; Neil *et al*., 2009). The infection causes vomiting, diarrhea, hemorrhagic colitis and hemolytic uraemic syndrome (HUS), a cause of renal failure in children, which can lead to long-term complications and death (Barrett *et al.*, 1994; Mead *et al.*, 1999; Mañas and Pagan, 2005; Osaili *et al*., 2007). The transmission of *E. coli* O157:H7 is due to the ingestion of contaminated food or water, or oral contact with contaminated surfaces (Mead *et al.*, 1999; Reiss *et al.*, 2006).

Several food preservation methods are currently used by food processing industries to maintain food safety by inactivating microorganisms or inhibiting their growth (Gould, 2001; Mañas and Pagan, 2005). There are different microbial inactivation methods: thermal treatment (Osaili *et al*., 2006; Osaili *et al*., 2007; Al-Qadiri *et al*., 2008; Espina *et a*l., 2010; Gabriel and Nakano, 2011), microwave processing (Gould, 1996; Mañas and Pagan, 2005), ultrasound under pressure (Pagan and Mackey, 2000), high hydrostatic processing (Wuytack *et al*., 2002; Mañas and Mackey, 2004; Somolinos *et al*., 2008a), UV irradiation (Basaran *et al*., 2004; Gabriel and Nakano, 2009), pressure-assisted thermal processing (Gould, 2001; Subramanian *et al*., 2006; Whitney *et al*., 2007) and pulsed electric fields (Garcia *et al*., 2005a; Garcia *et al*., 2007; Somolinos *et al*., 2008b). Among these methods, thermal treatment is the most widely used for the inactivation of foodborne pathogens (Murphy *et al*., 2004; O'Bryan *et al*., 2006; Osaili *et al*., 2007; Al-Qadiri *et al*., 2008). It has been reported that, temperature controls the rate of biochemical reactions taken place in the bacterial cells as well as the 3-dimensional structure of proteins (Bozoglu *et al*., 2004; Mañas and Pagan, 2005; Al-Qadiri *et al*., 2008; Hu *et al*., 2009). Due to the adverse effect of thermal processes on nutritional, sensory and functional properties of food, there is a strong need of alternative food preservation methods. Pulsed electric field (PEF) has been used as a nonthermal process to inactivate pathogenic microorganisms in food (Aronsson *et al*., 2005; Garcia *et al*., 2007). The degree of inactivation strongly depends on the

intensity of the pulses in terms of field strength, energy and number of pulses applied on the microbial strain and the treatment medium pH (Garcia *et al*., 2005b; Toepfl *et al*., 2007). Garcia *et al*. (2005c) studied the pH dependence of PEF treatments of Gram-positive and Gram-negative bacteria. At acidic pH (pH 4), Gram-negative bacteria had higher PEF resistance than at neutral pH (pH 7) and large proportion of survivor bacteria (>90%) were sublethally injured at maximum this pH (Garcia *et al*., 2003; Garcia *et al*., 2005c). No sublethal injuries were reported when Gram-negative bacteria were treated at pH 7(Garcia *et al*., 2005b). The ability of repairing their damaged cytoplasmic membrane seemed to be the reason behind the bacterial PEF resistance (Garcia *et al*., 2007).

However, during thermal and nonthermal treatment procedures, in addition to the dead cells, injured cells can be formed. Sublethally injured pathogenic microorganisms may cause significant health threat because they can repair themselves and start to grow in food products when the environmental conditions are suitable (Williams and Golden, 2001; Lin *et al*., 2004; Alvarez-Ordonez, *et al*., 2011). Moreover, routine microbiological procedures may yield negative results for detection of sublethally injured cells. Hence, food could be assumed to be safe and free from pathogenic cells, however during storage it become dangerous due to the re-growth and recovery of the injured cells (Bozoglu *et al*., 2004; Alvarez-Ordonez, *et al*., 2010).

In literature, different procedures are reported for the detection and identification of sublethally injured foodborne pathogens such as enumeration on conventional and modified enrichment media, direct epifluorescent filter technique, enzyme-linked immunosorbent assay and DNA probe for gene detection (Busch and Donnelly, 1992; Peng *et al*., 2001; Restaino *et al*., 2001; Kobayashi *et al*., 2005; Al-Qadiri *et al*., 2008). However, these methods are time consuming and usually require pre enrichments steps or selective media to inhibit the growth of competitive bacterial population. Hence, there is a significant need for a reliable, rapid and high-throughput method to discriminate and detect alive and sublethally injured pathogenic foodborne microbial.

Fourier transform infrared (FTIR) spectroscopy in mid infrared range can be used for identification and detection of microorganisms (Subramanian *et al*., 2006; Lin *et al*., 2004; Al-Qadiri *et al*., 2008; Grasso *et al*., 2009). In the past decades, this technique has been used to the identification and classification of different microorganisms. FTIR spectrum provides bands from all the cellular components of microorganism (e.g. cell membrane and wall components, proteins and nucleic acid), giving spectral signatures or "fingerprints" that permit the classification of microorganisms at strain and serovar level (Rodriguez-Saona *et al*., 2001; Baldauf *et al*., 2007; Alvarez-Ordonez, *et al*., 2011). Hence, FTIR should be able to detect the changes occurring in bacterial cells and indicate the physiological state in response to the inactivation conditions. The main objective of this research was to show the potential of attenuated total reflectance infrared microspectroscopy (ATR-IRMS) combined with soft independent modeling of class analogy multivariate analysis to detect and discriminate between injured and alive *E .coli* O157:H7 cells during thermal and pulsed electric fields treatments at pH 7 and 4. In addition, partial least square regression (PLSR) models were used to quantify bacterial cells by ATR-IRMS after the treatments.

4.2. MATERIALS and METHODS

4.2.1. Bacterial Strain and Culture Preparation

Escherichia coli O157:H7 culture used for this study was isolated by P. A. Chapman (Chapman *et al*., 1993) and obtained from Dr B. Mackey (Reading, UK). A broth subculture was prepared by inoculating with one single colony, a test tube containing 5 mL of sterile Tryptic Soy Broth (Biolife, Milan, Italy) with 0.6% of Yeast Extract added (Biolife) (TSBYE). After inoculation, this tube was incubated at 37^{o}C overnight. With this subculture, 250 mL Erlenmeyer flasks containing 50 mL of TSBYE were inoculated to a final concentration of 10^4 CFU/mL. These flasks were incubated under agitation (130 rpm; Selecta, mod. Rotabit, Barcelona, Spain) at 37^{o}C until the stationary growth phase was reached (24 h).

4.2.2. Sample Preparation for Thermal Treatments

An aliquot of 20 mL *E. coli* O157:H7 culture was centrifuged at 3800 rpm for 20 min at 20 ^{o}C in a sterile falcon tube. The supernatant was removed and the bacteria cells were re-suspended in 0.5 mL sterile citrate phosphate (McIlvaine buffer) at pH 4 and 7. From this suspension, an aliquot of *E. coli* O157:H7 cell (0.25 mL) was inoculated into each tube (4 tubes for 5, 10, 20 and 90 min thermal treatments) to a final concentration of 10^{8} CFU/mL.

4.2.3. Thermal Treatment

Inoculated samples were treated by heat at 54 ± 0.2^{o}C for 5, 10, 20 and 90 min using a thermostatic bath provided with a shaking system (120 rpm,). The temperature of the bath was monitored by a K-type thermocouple. At specific holding times, each tube was removed from the thermostatic bath and immediately immersed into an ice–water bath (4^{o}C) to avoid further inactivation. After the heat treatment, samples were centrifuged at 10000 rpm for 5 min at 20ºC and the pellets were resuspended into 1 mL of Maximum Recovery Diluent. Medium (Oxoid, Unipath, Basingtoke, UK) and stored at 4^{o}C until being analyzed by conventional method (plate counts) and attenuated total reflectance infrared microspectroscopy. These experiments were performed by research group “Nuevas tecnologías de conservación de alimentos” at Universidad de Zaragoza (Spain)

4.2.4. Sample Preparation for Pulsed Electric Field Treatment

For PEF treatment, bacterial cultures were centrifuged at 10000 rpm for 5 min. The supernatant was removed and re-suspended in 1 mL of sterile McIlvaine buffer at pH 4 and 7 with a conductivity of 2 mS/cm.

4.2.5. Pulsed Electric Field Treatment

The re-suspended cultures were treated by PEF with 35 kV/cm for 10, 25, 50 and 60 pulses. The PEF treated cultures (0.5 mL) were immediately removed and placed into an eppendorf tube in ice and the samples were centrifuged at 10000 rpm for 5 min. The supernatant were removed and the pellets were re-suspended into 1 mL of Maximum Recovery Diluent. Medium (Oxoid, Unipath, Basingtoke, UK) and stored at 4^{o}C until being analyzed by conventional method (plate counts) and attenuated total reflectance infrared microspectroscopy. These experiments were performed by research group “Nuevas tecnologías de conservación de alimentos” at Universidad de Zaragoza (Spain)

4.2.6. Microbiological Analyses

Cell populations were estimated using the pour plate method. After treatments, the samples were adequately diluted and 0.1 mL samples were pour plated onto Tryptic Soy Agar (Biolife) with 0.6% of Yeast Extract added (TSAYE) as a recovery medium. Plates were incubated for 24 h at 37^{o}C. Previous experiments showed that longer incubation times did not influence survival counts. After incubation, colony forming units were counted with an improved image analyzer automatic counter (Protos, Analytical Measuring Systems, Cambridge, UK). In order to determine bacterial cell injury, treated samples were also pour plated onto TSAYE with 3% of sodium chloride (Probus, Barcelona, Spain, TSAYE-SC) to evaluate cytoplamatic membrane damage and onto TSAYE with 0.35% of bile salts (Biolife, TSAYE-BS) to detect outer membrane damage. These levels of sodium chloride and bile salts had previously been determined as the maximum non-inhibitory concentrations for native cells. Plates containing selective media were incubated for 48 h at 37^{o}C. Previous experiments showed that longer incubation times did not influence survival counts. Inactivation was calculated as the difference between the logarithm of colony counts of the treated and untreated samples (log N-log N_0).

4.2.7. Sample Preparation for Attenuated Total Reflectance Infrared Microspectroscopy Analysis

An aliquot of cell suspensions (1 mL) was centrifuged at 6000 rpm for 10 min at 4^{o}C. Pellets were washed three times with 1 mL of 0.9% NaCl and centrifuged using the same conditions (6000 rpm and 10 min). Pellets were placed onto grids of hydrophobic membrane (HGM; ISO-GRID, Neogen Corporation, Lansing, MI, USA) and dried out under laminar flow at room temperature for 1 h to obtain a dry, homogeneous film of bacterial cells. The drying step is crucial to avoid the overlapping effect of the O-H band coming from water during the IR spectra measurements of the samples.

4.2.8. Attenuated Total Reflectance Infrared Microspectroscopy (ATR-IRMS)

Samples were analyzed by IR equipment (Illuminate IR, Smiths detection, The Genesis Centre Science Park South Birchwood Warrington, WA3 7BH, England) interfaced with mercury-cadmium-telluride (MCT) photoconductive detector and equipped with a microscope with a motorized x-y stage, 5x, 20x and 50x objectives, and slide-on attenuated total reflection (ATR) diamond objective (Smiths detection, The Genesis Centre Science Park South Birchwood Warrington, WA3 7BH, England). The hydrophobic membranes were placed on the stage of the microscope and a specific position of the microbial pellet was selected with the assistance of the microscope and live camera (Lecica OM 2500, Modulo FTIR, Renishaw plc). Spectra were collected from 4000 to 800 cm^{-1} with a resolution of 4 cm^{-1}. The spectrum of each sample was obtained by taking the average of 128 scans to improve the signal-to-noise ratio. Spectra were displayed in terms of absorbance obtained by rationing the single beam spectrum against that of the air background. The spectrometer was completely software controlled by synchronize IR basic version 1.1 software (SensIR Technologies, Smiths detection).

4.2.9. Multivariate Analysis

Pirouette® multivariate analysis software (version 4.0, InfoMetrix, Inc., Woodville, WA) was used to analyze the raw spectra of bacterial cells. IR spectral data were mean-centered, transformed to their second derivative using a 15-point Savitzky-Golay polynomial filter, and vector-length normalized; sample residuals and Mahalanobis distance were used to determine outliers (Kansiz *et al*., 1999; De Maesschalck *et al*., 2000). Spectral data were statistically analyzed using soft independent modeling of class analogy (SIMCA). SIMCA was used to build a predictive model based on the construction of separate principal component analysis (PCA) models for each class to describe and model the variation (De Maesschalck *et al*., 1999; Kansiz *et al*., 1999). SIMCA class models were interpreted based on class projections, misclassifications, discriminating power, and interclass distances. Class projections were visible through a three-dimensional graph of clustered membranes. Discriminating power was used to define the variables (wavenumbers) that have a predominant effect on classification of bacterial cells (Pirouette, Version 4.0, 2008; Grasso *et al*., 2009). SIMCA analysis assesses itself by predicting each sample included in the training set comparing that prediction to its assigned class; this assessment is referred to misclassifications. Zero misclassifications typify a model in which all samples were correctly predicted to the preassigned class (De Nardo *et al*., 2009). The transformed spectra were analyzed by partial least-squares regression (PLSR) that was cross-validated (leave-one-out) to generate calibration models. The reference data (x variable) used in this study was the bacterial counts measured by conventional culture method and the y variable was the bacterial count predicted from the infrared spectra (Al-Qadiri *et al*., 2008; De Nardo *et al*., 2009). Models were evaluated in terms of loading vectors, standard error of cross-validation (SECV), determination coefficient (R^2), and outlier diagnostics.

4.3. RESULTS and DISCUSSION

4.3.1. Discrimination of Alive and Thermal Treated E. coli *O157:H7 Cells by ATR-IRMS*

Classification models of SIMCA were developed using transformed spectra of alive and thermal treated *E. coli* O157:H7 cells at pH 4 and pH 7. Class projection plot (**Figure 4.1a** and **b**) of SIMCA classification model of transformed spectra (1810-1042 cm^{-1}) of alive and thermal processed samples showed tight clustering and clear differentiation among samples at both pH values. In each principal component direction, a 95% confidence interval probability cloud is assigned around each class (Subramanian *et al*., 2007; Pirouette, Version 4.0, 2008; Grasso *et al*., 2009).

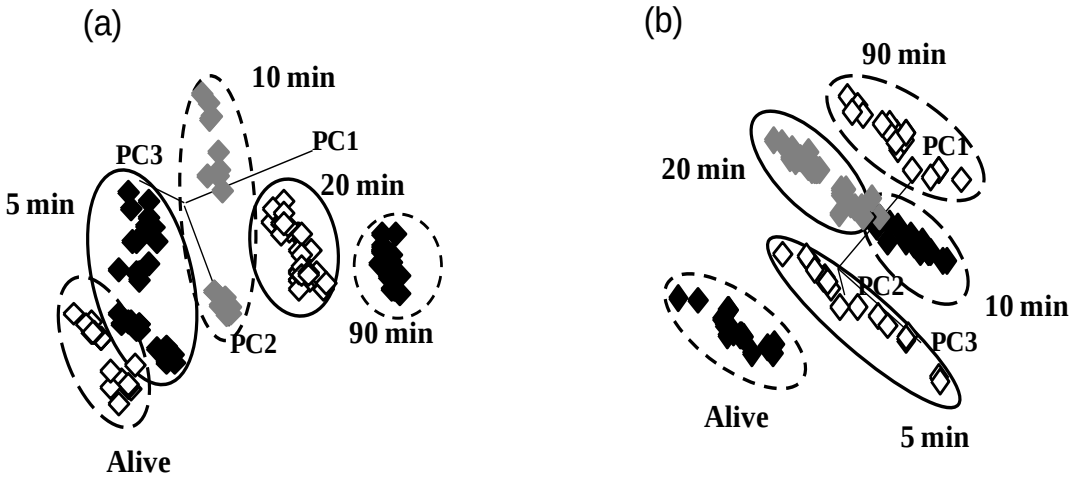

Figure 4.1. Soft independent modeling of class analogy (SIMCA) class projections of transformed (second derivative, 15 points window) attenuated total reflectance infrared microspectroscopy (ATR-IRM) spectra of thermal treated for 5, 10, 20 and 90 min and alive *E. coli* O157:H7 at pH 4 (a) and 7 (b)

The distance between the clusters of alive *E. coli* O157:H7 cells and each heat treated sample increased with the duration of the heat treatment applied. This trend was observed for both pH values used for this research. For instance, *E. coli* O157:H7 cells heat treated at pH 7 for 90 min (with 4.15 log units of inactivation in TSAYE) were biochemically very different than alive or

heat treated cells for 5 min (with 0.17 log units of inactivation in TSAYE). Interclass distance (ICD), which is the measure of the distance between samples based on factor loadings (Subramanian *et al*., 2007; Pirouette, Version 4.0, 2008; Grasso *et al*., 2009), of this SIMCA model further proved this finding. ICD values above 3.0 are considered significant to discriminate two clusters of samples as a different class (Subramanian *et al*., 2007; Pirouette, Version 4.0, 2008; Grasso *et al*., 2009). ICD values between alive and thermal treated *E. coli* O157:H7 cells (**Table 4.1**) ranged from 7.3 to 39.1 (pH 4) and from 3.7 to 22.1 (pH 7) confirming these biochemical differences among all the clusters.

Table 4.1. *Soft independent modeling of class analogy (SIMCA) of interclass distance of intact and thermal processed (for 5, 10, 20 and 90 minutes)* Escherichia coli *O157:H7 at pH 4 and 7 of transformed (second derivative, 15 points window) attenuated total reflectance infrared microspectroscopy (ATR-IRM) spectra.*

pH 4	Alive	5 min	10 min	20 min	90 min
Alive	0.0				
5 min	7.3	0.0			
10 min	20.2	8.4	0.0		
20 min	28.1	12.5	11.7	0.0	
90 min	39.1	23.4	21.8	8.1	0.0
pH 7	Alive	5 min	10 min	20 min	90 min
Alive	0.0				
5 min	9.6	0.0			
10 min	18.2	8.2	0.0		
20 min	17.2	7.5	3.7	0.0	
90 min	22.1	12.5	6.9	6.2	0.0

Wavenumbers in the spectral range are plotted against their power to classify and discriminate the samples that are being compared (Pirouette, Version 4.0, 2008; Grasso *et al*., 2009; De Lamo-Castellví and Rodriguez-Saona, 2011). Discriminating power plot of alive *E. coli* O157:H7

cells and thermal treated samples at pH 4 are shown in **Figure 4.2**. In this plot, two spectral bands at 1618 and 1638 cm^{-1} were mainly responsible to explain the differences among these samples. These IR bands were linked to amide I group vibrations of peptides and β-pleated secondary protein structure (Kansiz *et al*., 1999; Al-Qadiri *et al*., 2006; Beekes *et al*., 2007; Alvarez-Ordonez *et al*., 2011).

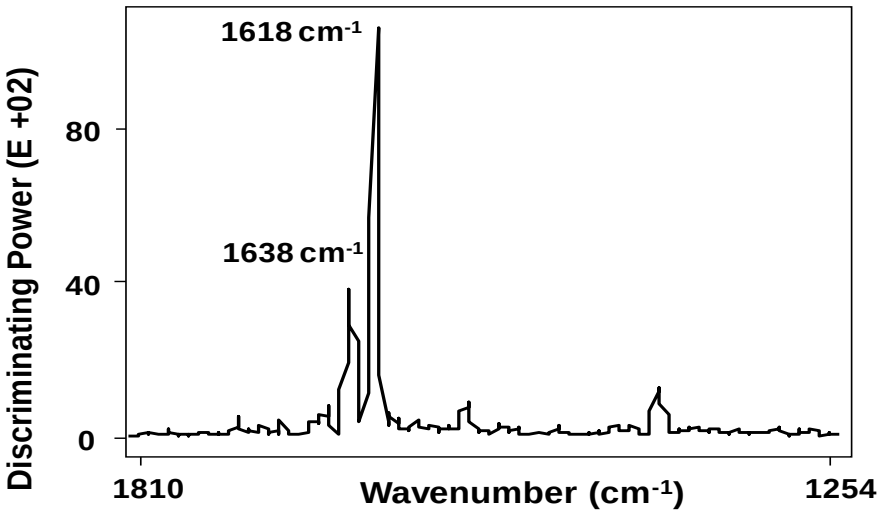

Figure 4.2. Soft independent modeling of class analogy (SIMCA) of discriminating power of intact and thermal processed (for 5, 10, 20 and 90 min.) *E. coli* O157:H7 at pH 4 of transformed (second derivative, 15 points window) attenuated total reflectance infrared microspectroscopy (ATR-IRM) spectra

Similarly, the amide I band of β-pleated sheet secondary protein at 1618 cm^{-1} was the discriminating band of alive and thermally treated at 5, 10, 20, and 90 min and pH 7 *E. coli* cells (**Figure 4.3**). In addition to this amide I band, there was another at 1215 cm^{-1} that also had a contribution to classify and discriminate alive and thermal treated *E. coli* cells. The discriminating band at 1215 cm^{-1} was related to the asymmetric stretching of P=O (PO_2^-) in phosphodiesters (Kansiz *et al*., 1999; Jiang *et al*., 2004; Al-Qadiri *et al*., 2006; Beekes *et al*., 2007; Alvarez-Ordonez *et al*., 2011). Phosphodiester bounds have been linked to phospholipids

presents in the cytoplasmic membrane and in the inner leaflet of the outer membrane (Ait-Ouazzou *et al*., 2012).

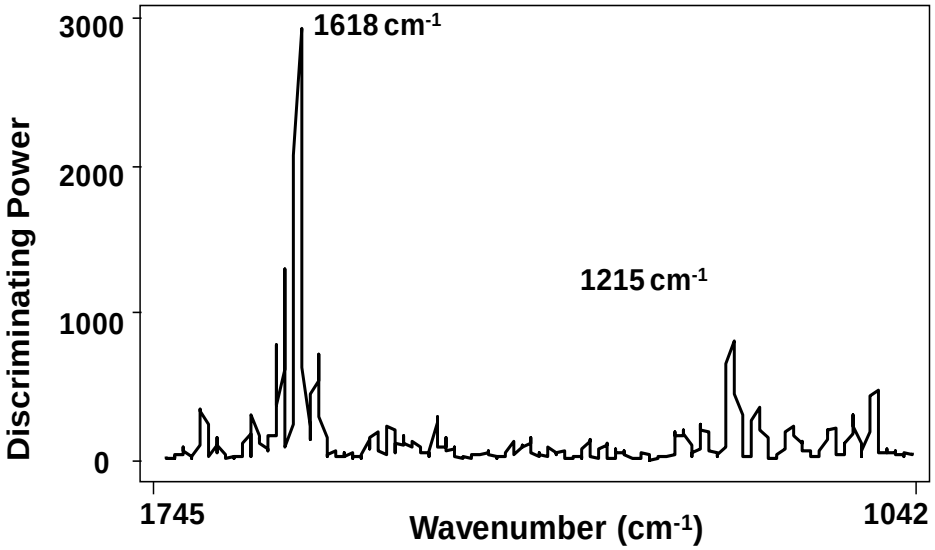

Figure 4.3. Soft independent modeling of class analogy (SIMCA) of discriminating power of intact and thermal processed (for 5, 10, 20 and 90 min.) *E. coli* O157:H7 at pH 7 of transformed (second derivative, 15 points window) attenuated total reflectance infrared microspectroscopy (ATR-IRM) spectra

Moreover, it is worth to mention that the discriminating power value of the model obtained comparing alive and thermal treated *E. coli* O157:H7 cells at pH 4 for the band 1618 cm^{-1} (**Figure 4.2**) was higher (8000 units) than the one comparing alive and thermal treated *E. coli* cells at pH 7 3000 units (**Figure 4.3**). It is well documented that, the higher the value of discriminating power is the greater is the influence of that wavenumber in classifying the samples (Subramanian *et al*., 2007; Pirouette, Version 4.0, 2008). These results have showed that when the thermal treatment was applied to *E. coli* O157:H7 cells at pH 4, outer membrane proteins were the cell structures mainly affected and when the treatment was applied at pH 7 the phospholipids were also involved.

4.3.2. Discrimination of Alive and PEF Treated E. coli *O157:H7 Cells by ATR-IRMS*

SIMCA classification models were developed using transformed spectra of alive and PEF treated *E. coli* O157:H7 cells at pH 4 and 7. Class projection plot (**Figure 4.4 a** and **b**) of SIMCA classification model (1888-882 cm^{-1} at pH 7 and 2022-1026 cm^{-1} at pH 4) of alive and PEF treated samples showed clear differentiation among samples at both pH values.

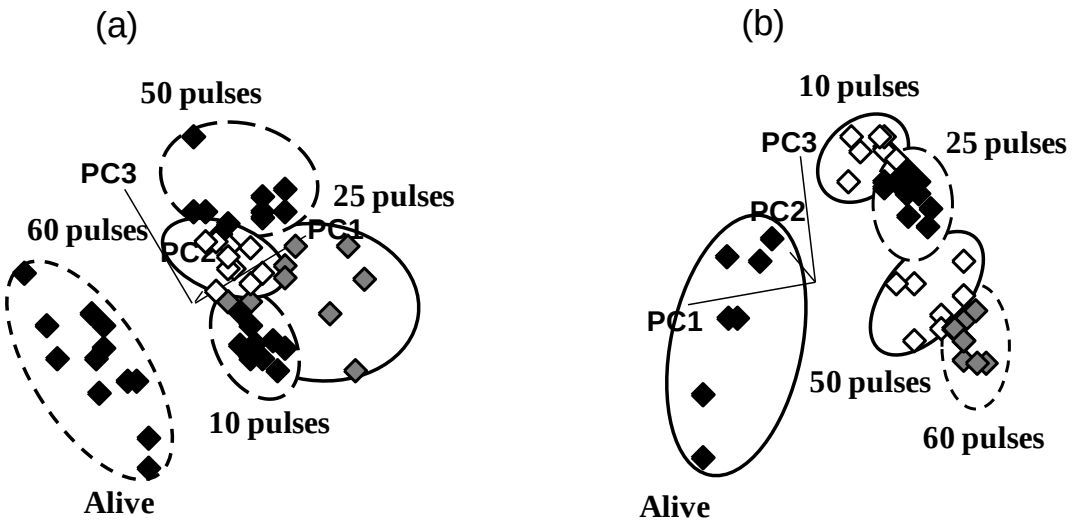

Figure 4.4. Soft independent modeling of class analogy (SIMCA) class projections of transformed (second derivative, 15 points window) attenuated total reflectance infrared microspectroscopy (ATR-IRM) spectra of pulsed electric field treated for 10, 25, 50 and 60 pulses and intact *E. coli* O157:H7 at pH 4 (a) and 7 (b)

ICD values (**Table 4.2**) showed differences between alive *E. coli* O157:H7 cells and PEF treated samples. These values increased with the number of pulses applied in a similar trend for both pH values tested.

Table 4.2. *Soft independent modeling of class analogy (SIMCA) of interclass distance of intact and pulsed electric field treated (for 10, 25, 50 and 60 pulses)* Escherichia coli *O157:H7 at pH 4 and 7 of transformed (second derivative, 15 points window) attenuated total reflectance (ATR) infrared microspectroscopy (IRM) spectra.*

pH 4	Alive	10 pulses	25 pulses	50 pulses	60 pulses
Alive	0.0				
10 pulses	2.8	0.0			
25 pulses	2.8	1.6	0.0		
50 pulses	2.9	0.9	1.2	0.0	
60 pulses	3.3	0.8	1.5	0.8	0.0
pH 7	Alive	10 pulses	25 pulses	50 pulses	60 pulses
Alive	0.0				
10 pulses	2.9	0.0			
25 pulses	3.4	1.0	0.0		
50 pulses	3.6	1.5	1.3	0.0	
60 pulses	4.1	1.9	1.4	0.9	0.0

The discriminating power (**Figure 4.5**) of alive and PEF treated samples at pH 4 showed two IR bands (1638 and 1618 cm^{-1}) responsible of the differences between alive and PEF treated *E. coli* O157:H7 cells. These bands were linked to the amide I of β-pleated secondary structure of proteins (Kansiz *et al*., 1999; Al-Qadiri *et al*., 2006; Beekes *et al*., 2007; Burgula *et al*., 2007; Alvarez-Ordonez *et al*., 2011).

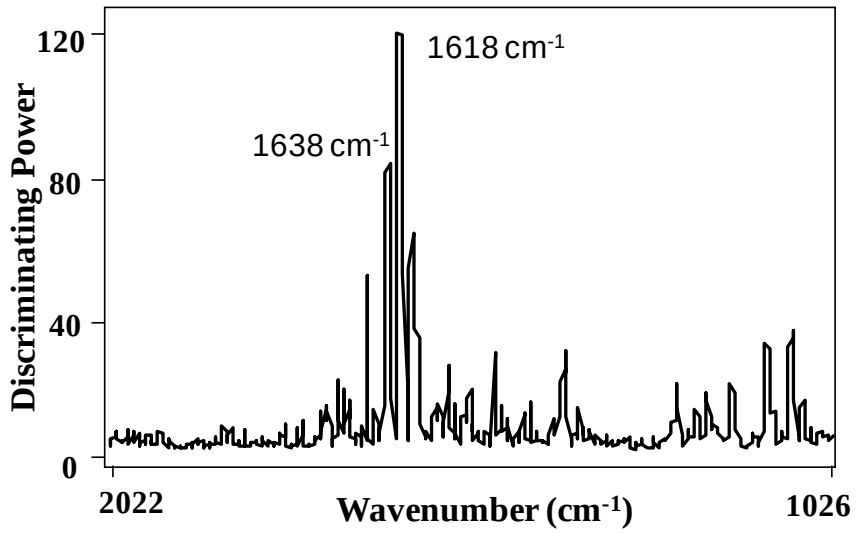

Figure 4. 5. Soft independent modeling of class analogy (SIMCA) of discriminating power of alive and pulsed electric field treated (for 10, 25, 50 and 60 pulses) *E. coli* O157:H7 at pH 4 of transformed (second derivative, 15 points window) attenuated total reflectance infrared microspectroscopy (ATR-IRM) spectra

The major discriminating bands observed during PEF treatments at pH 7 were 1078 and 993 cm^{-1} (**Figure 4.6**). These bands were linked to the symmetric stretching of P=O (PO_2^-) in phosphodiesters and C-O-C and C-O of different polysaccharides (dominated by the ring vibration of carbohydrates) respectively (Kansiz *et al*., 1999; Jiang *et al*., 2004; Al-Qadiri *et al*., 2006; Naumann, 2006; Beekes *et al*., 2007; Alvarez-Ordonez *et al*., 2011). In addition to the major discriminating bands, there was a small contribution of amide I band at 1620 cm^{-1} in the discriminating of alive and PEF treated *E. coli* O157:H7 at pH 7 (**Figure 4.6**). The membrane permeabilization caused by PEF treatment can affect the inner cell content such as DNA/RNA. Phosphate groups are found in the back bone of DNA/RNA structure and polysaccharides (lipopolysaccharides) also found on the outer membrane of Gram-negative bacteria (Mañas and Pagan, 2005). Several authors have reported that Gram-negative bacteria are more PEF resistant at pH 4 than at pH 7 (Garcia et al., 2003). These researchers have related this behavior to their outer membrane that might be protecting cells from electropermeabilization (García *et al*., 2005b; García *et al*., 2005c; García *et al*., 2007). The SIMCA models have confirmed this hypothesis.

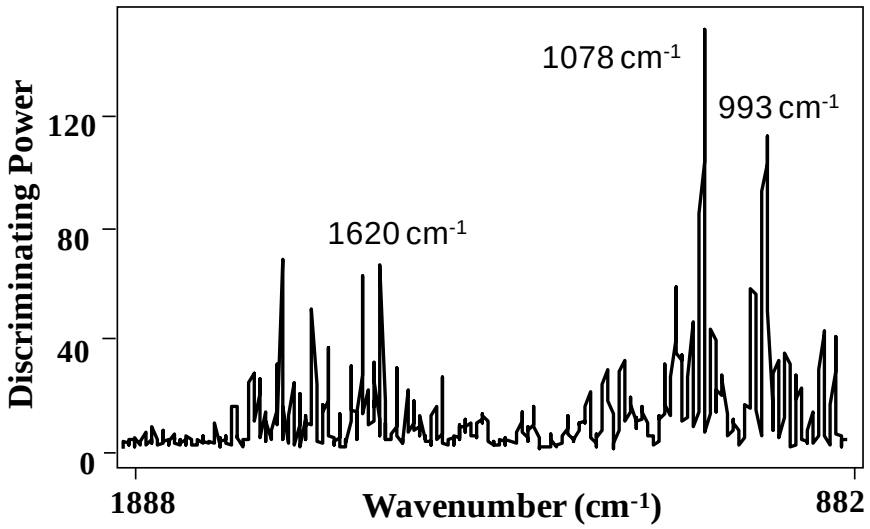

Figure 4. 6. Soft independent modeling of class analogy (SIMCA) of discriminating power of intact and pulsed electric field treated (for 10, 25, 50 and 60 pulses) *E. coli* O157:H7 at pH 7 of transformed (second derivative, 15 points window) attenuated total reflectance infrared microspectroscopy (ATR-IRM) spectra.

4.3.3. Quantitative Prediction of Thermal and PEF Treated Escherichia coli *O157:H7 Cells By Multivariate Analysis Technique*

A quantitative analysis was performed based on PLSR analysis to predict bacterial inactivation after thermal and PEF treatments from the IR data. The correlation was based on the measured inactivation values in each culture medium (reference data) and the ATR-IRMS spectral data to predict inactivation. The inactivation values (reference data) were obtained from three different media, TSAYE, TSAYE-SC and TSAYE-BS used to have total cell counts, cells that have cytoplasmic membrane damaged and cells with outer membrane damaged, respectively. The PLSR models built for predicting inactivation of thermal treatment at pH 4 (**Figure 4.7, A, B** and **C**) had higher coefficient of determination for TSAYE and TSAYE-SC models and lower for TSAYE-BS model (**Table 4.3**). The SECV values obtained for the cross validation models for predicting the thermal inactivation at pH 4 were 0.265, 0.213 and 0.244 log units in TSAYE, TSAYE-SC and TSAYE-BS, respectively (**Table 4.3**). The PLSR models for thermal inactivation at pH 7 (**Figure 4.8,**

A, B and **C**) had a similar trend with higher values of the coefficient of determination for TSAYE and TSAYE-SC models and lower value for TSAYE-BS model(**Table 4.3**) with SECV values of 0.271, 0.114, 0.233 log units in TSAYE, TSAYE-SC and TSAYE-BS, respectively (**Table 4.3**).

Table 4.3. *Partial least-squares model parameters for* Escherichia coli *O157:H7 cells treated by heat and PEF*

Recovery medium	TP			PEF		
	SECV	determination coefficient (R^2)	latent variables	SECV	determination coefficient (R^2)	latent variables
TSAYE pH 4	0.265	0.966	3	0.243	0.832	6
TSAYE pH 7	0.271	0.961	8	0.369	0.968	7
TSAYE-SC pH 4	0.213	0.976	4	0.128	0.858	6
TSAYE-SC pH 7	0.114	0.991	8	0.216	0.958	7
TSAYE-BC pH 4	0.244	0.916	3	0.127	0.846	6
TSAYE-BC pH 7	0.233	0.935	7	0.358	0.962	7

The PLSR models for predicting the PEF inactivation at pH 4 (**Figure 4.9 A, B** and **C**) showed lower correlation trends (**Table 4.3**) in all recovery medium (TSAYE, TSAYE-SC and TSAYE-BS) compared to the coefficient of determination of The PLSR predicting models for PEF inactivation at pH 7(**Figure 4.10 A, B** and **C**). As mentioned before, Gram-negative bacteria such as *E. coli* O157:H7 have higher PEF resistance at pH 4 than at 7 (Garcia *et al*., 2003; Garcia *et al*., 2005b; Garcia *et al*. 2005c; Garcia *et al*. 2007). When the inactivated bacteria recovered in selective medium (TSAYE-SC), the inactivation log values at pH 4 and 7 were different due to the presence of sublethal injury at pH 4 (Garcia *et al*., 2003; Garcia *et al*. 2005c). However, the PEF treatment injury detected by ATR-IRMS could be total sublethal injury (cythoplasmic and outer membrane damage). This could leads to a lower coefficient of determination of the PLSR prediction model at pH 4. It has been reported that, at pH 7 there was no sublethal injury observed by the PEF treatment, rather it either causes total inactivation or no inactivation and this event is known as “all or nothing” event (Garcia *et al*., 2003).

The SECV values of the model for PEF treated bacterial at pH 4 were 0.243, 0.128 and 0.127 log units in TSAYE, TSAYE-SC and TSAYE-BS, respectively (**Table 4.3**). Similarly, the SECV values of the PLSR model for PEF treated at pH 7 were 0.369, 0.216 and 0.358 log units in TSAYE, TSAYE-SC and TSAYE-BS, respectively (**Table 4.3**). Generally, these results show that the bacterial counts (quantitative data) can be predicted using ATR-IRMS based on PLS analysis technique after different thermal and pulsed electric field treatments.

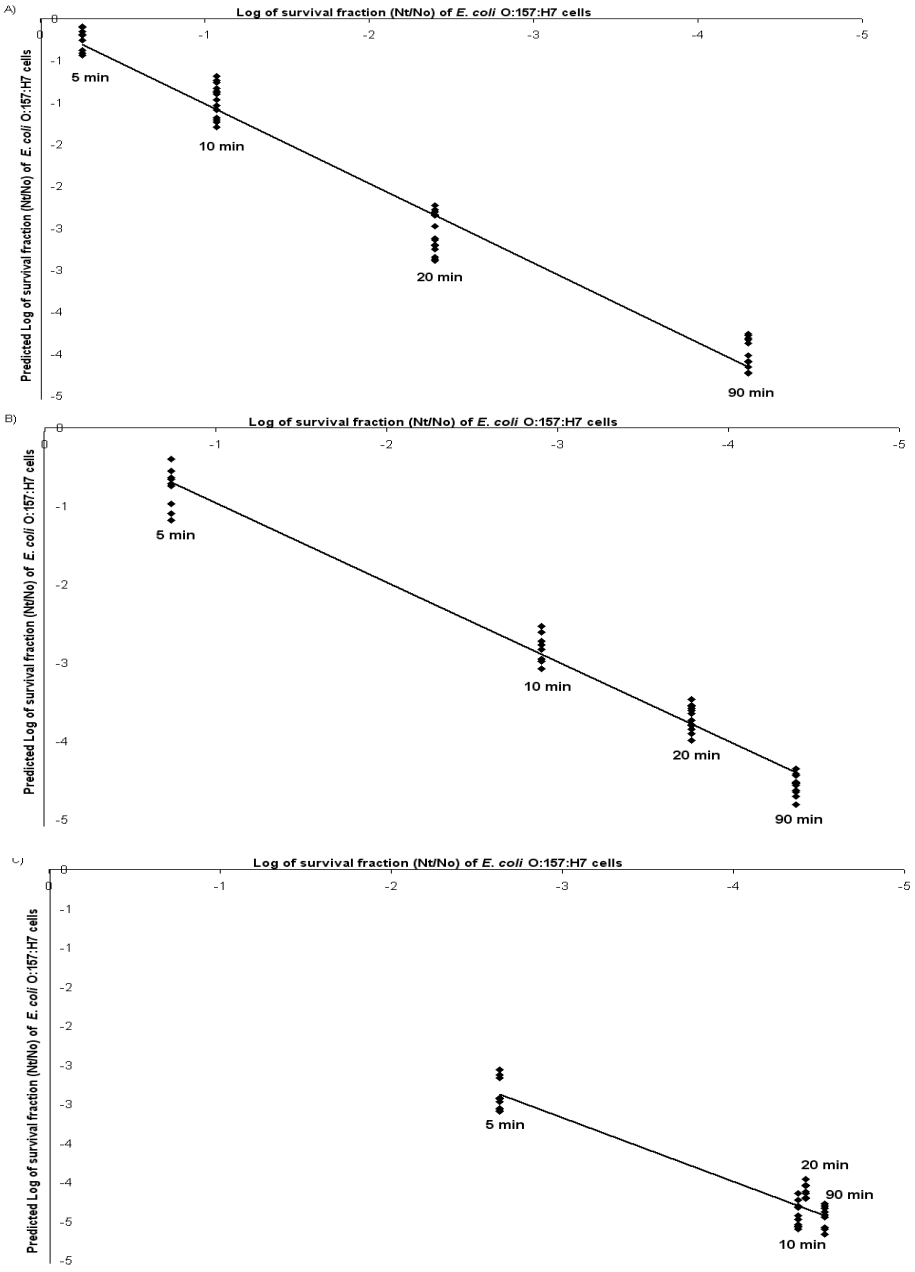

Figure 4.7. Calibration curve of measured and IRMS predicted thermal treated bacterial count: (A), (B) and (C) are bacterial counts in TSAYE, TSAYE-SC and TSAYE-BS respectively at pH 4

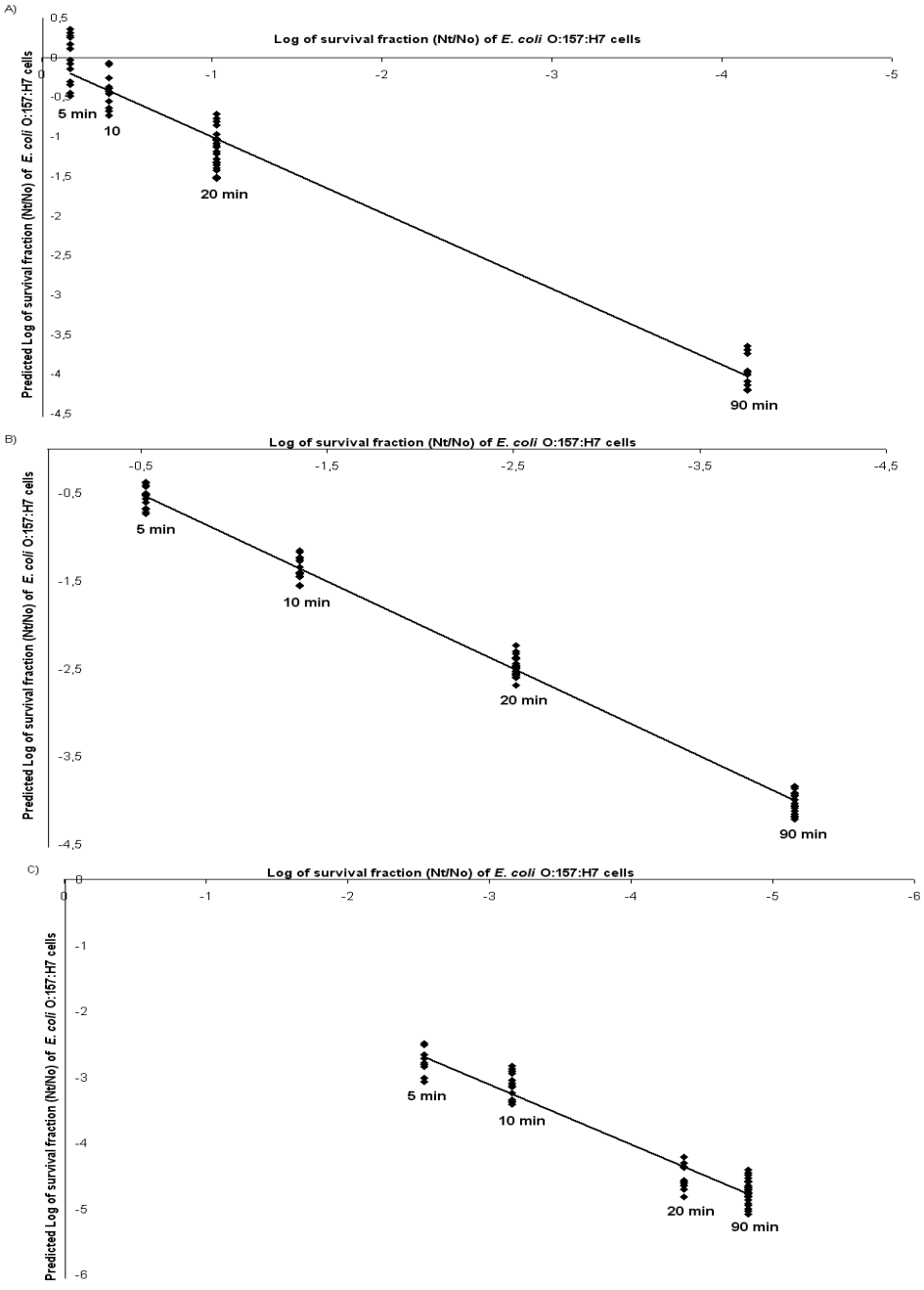

Figure 4.8. Calibration curve of measured and IRMS predicted thermal treated bacterial count: (A), (B) and (C) are bacterial counts in TSAYE, TSAYE-SC and TSAYE-BS respectively at pH 7

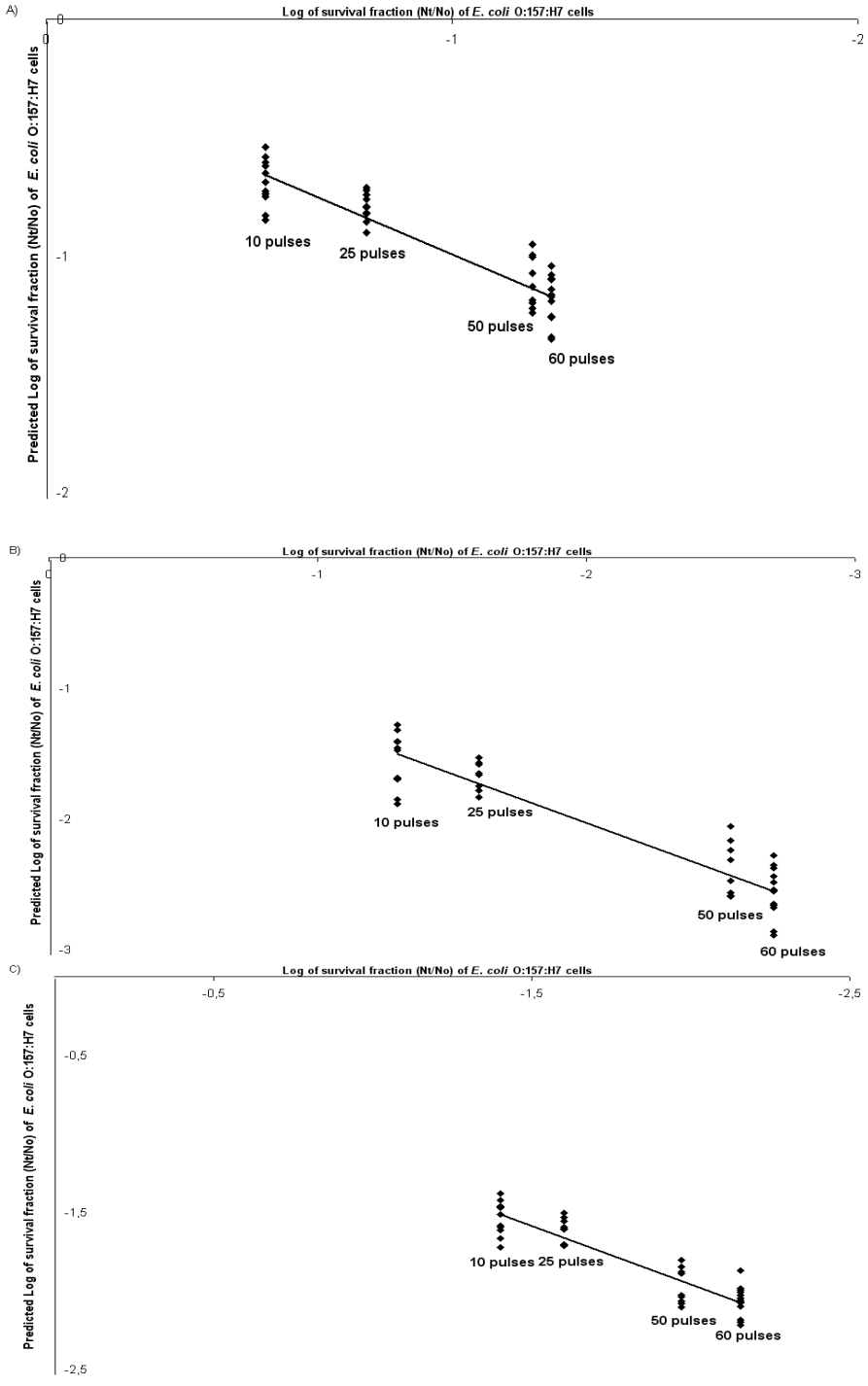

Figure 4.9. Calibration curve of measured and IRMS predicted pulsed electric field treated bacterial count: (A), (B) and (C) are bacterial counts in TSAYE, TSAYE-SC and TSAYE-BS respectively at pH 4

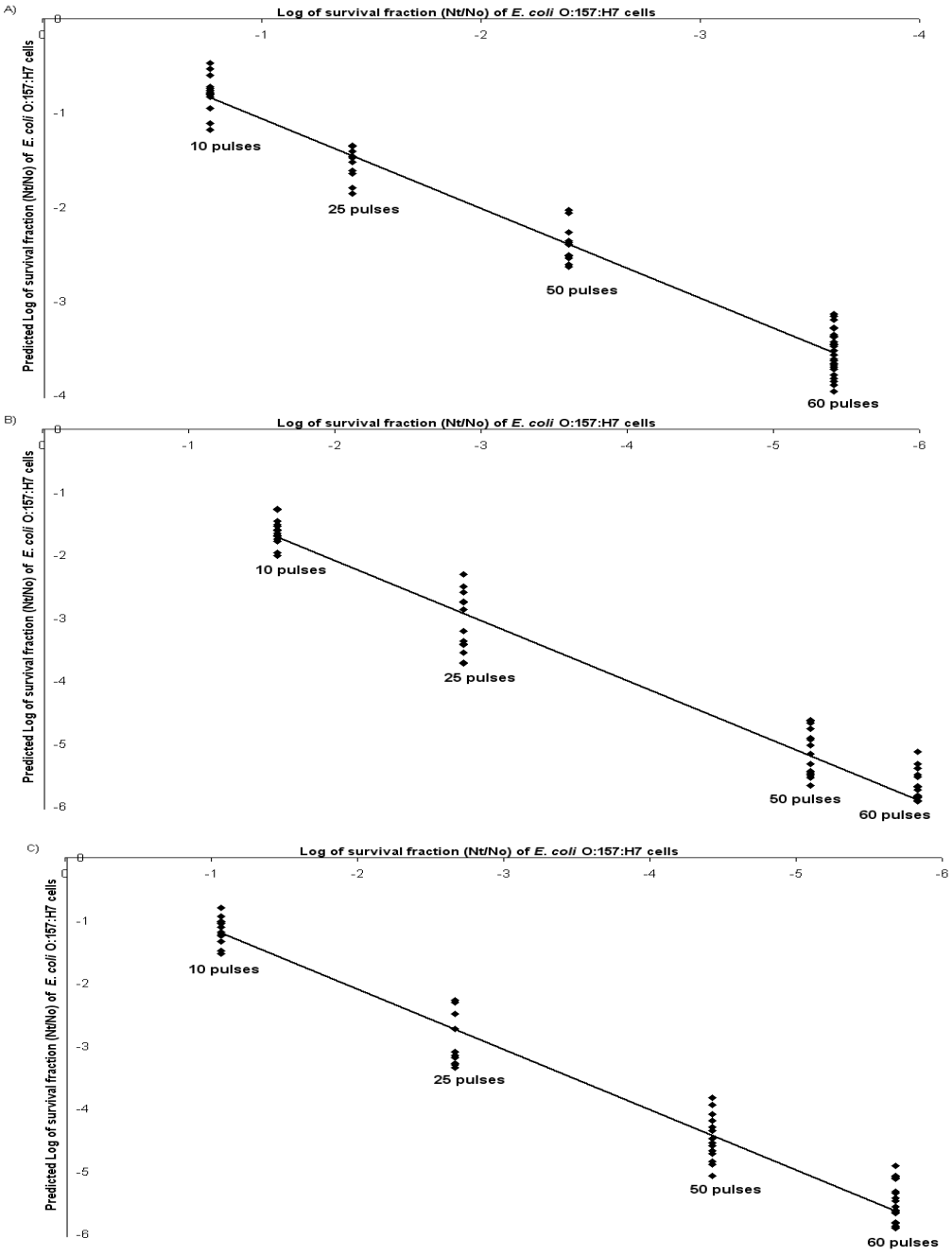

Figure 4.10. Calibration curve of measured and IRMS predicted pulsed electric field treated bacterial count: (A), (B) and (C) are bacterial counts in TSAYE, TSAYE-SC and TSAYE-BS respectively at pH 7

4.4. CONCLUSIONS

ATR- IRMS combined with multivariate analysis was used to study the effect of thermal and pulsed electric field treatment on *E. coli* O157:H7 cells. This technique was used to detect sublethlly injured and alive bacterial cells after the treatments for different length of time and pulses. The raw IR spectra were further analyzed using SIMCA to classify and discriminate between alive, injured and dead cells. The degree of injury by the thermal pulsed electric field treatments produced distinct difference in the infrared spectral features of the biochemical components of the bacterial cell. The results showed that, the components affected the most were proteins of the outer membrane of the cell and the phosphodiester bonds in the DNA/RNA structures. The quantitative prediction of the injured cells using the ATR- IRMS spectral data showed good correlation with the bacteria count measured using conventional culture method. Hence, this method could be used for determining the presence and quantity of injured pathogens in food products. This technique can be used to examine other novel treatments such as high pressure processing, microwave, ultrasound and various chemical treatments

4.5. REFERENCES

Al-Qadiri, H.M.; Lin, M.S.; Cavinato, A.G.; Rasco, B.A. Fourier transform infrared spectroscopy, detection and identification of *Escherichia coli* O157:H7 and *Alicyclobacillus* strains in apple juice. *International Journal of Food Microbiology* **2006**, 111, (1), 73-80

Al-Qadiri, H.M.; Lin, M.; Al-Holy, M.A.; Cavinato, A.G.; Rasco, B.A. Detection of sublethal thermal injury in *Salmonella enterica* serotype typhimurium and *Listeria monocytogenes* using Fourier transform infrared (FT-IR) spectroscopy (4000 to 600 cm^{-1}). *Journal of Food Science* **2008**, 73, (2), M54-M61.

Alvarez-Ordonez, A.; Halisch, J.; Prieto, M. Changes in Fourier transform infrared spectra of *Salmonella enterica* serovars Typhimurium and Enteritidis after adaptation to stressful growth conditions. *International Journal of Food Microbiology* **2010**, 142, (1-2), 97-105.

Alvarez-Ordonez, A.; Mouwen, D.J.M.; Lopez, M.; Prieto, M. Fourier transform infrared spectroscopy as a tool to characterize molecular composition and stress response in foodborne pathogenic bacteria. *Journal of Microbiological Methods* **2011**, 84, (3), 369-378.

Angersbach, A.; Heinz, V.; Knorr, D. Effects of pulsed electric fields on cell membranes in real food systems. *Innovative Food Science & Emerging Technologies* **2000**, 1, (2), 135-149.

Aronsson, K.; Rönner, U.; Borch, E. Inactivation of *Escherichia coli*, *Listeria innocua* and *Saccharomyces cerevisiae* in relation to membrane permeabilization and subsequent leakage of intracellular compounds due to pulsed electric field processing. *International Journal of Food Microbiology* **2005**, 99, (1), 19-32.

Baldauf, N.A.; Rodriguez-Romo, L.A.; Mannig, A.; Yousef, A.E.; Rodriguez-Saona, L.E. Effect of selective growth media on the differentiation of *Salmonella enterica* serovars by Fourier-transform mid-infrared spectroscopy. *Journal of Microbiological Methods* **2007**, 68, (1), 106-114.

Barrett, T.J.; Lior, H.; Green, J.H.; Khakhria, R.; Wells, J.G.; Bell, B.P.; Greene, K.D.; Lewis, J.; Griffin, P.M. Laboratory investigation of a multistate food-borne outbreak of *Escherichia coli* O157:H7 by using pulsed field gel-electrophoresis and phage typing. *Journal of Clinical Microbiology* **1994**, 32, (12), 3013-3017.

Barsotti, L.; Cheftel, J.C. Food processing by pulsed electric fields. II. Biological aspects. *Food Reviews International* **1999**, 15, (2), 181-213.

Basaran, N.; Quintero-Ramos, A.; Moake, M.M.; Churey, J.J.; Worobo, R.W. Influence of apple cultivars on inactivation of different strains of a *Escherichia coli* O157: H7 in apple cider by UV irradiation. *Applied and Environmental Microbiology* **2004**, 70, (10), 6061-6065.

Beekes, M.; Lasch, P.; Naumann, D. Analytical applications of Fourier transform-infrared (FT-IR) spectroscopy in microbiology and prion research. *Veterinary Microbiology* **2007**, 123, (4), 305-319.

Bozoglu, F.; Alpas, H.; Kaletunc, G. Injury recovery of foodborne pathogens in high hydrostatic pressure treated milk during storage. *Fems Immunology and Medical Microbiology* **2004**, 40, (3), 243-247.

Burgula, Y.; Khali, D.; Kim, S.; Krishnan, S.S.; Cousin, M.A.; Gore, J.P.; Reuhs, B.L.; Mauer, L.J. Review of mid-infrared Fourier transform-infrared spectroscopy applications for bacterial detection. *Journal of Rapid Methods & Automation in Microbiology* **2007**, 15, (2), 146-175.

Busch, S.V.; Donnelly, C.W. Development of a repair-enrichment broth for resuscitation of heat-injured *Listeria monocytogenes* and *Listeria innocua*. *Applied and Environmental Microbiology* **1992**, 58, (1), 14-20.

Chapman, P.A., Wright D.J., Norman P., Fox J., and Crick E. Cattle as a possible source of verocytotoxin-producing *Escherichia coli* O157 infections in man. *Epidemiology and Infection* **1993**, 111, 439-447

De Lamo-Castellví, S.; Rodríguez-Saona, L.E. Use of attenuated total reflectance infrared microspectroscopy to discriminate *Bacillus* spores. *Journal of Food Safety* **2011**, 31, (3), 401-407.

De Maesschalck, R.; Candolfi, A.; Massart, D.L.; Heuerding, S. Decision criteria for soft independent modelling of class analogy applied to near infrared data. *Chemometrics and Intelligent Laboratory Systems* **1999**, 47, (1), 65-77.

De Maesschalck, R.; Jouan-Rimbaud, D.; Massart, D.L. The Mahalanobis distance. *Chemometrics and Intelligent Laboratory Systems* **2000**, 50, (1), 1-18.

De Nardo, T.; Shiroma-Kian, C.; Halim, Y.; Francis, D.; Rodriguez-Saona, L.E. Rapid and simultaneous determination of lycopene and beta-carotene contents in tomato juice by infrared spectroscopy. *Journal of Agricultural and Food Chemistry* **2009**, 57, (4), 1105-1112.

Espina, L.; Somolinos, M.; Pagan, R.; Garcia-Gonzalo, D. Effect of citral on the thermal inactivation of *Escherichia coli* O157:H7 in citrate phosphate buffer and apple juice. *Journal of Food Protection* **2010**, 73, (12), 2189-2196.

Gabriel, A.A.; Nakano, H. Inactivation of *Salmonella*, *E. coli* and *Listeria monocytogenes* in phosphate-buffered saline and apple juice by ultraviolet and heat treatments. *Food Control* **2009**, 20, (4), 443-446.

Gabriel, A.A.; Nakano, H. Effects of culture conditions on the subsequent heat inactivation of *E. coli* O157:H7 in apple juice. *Food Control* **2011**, 22, (8), 1456-1460.

Garcia, D.; Gomez, N.; Condon, S.; Raso, J.; Pagan, R. Pulsed electric fields cause sublethal injury in *Escherichia coli. Letters in Applied Microbiology* **2003,** 36, (3), 140-144.

Garcia, D.; Hassani, M.; Manas, P.; Condon, S.; Pagan, R. Inactivation of *Escherichia coli* O157:H7 during the storage under refrigeration of apple juice treated by pulsed electric fields. *Journal of Food Safety* **2005a**, 25, (1), 30-42.

Garcia, D.; Gomez, N.; Mañas, P.; Condon, S.; Raso, J.; Pagan, R. Occurrence of sublethal injury after pulsed electric fields depending on the micro-organism, the treatment medium ph and the intensity of the treatment investigated. *Journal of Applied Microbiology* **2005b**, 99, (1), 94-104.

Garcia, D.; Gomez, N.; Raso, J.; Pagan, R. Bacterial resistance after pulsed electric fields depending on the treatment medium pH. *Innovative Food Science and Emerging Technologies* **2005c,** 6, (4), 388-395.

Garcia, D.; Gomez, N.; Manas, P.; Raso, J.; Pagan, R. Pulsed electric fields cause bacterial envelopes permeabilization depending on the treatment intensity, the treatment medium pH and the microorganism investigated. *International Journal of Food Microbiology* **2007**, 113, (2), 219-227.

Grasso, E.M.; Yousef, A.E.; De Lamo-Castellvi, S.; Rodriguez-Saona, L.E. Rapid Detection and Differentiation of *Alicyclobacillus* species in fruit juice using hydrophobic grid membranes and attenuated total reflectance infrared microspectroscopy. *Journal of Agricultural and Food Chemistry* **2009**, 57, (22), 10670-10674.

Gould, G.W. Methods for preservation and extension of shelf life. *International Journal of Food Microbiology* **1996**, 33, (1), 51-64.

Gould, G.W., New processing technologies: an overview. *Proceedings of the Nutrition Society* **2001**, 60, (4), 463-474.

Hu, X.; Qiu, Z.N.; Wang, Y.R.; She, Z.C.; Qian, G.R.; Ren, Z.M. Effect of ultra-strong static magnetic field on bacteria: application of Fourier-transform infrared spectroscopy combined with cluster analysis and deconvolution. *Bioelectromagnetics* **2009**, 30, (6), 500-507.

Jiang, W.; Saxena, A.; Song, B.; Ward, B.B.; Beveridge, T.J.; Myneni, S.C.B. Elucidation of functional groups on gram-positive and gram-negative bacterial surfaces using infrared spectroscopy. *Langmuir* **2004**, 20, (26), 11433-11442.

Kansiz, M.; Heraud, P.; Wood, B.; Burden, F.; Beardall, J.; McNaughton, D. Fourier transform infrared microspectroscopy and chemometrics as a tool for the discrimination of *cyanobacterial* strains. *Phytochemistry **1999***, 52, (3), 407-417.

Kobayashi, H.; Miyamoto, T.; Hashimoto, Y.; Kiriki, M.; Motomatsu, A.; Honjoh, K.; Iio, M. Identification of factors involved in recovery of heat-injured *Salmonella enteritidis*. *Journal of Food Protection* **2005**, 68, (5), 932-941.

Lin, M.S.; Al-Holy, M.; Al-Qadiri, H.; Kang, D.H.; Cavinato, A.G.; Huang, Y.Q.; Rasco, B.A. Discrimination of intact and injured *Listeria monocytogenes* by Fourier transform infrared spectroscopy and principal component analysis. *Journal of Agricultural and Food Chemistry* **2004**, 52, (19), 5769-5772.

Mañas, P.; Mackey, B.M. Morphological and physiological changes induced by high hydrostatic pressure in exponential- and stationary-phase cells of *Escherichia coli*: Relationship with cell death. *Applied and Environmental Microbiology* **2004**, 70, (3), 1545-1554.

Mañas, P.; Pagan, R. Microbial inactivation by new technologies of food preservation. *Journal of Applied Microbiology* **2005**, 98, (6), 1387-1399.

Mead, P.S.; Slutsker, L.; Dietz, V.; McCaig, L.F.; Bresee, J.S.; Shapiro, C.; Griffin, P.M.; Tauxe, R.V. Food-related illness and death in the United States. *Emerging Infectious Diseases* **1999**, 5, (5), 607-625.

Murphy, R.Y.; Beard, B.L.; Martin, E.M.; Duncan, L.K.; Marcy, J.A. Comparative study of thermal inactivation of *Escherichia coli* O157:H7, *Salmonella*, and *Listeria monocytogenes* in ground pork. *Journal of Food Science* **2004**, 69, (4), M97-M101.

Naumann, D. Infrared spectroscopy in microbiology. *Encyclopedia of Analytical Chemistry*, John Wiley & Sons, Ltd: **2006**.

Neil, K.P.; Biggerstaff, G.; MacDonald, J.K.; Trees, E.; Medus, C.; Musser, K.A.; Stroika, S.G.; Zink, D.; Sotir, M.J. A Novel vehicle for transmission of *Escherichia coli* O157:H7 to humans: multistate outbreak of *E. coli* O157:H7 infections associated with consumption of ready-to-bake commercial prepackaged cookie dough-United States, 2009. *Clinical Infectious Diseases* **2011**, 54(4), 511-518.

O'Bryan, C.A.; Crandall, P.G.; Martin, E.M.; Griffis, C.L.; Johnson, M.G. Heat resistance of *Salmonella* spp., *Listeria monocytogenes*, *Escherichia coli* O157:H7 and *Listeria innocua* M1, a potential surrogate for *Listeria monocytogenes*, in meat and poultry: A review. *Journal of Food Science* **2006**, 71, (3), R23-R30.

Osaili, T.; Griffis, C.L.; Martin, E.M.; Beard, B.L.; Keener, A.; Marcy, J.A. Thermal inactivation studies of *Escherichia coli* O157 : H7, *Salmonella*, and *Listeria monocytogenes* in ready-to-eat chicken-fried beef patties. *Journal of Food Protection* **2006**, 69, (5), 1080-1086.

Osaili, T.M.; Griffis, C.L.; Martin, E.M.; Beard, B.L.; Keener, A.E.; Marcy, J.A. Thermal inactivation of *Escherichia coli* O157: H7, *Salmonella*, and *Listeria monocytogenes* in breaded pork patties. *Journal of Food Science* **2007**, 72, (2), M56-M61.

Pagan, R.; Mackey, B. Relationship between membrane damage and cell death in pressure-treated *Escherichia coli cells*: Differences between exponential- and stationary-phase cells and variation among strains. *Applied and Environmental Microbiology* **2000**, 66, (7), 2829-2834.

Peng, H.; Ford, V.; Frampton, E.W.; Restaino, L.; Shelef, L.A.; Spitz, H. Isolation and enumeration of *Bacillus cereus* from foods on a novel chromogenic plating medium. *Food Microbiology* **2001**, 18, (3), 231-238.

Pirouette, Multivariate Data Analysis Version 4.0 User Manual [online]. *Infometrix, Inc. Bothell, WA,* 2008.

Reiss, G.; Kunz, P.; Koin, D.; Keeffe, E.B. *Escherichia coli* O157:H7 infection in nursing homes: review of literature and report of recent outbreak. *Journal of the American Geriatrics Society* **2006**, 54, (4), 680-684.

Restaino, L.; Frampton, E.W.; Spitz, H. Repair and growth of heat- and freeze-injured *Escherichia coli* O157:H7 in selective enrichment broths. *Food Microbiology* **2001**, 18, (6), 617-629.

Rodriguez-Saona, L.E.; Khambaty, F.M.; Fry, F.S.; Calvey, E.M. Rapid detection and identification of bacterial strains by Fourier transform near-infrared spectroscopy. *Journal of Agricultural and Food Chemistry* **2001**, 49, (2), 574-579.

Somolinos, M.; Garcia, D.; Pagan, R.; Mackey, B. Relationship between sublethal injury and microbial inactivation by the combination of high hydrostatic pressure and citral or tert-butyl hydroquinone. *Applied and Environmental Microbiology* 2008a, 74, (24), 7570-7577.

Somolinos, M.; Garcia, D.; Mañas, P.; Condon, S.; Pagan, R. Effect of environmental factors and cell physiological state on pulsed electric fields resistance and repair capacity of various strains of *Escherichia coli*. *International Journal of Food Microbiology* **2008b**, 124, (3), 260-267.

Subramanian, A.; Ahn, J.; Balasubramaniam, V.M.; Rodriguez-Saona, L. Determination of spore inactivation during thermal and pressure-assisted thermal processing using FT-IR spectroscopy. *Journal of Agricultural and Food Chemistry* **2006**, 54, (26), 10300-10306.

Subramanian, A.; Ahn, J.; Balasubramaniam, V.M.; Rodriguez-Saona, L. Monitoring biochemical changes in bacterial spore during thermal and pressure-assisted thermal processing using FT-IR Spectroscopy. *Journal of Agricultural and Food Chemistry* **2007**, 55, (22), 9311-9317.

Toepfl, S.; Heinz, V.; Knorr, D. High intensity pulsed electric fields applied for food preservation. *Chemical Engineering and Processing: Process Intensification* **2007**, 46, (6), 537-546.

Whitney, B.M.; Williams, R.C.; Eifert, J.; Marcy, J. High-pressure resistance variation of *Escherichia coli* O157: H7 strains and *Salmonella serovars* in tryptic soy broth, distilled water, and fruit juice. *Journal of Food Protection* **2007**, 70, (9), 2078-2083.

Williams, R.C.; Golden, D.A. Influence of modified atmospheric storage, lactic acid, and NaCl on survival of sublethally heat-injured *Listeria monocytogenes. International Journal of Food Microbiology* **2001**, 64, (3), 379-386.

Wuytack, E.Y.; Diels, A.M.J.; Michiels, C.W. Bacterial inactivation by high-pressure homogenisation and high hydrostatic pressure. *International Journal of Food Microbiology* **2002**, 77, (3), 205-212.

CHAPTER 5

Conclusions

5.1. CONCLUSIONS

The main conclusion of this thesis is that: The use of ATR-IRMS combined with multivariate analysis technique such as SIMCA and PLSR as a rapid, sensitive and robust technique was showed for the characterization of membrane fouling and for the determination of the efficiencies of different cleaning protocols used to remove the foulants during membrane emulsification as well as for the detection and classification of different microorganisms.

The following conclusions can be also made:

- The fouling components were identified based on the discriminating bands obtained from the SIMCA analysis of the ATR-IRMS spectra of new, fouled and cleaned membranes (nylon and MCE). From this analysis, sunflower oil was the most prominent surface foulant on both nylon and MCE membranes. Moreover, the class projection and interclass distance results of the SIMCA analysis of new, fouled and cleaned membranes were classified and separated these samples into different classes. Furthermore, efficiencies of different membrane cleaning protocols obtained throught IR data showed that the cleaning protocols applied with 3% Tween 20 at 700 kPa N_2 pressure and with 4% Tween 20 at 500 kPa N_2 pressure had the highest cleaning efficiency and the cleaning protocol with 2% Tween 20 at 150 kPa N_2 pressure had lowest efficiency among the protocols tested independently of the type of membrane used. The cleaning efficiencies obtained from the IR spectral data were compared with the results found from conventional method (WFR %) and the results showed a similar trend on both methods.

- Acetic acid bacteria (*Gluconobacter oxydans* and *Gluconacetobacter xylinus*) and *Saccharomyces cerevisiae* strains were differentiate and correctly classified into the respective bacteria yeast clusters using ATR-IRMS combined with SIMCA.

- *Saccharomyces cerevisiae* and acetic acid bacteria strains were discriminated mainly due to the difference in their cell wall composition.

- Alive and inactivated *Escherichia coli* O157:H7 cells produced by thermal and PEF treatments were correctly classified and discriminated based on the ATR-IRMS spectral differences of the cells detected using SIMCA analysis.

- The classification and discrimination of alive and inactivated (thermal and PEF) *Escherichia coli* O157:H7 cells were mainly due to the difference on the cell membrane composition, cytoplasmic and outer cell membranes.

- SIMCA models showed that the biochemical differences between alive and thermal or PEF treated *Escherichia coli* O157:H7 cells increased with the thermal treatment time and number of pulses applied. These results were also onfirmed with the plate counts obtained.

- The PLSR analysis of ATR-IRMS spectra of treated (thermal and PEF) *Escherichia coli* O157:H7 demonstrates the quantitative application of this technique in the prediction of injured/alive foodborne pathogen microorganisms after different thermal and PEF treatment conditions.

CHAPTER 6

Appendix

6.1. ABOUT THE AUTHOR

6.1.1. Published articles

Espina, L.; **Gelaw, T.K.**; De Lamo-Castellví, S.; Pagán, R. and García-Gonzalo, D. Mechanism of bacterial inactivation by (+)-limonene and its potential use in food preservation combined processes. *PLoS ONE* **2013**, 8(2): e56769. doi:10.1371/journal.pone.0056769

Ait-Ouazzou, A.; Espina, L.; **Gelaw, T.K.;** De Lamo-Castellví, S.; Pagán, R. and García-Gonzalo, D. New insights in mechanisms of bacterial inactivation by carvacrol. *Journal of applied microbiology* **2012**, DOI: 10.1111/jam.12028

Trentin, A.; Güell, C.; **Gelaw, T.K.**; De Lamo-Castellví, S.; Ferrando, M. Cleaning protocols for organic microfiltration membranes used in premix membrane emulsification. *Separation and Purification Technology* **2012**; 88: 70-78.

Gelaw, T.K.; Trentin, A.; Güell, C.; Ferrando, M.; Rodríguez-Saona, L.E. and De Lamo-Castellví, S. Attenuated total reflectance infrared microspectroscopy combined with multivariate analysis, a novel tool to characterize cleaning efficiency of organic microfiltration membranes. *Journal of Membrane Science* **2011**; 376: 35-39.

6.1.2. Conference proceeding

Gelaw, T.K.; Trentin, A.; Güell, C.; Ferrando, M. and De Lamo-Castellví, S. Study of cleaning efficiency of organic microfiltration membranes by attenuated total reflectance infrared microspectroscopy: In Proceedings of 11th International Congress on Engineering and Food (ICEF11),Volume III, Athens, Greece, **2011**.

6.1.3. Articles in preparation

Gelaw, T.K.; Espina, L.; Pagan, R.; García-Gonzalo, D. and De Lamo-Castellví, S. Detection of injured population of *Escherichia coli* O157:H7 produced by thermal and pulsed electric field treatment with attenuated total reflectance infrared microspectroscopy. Journal of Food Protection, to be submitted **2013**.

Gelaw, T.K. and De Lamo-Castellví, S. Discrimination and classification of acetic acid bacteria and *Saccharomyces cerevi*siae strains by attenuated total reflectance microspectroscopy. *Journal of Microbiological Methods*, to be submitted **2013.**

Gelaw, T.K.; Güell, C.; Ferrando, M.; and De Lamo-Castellví, S. Use of attenuated total reflectance infrared microspectroscopy combined with multivariate analysis to study membrane fouling. *Desalination,* to be submitted **2013**.

6.1.4. Conference presentation

Gelaw, T.K.; Güell, C.; Ferrando, M. and De Lamo-Castellví, S. Attenuated total reflectance infrared microspectroscopy combined with multivariate used to study membrane fouling and different cleaning procedures. 12th Mediterranean Congress of Chemical Engineering, Barcelona, **2011**.

Gelaw T.K.; Espina, L.; Pagan, R.; García-Gonzalo, D. and De Lamo-Castellví, S. Detection and discrimination of *Escherichia coli* O157:H7 inactivated with thermal and pulsed electric fields using attenuated total reflectance infrared microspectroscopy combined with multivariate analysis. EFFOST 2011, Berlin, **2011**.

Espina, L.; **Gelaw, T.K.**; De Lamo-Castellví, S.; Pagan, R. and García-Gonzalo, D. Detection and discrimination of *Escherichia coli* O157:H7 inactivated with citral and limonene using attenuated total reflectance infrared microspectroscopy combined with multivariate analysis. EFFOST 2011, Berlin, 2011.

Gelaw, T.K.; Trentin, A.; Güell, C.; Ferrando, M. and De Lamo-Castellví, S. Evaluation of the efficacy of cleaning protocols on membrane emulsification by attenuated total reflectance infrared microspectroscopy (ATR-IRMS). ICOM 2011, Amsterdam, 2011.

Gelaw, T.K.; Puxeu, M. and De Lamo-Castellví, S. Discrimination and classification of acetic acid bacteria and *Saccharomyces cerevisiae* strains by attenuated total reflectance microspectroscopy. IAFP European Symposium on Food Safety, Ede, **2011**.

Gelaw, T.K.; Trentin, A.; Güell, C.; Ferrando, M. and De Lamo-Castellví, S. Study of cleaning efficiency of organic microfiltration membranes by attenuated total reflectance infrared microspectroscopy. 11th International Congress on Engineering and Food (ICEF11), Athens, **2011**.